

## Preface

It is in 1997 that I had the first contact with the Bose-Einstein Condensation and right away I was crazy for it. It is so cool for me that men can cool atoms and catch them ! In that period I attended all of Prof. Chu's speech in Taiwan though I didn't catch the English and the physics most of time. I asked for a poster with the print of the optical molasses and Chu. It's the first and the only one poster I have. I went on listening to the talks about '*Laser Cooling and Trapping*' and expected someday I can see the atom too.

Before the successful cooling and trapping technology, we see the skin of objects because men can only investigate the surface of a material. Actually it is impossible for us to precisely understand the mechanism of behaviors of great amount particles. The manipulation of atoms by light gives us an opportunity to observe the microscopic dynamics even in femto-second time order.

The most spectacular application of laser trapping and atom trapping was recognized on the Nobel prize in 2001. The realization of Bose-Einstein condensation fulfills a 70-year-old dream since the prediction of Einstein in 1925. Physicists call BEC '*The Final Grail*' of science development. And the condensate is suggested to be the fourth phase of matters. The achievement of Bose-Einstein condensation is one of the highlight that men can control the position and the velocity of atoms. We can coherent control the quantum states of atoms and molecules. We can control spontaneous emission, control cold collisions, control the many-body macroscopic wavefunctions. It seems that we are going to be able to unravel all puzzles in the low-energy physics.

The dynamics of the Bose-Einstein condensate can be described through the giant order parameter. The weakly interaction between atoms gives rise to the nonlinearity in the system which enriches investigations into the cold world. With a macroscopic population in the lowest quantum state, cold atoms in the condensate move collectively and show the coherence and the superfluidity. These are very important features below the critical temperature. Therefore in the thesis, we focus on the topics in studying coherent and superfluid behaviors of the condensate.

In chapter one, I make a brief introduction of the route to Bose-Einstein condensation. For experimentalists it is a long and difficult way to develop and improve the cooling and trapping technology. Now, BEC can be reached in few minutes and moreover, in few seconds with all-optical set-up. So it is necessary to understand some important steps in the cooling and trapping processes.

In chapter two, I will introduce one of the nature of the condensate: the coherence, from a theoretical point of view. From the second quantization descriptions, we show the order parameter is a coherent state with a definite phase. Then, by reviewing the interference experiments we see the evidence of coherence. In addition to photons of lasers and cooper pairs in superconductors, the manifestation of coherent property in the neutral atomic system provides more opportunities in further researches. It will be great if we can save and extract the phase information randomly. Combine with concept of adiabatic

exciting process, we design a model to measure an accumulated phase in the time-dependent process. It's very cute that the additional phase can be directly read-out from the interference patterns.

In chapter three, we discuss another nature of the condensate: the superfluid. The historical review of discovery and survey on the superfluid in Helium-4 gives us a better understanding of Two-fluid model, Landau's criterion of the critical velocity, and Bogoliubov's approach to explain the excitation spectrum. Follow Landau's idea, we know an ideal Bose gas is not the superfluid. The weakly interaction again plays an important role on determination of fundamental properties of the condensate. By loading the condensate into an optical lattice, we can investigate the transport property of the condensate. With a little boost, atoms will collectively flow through the periodic wells. By using the band structure method, we find while the group velocity of the flow is larger than the sound velocity, thermal atoms will be created to destroy the superfluid, and the system enters the Landau instability regime. However, if the effective mass of the condensate becomes negative, the condensate will become unstable against the exponential growth of thermal atoms. In this dynamical instability regime, the superfluid model will totally breakdown. Through the study on instability occurrence in the quantum transport process of a condensate, we do observe and prove Landau's theory in BEC, and find the periodic potential provides the roughness to destroy the superfluid.



# Contents

<b>1</b>	<b>Making Atoms a Bose-Einstein Condensate</b>	<b>7</b>
1.1	Very Cold Indeed . . . . .	7
1.2	Properties of an Ideal Bose Gas . . . . .	13
1.3	The Gross-Pitaevskii Equation . . . . .	16
1.4	Summary . . . . .	19
<b>2</b>	<b>The Measurement of the Phase of Bose-Einstein Condensates by Interference of Matter Waves</b>	<b>23</b>
2.1	Why Can We Measure the Phase Between Condensates? . . . . .	23
2.1.1	A Definite Phase of the Giant Matter Wave . . . . .	23
2.1.2	The Coherent State . . . . .	25
2.1.3	Quantum Fields and the Long Range Order Parameter . . . . .	26
2.2	Evidence of Coherence - Manifestation by Interference Patterns . . . . .	29
2.3	The Read-Out Phase Measurement by Simulation of Interference of Two Condensates . . . . .	32
2.3.1	The Model . . . . .	32
2.3.2	Generation of an Additional Phase . . . . .	34
2.3.3	The Method to Produce a Relative Phase Between Con- densates . . . . .	37
2.4	Summary . . . . .	43
<b>3</b>	<b>Instabilities of a Bose-Einstein Condensate in an Optical Lat- tice</b>	<b>47</b>
3.1	Introduction . . . . .	47
3.2	How Does an Optical Lattice Work? . . . . .	48
3.3	Superfluidity and Dissipations of the BEC . . . . .	49
3.3.1	Historical Review of Superfluidity: From $He^4$ to BEC . . . . .	49
3.3.2	Bose-Einstein Condensation and Superfluidity . . . . .	54
3.3.3	Summary . . . . .	57
3.4	Landau and Dynamical Instability of a Bose-Einstein Condensate in an Optical Lattice . . . . .	59
3.4.1	Motivation . . . . .	59
3.4.2	The Effective 1D Gross-Pitaevskii Equation . . . . .	61

3.4.3	k-p Method and 1-band Approximation . . . . .	62
3.4.4	Collective Excitations . . . . .	64
3.5	Numerical Results and Discussions . . . . .	68
3.6	Summary . . . . .	74
<b>A</b>	<b>Derivation of Interaction Potential in Terms of Scattering Length</b>	<b>77</b>
A.1	Relative Magnitude of Phase Shifts . . . . .	78
A.2	Viewpoints From Quantum Mechanics . . . . .	79
<b>B</b>	<b>Analytical Expressions for Band Structures by Plane Wave Method</b>	<b>85</b>
<b>C</b>	<b>Bloch Theorem and k-p Method</b>	<b>89</b>
C.1	General Remarks About Bloch's Theorem . . . . .	89
C.2	k-p Perturbation, Group Velocity, and Effective Mass . . . . .	90
<b>D</b>	<b>The Collective Excitation in The Mean Field Approximation</b>	<b>95</b>



# List of Figures

1.1	The density distribution of expanded clouds. . . . .	8
1.2	Doppler cooling mechanism. . . . .	10
1.3	Cooling and trapping in the magneto-optical trap. . . . .	11
1.4	Energy levels of Na in a magnetic trap. . . . .	12
1.5	A table of temperatures and phase space densities of cold atoms. . . . .	12
1.6	The fraction of particles in the condensate of the function of T. . . . .	14
1.7	Heat capacity of an ideal Bose gas . . . . .	15
1.8	Ground state wave function of a condensate in the isotropic magnetic trap. . . . .	18
1.9	Density profile of a condensate in the axial-symmetric double well . . . . .	19
2.1	The criterion for Bose-Einstein condensation. . . . .	24
2.2	Temperature dependent one particle density matrix. . . . .	28
2.3	Interference patterns of two expanding condensates. . . . .	30
2.4	Macroscopic quantum interference from atomic tunnel arrays. . . . .	31
2.5	Density profiles of a condensate in single- and double-well. . . . .	33
2.6	The wall of a box moved in adiabatic and nonadiabatic processes. . . . .	35
2.7	Density profiles of clouds at the initial time. . . . .	39
2.8	The additional phase of the condensate accumulated after a loop of perturbation. . . . .	40
2.9	The phase functions at the end of adiabatically added perturbing potential to the left well. . . . .	41
2.10	Free expansion interference patterns for the pure double-well BEC and the two condensates with a difference of the additional phase. . . . .	42
3.1	One dimensional optical lattice. . . . .	49
3.2	Two dimensional optical lattice. . . . .	50
3.3	Heat capacity of $He^4$ . . . . .	51
3.4	Dispersion relation of $He^4$ . . . . .	52
3.5	Measurement and theoretical calculations of collective excitation spectra. . . . .	53
3.6	Galilean transformation for the excitation spectrum. . . . .	56
3.7	Evidence for a critical velocity in BEC. . . . .	57
3.8	Ratio of the first peak amplitude of the oscillation to the free oscillation amplitude. . . . .	59

3.9	The fraction of atoms remains in the condensate as the function of the velocity. . . . .	60
3.10	Periodic potential and the band structure of $V = 0.7 \sin^2 \frac{\pi x}{2}$ . . .	62
3.11	Effective mass and group velocity of the BEC in an optical lattice.	70
3.12	Fraction $N_0/N$ of $k$ at $V_0 = 2$ , $T = 0$ K, $30$ nK. . . . .	71
3.13	Low energy branch of the excitation energy spectra . . . . .	72
3.14	High energy branch of the excitation energy spectra. . . . .	73
A.1	Classical scattering between two particles. . . . .	79
D.1	Excitation energy spectra of the three lowest collective excitation modes . . . . .	98



# Chapter 1

## Making Atoms a Bose-Einstein Condensate

The Basic idea of Bose Einstein condensation (BEC) goes back to 1924 when Bose proposed the concept of statistical description on a new derivation of Planck's radiation law to the light quanta. Then Einstein presented in 1925 a similar treatment for the ideal indistinguishable particles. He predicted the occurrence of a phase transition of noninteracting atoms. The phase transition associated with the condensation of atoms in the lowest energy state and, irrelevant to interactions between atoms, is purely the consequence of quantum statistical effects. But for a long time there are no practical verifications of predictions. It's not until the discovery of superfluidity in liquid helium that efforts to realize BEC in  $He^4$  comes to bloom.

However, the quantum statistical properties in description of route to BEC is valid only for *gases*. The first BEC is realized in 1995. Before 2001 there are five groups that successfully create condensates[1, 2, 3, 4, 5]. And over 150 groups world-wide are working on BEC in cold atomic gases. Fig. 1.1 shows the evidence of creation of the condensate for Na. When  $T \ll T_c \sim 2\mu K$  where most of atoms occupy the lowest quantum state and have a very narrow momentum distribution. We have not only to sit and enjoy the beautiful 'product' but attribute great success to the efforts on development of cooling techniques. So in the next section, we try to simply and briefly introduce the complex cooling processes. Detailed references are available in Ref. [6].

### 1.1 Very Cold Indeed

In general there are three 'stops' in the cooling processes[7]:

- Doppler molasses:  
An optical molasses is usually constructed by six intersecting beams tuned below resonance to reduce velocity of atoms at beam intersection. The

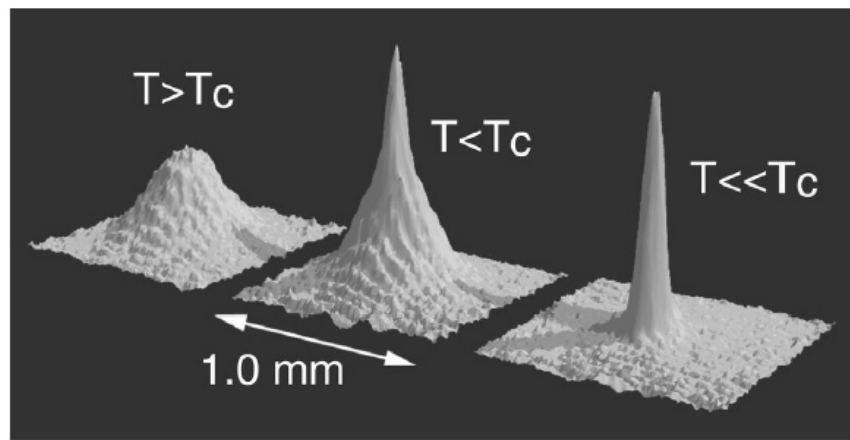


Figure 1.1: The density distribution of expanded clouds of Na atoms at different temperatures. When  $T > T_c$  the distribution of the cloud in momentum space represents uniformly thermal expansion. When  $T \ll T_c$  it shows the evidence of formation of the condensate where a sharp and nonuniform distribution in momentum space represents a macroscopic occupation of a low quantum state and manifestation of the uncertainty principle. *From web page of W. Ketterle in MIT group.*



Doppler effect is demonstrated in preference of absorption of the photon counter-propagating to an atom. As shown in Fig. 1.2, when an atom with velocity  $v$  absorbs a photon with momentum  $p = \hbar k$ , the atom is slowed by  $\hbar k/m$  according to the momentum conservation law. After re-radiation randomly, on average the atom is slowed down. However, the molasses can not trap atoms. Even cold atoms are free to wander around out.

- Magneto-optical trap:

In order to confine atoms, we add a magnetic field gradient. As shown in Fig. 1.3, two coils with currents flowing in opposite directions generate a linear field gradient to provide a restoring force that pulls atoms back to the center. A defect at the origin can be made up by adding a rotating bias field. In this way, atoms are trapped in a time-averaged orbiting parabolic potential.

The trapping mechanism in the magnetic trap originates in kicking out hot atoms of high Zeeman energies. When Zeeman shifted energy levels are denoted by

$$U_Z = \mu|B|,$$

where  $\mu$  is the magnetic dipole moment and for hyperfine level  $F$ , sub-level  $m_F$ ,

$$\mu = \mu_B m_F g$$

where  $\mu_B$  is the Bohr magneton and  $g$  is Lande  $g$  factor. So Fig. 1.4 shows for Na, energies of  $\{F = 2, m_F = -1, 0, 1, 2\}$  states increase when B field increases. They are "weak-field seeking" states that can be confined in a magnetic field minimum.

- Evaporative cooling:

The optical cooling can reduce the temperature to orders about milli-Kelvin, but it's not cold enough. By tuning the frequency of the RF radiation we can make a hole at the side of the trap. Only atoms with energies less than that of the trap would stay in. The RF radiation can flip the spin state of an atom from low-field seeking one to the high-field seeking state, therefore expelling hot atoms from the trap. After the hot atoms are forced out, the rest re-thermalizes through elastic collisions to a lower temperature. After this process, the temperature can be lowered to at least micro-Kelvin, cold enough for creating a condensate.

So what is the temperature of atoms cooled in each steps? According to the Fig. 1.5 the laser cooling process lowers atoms to about  $50 \mu K$ , and  $T$  goes down to  $500 nK$  after the evaporative cooling process. Actually the results of evaporative cooling from the first three groups that achieved BEC are:

- Rice: for  $Li^7$ ,  $N = 0.1 \times 10^6$ ,  $T = 0.4 \mu K$ .

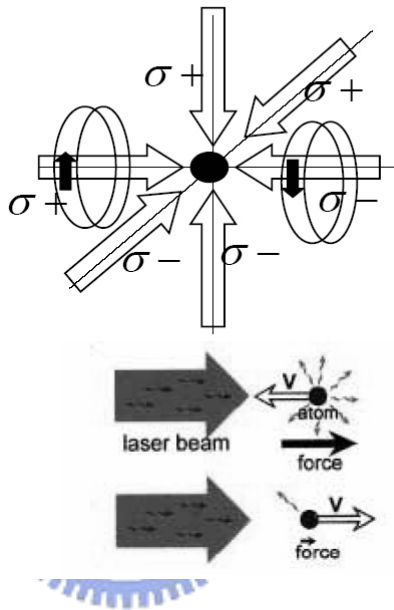


Figure 1.2: The optical molasses is constructed by focusing six lasers on atoms. Due to the motion of atoms, the laser frequency is detuned by the Doppler effect. When an atom with velocity  $v$  absorbs an off-resonance photon with energy  $E_{laser} = E_{res} - \Delta_{Doppler}$  and momentum  $p = \hbar k$ , the atom is slowed by  $\hbar k/m$  according to the momentum conservation law. After re-radiation randomly, on average the atom is slowed down.

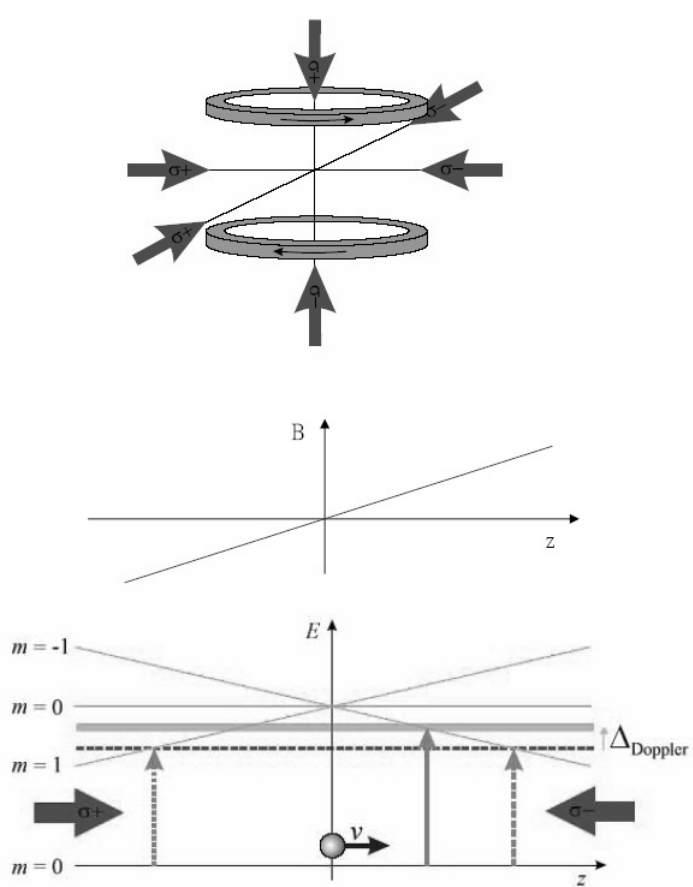


Figure 1.3: Two magnetic coils provides a linear field with  $B = A\sqrt{\rho^2 + 4z^2}$ . The presence of the B field causes the zeeman shift of magnetic quantum states and provides a trapping force to confine atoms. When the atom moves to right, it prefers to absorb a photon with  $\sigma_-$ . When it falls to the ground state by spontaneous emission, an atom is effectively driven towards the center. *From R. Roth in GSI group.*

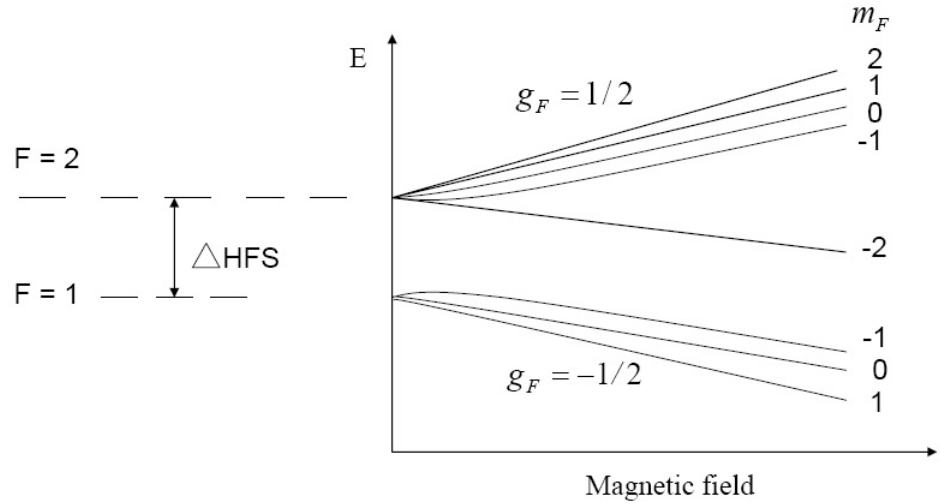
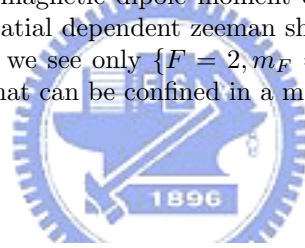


Figure 1.4: The magnetic dipole moment of the atom interacting with the B field induces a spatial dependent zeeman shift. Through energy levels of Na in a magnetic trap, we see only  $\{F = 2, m_F = -1, 0, 1, 2\}$  states are "weak-field seeking" states that can be confined in a magnetic field minimum.



	Temperature	Density[ $cm^{-3}$ ]	Phase-space density
<b>Oven</b>	500K	$10^{14}$	$10^{-13}$
<b>Laser cooling</b>	$50 \mu K$	$10^{11}$	$10^{-6}$
<b>Evaporative cooling</b>	500nK	$10^{14}$	2.612
<b>BEC</b>		$10^{15}$	$10^7$

Figure 1.5: A table of temperatures and phase space densities of cold atoms. When BEC is reached, almost all atoms populate in the lowest quantum state and the phase space density goes up to  $10^7$ . On the other hand, the particle density is only  $10^{15} cm^{-3}$ , much less than molecules in the air at room temperature and atmospheric pressure with density of  $10^{19} cm^{-3}$ , and the density in liquids or solids of order of  $10^{22} cm^{-3}$ . BEC is thus a dilute system.

- MIT: for  $Na^{23}$ ,  $N = 0.7 \times 10^6$ ,  $T = 2 \mu K$ .
- JILA: for  $Rb^{87}$ ,  $N = 4 \times 10^6$ ,  $T = 90 \mu K$ .

Compared with the temperature of the surface of the sun  $T = 3000 K$ , the BEC temperature in order of nano-Kelvin makes the condensate the coldest matter in the world!

While the chilly temperature serves as a macroscopic quantity giving the information of BEC, a very important symbol behind that guides settings of experimental parameters is the microscopic phase space density  $\rho$ . The condition to BEC requires  $\rho > 2.612$ . We will discuss it from the statistical properties of an ideal Bose gas in the next section. And then we can obtain more precise understandings of static properties of BEC.

## 1.2 Properties of an Ideal Bose Gas

It's convenient to investigate statistical properties for Bose gases from view point of the grand canonical ensemble theory[16]. With partition function  $Z$  we can evaluate all thermodynamical quantities of the system via the grand potential

$$\Omega = -k_B T \ln Z. \quad (1.1)$$

For an ideal Bose gas in the box of volume  $V$  the grand canonical potential is

$$\Omega = k_B T \sum_k \ln(1 - e^{(\mu - \epsilon_k)/k_B T}), \quad (1.2)$$

where  $\mu$  is chemical potential and  $\epsilon_k = \hbar^2 k^2 / 2m$  is the single particle energy state. By using  $N = -\partial\Omega/\partial\mu$ , the total number of particles is given by

$$N = \sum_k \frac{1}{\exp[(\epsilon_k - \mu)/k_B T] - 1}. \quad (1.3)$$

In the thermodynamical limit  $V \rightarrow \infty$ , and we rewrite above equation in an integration form. By calculating number of states in a unit shell of a  $k$ -space sphere, we obtain  $4\pi k^2 dk V / (2\pi)^3 = V g(\epsilon) d\epsilon$ , where  $g(\epsilon) = m^{3/2} \epsilon^{1/2} / \sqrt{2\pi^2 \hbar^3}$  is the density of state. Then the particle density can be written as

$$n = \int d\epsilon \frac{1}{e^{\beta(\epsilon - \mu)} - 1} g(\epsilon), \quad (1.4)$$

where  $\beta = 1/k_B T$ . Set  $z = e^{\beta\mu}$  and use the Gamma function the integration can be analytically calculated. And the particle density is expressed as

$$n = \frac{mk_B T^{3/2}}{2\pi\hbar^2} g_{3/2}(z), \quad (1.5)$$

where  $g_{3/2}(z)$  is defined by

$$g_{3/2}(z) = \sum_{p=1}^{\infty} \frac{z^p}{p^{3/2}}.$$

The series is convergent at  $z = 1$  and  $g_{3/2}(1) = 2.612$  can be calculated from the Riemann zeta function. By using small  $z$  expansion the chemical potential is approximated to

$$\mu \simeq \frac{3}{2}k_B T \ln\left(\frac{mk_B T}{2\pi\hbar^2 n^{3/2}}\right). \quad (1.6)$$

From Eq. 1.3 we know that the phase transition occurs as  $\mu$  becomes zero, if we neglect the zero-point energy and set the lowest state energy as zero. Therefore we define the BEC temperature

$$T_c = \frac{2\pi\hbar^2}{k_B m} \left(\frac{n}{2.612}\right)^{3/2}. \quad (1.7)$$

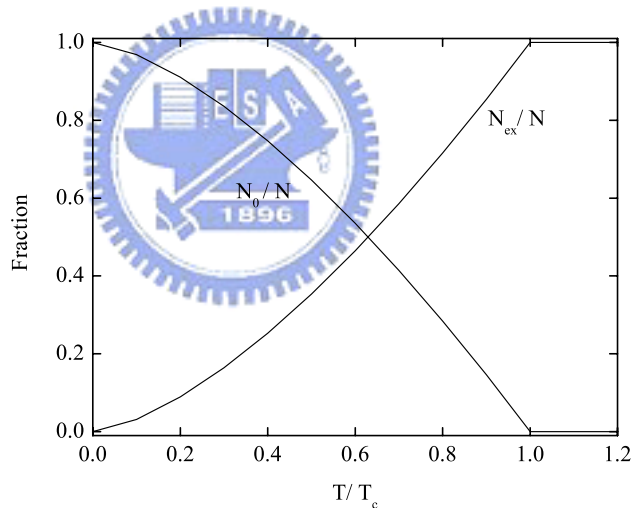


Figure 1.6: The fraction of particles in the condensate of the function of  $T$ :  $N_0/N = 1 - (T/T_c)^{3/2}$ . Here we consider the noninteracting gas in the box of volume  $V$ . If atoms are confined in an isotropic harmonic trap, the relation of the fraction and the temperature becomes  $N_0/N = 1 - (T/T_c)^3$ .

We mentioned that the phase space density must be increased to achieve BEC. The phase space density is defined as the number of particles contained

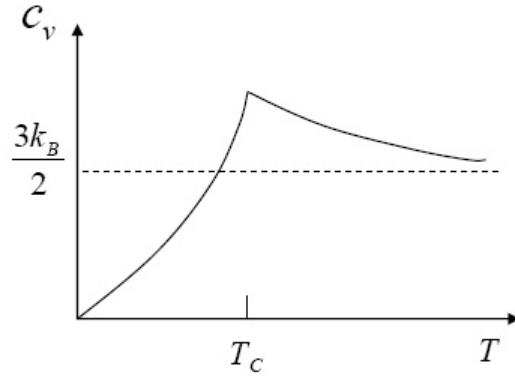


Figure 1.7: Heat capacity of an ideal Bose gas. At  $T_c$  the heat capacity has a cusp, or a discontinuity in the slope. We say that a first-order phase transition occurs at  $T_c$ . At any nonzero temperature below  $T_c$ , we have a mixture of the normal and condensate phases.

within a volume of cubic length of the de Broglie wavelength  $\lambda_{dB} = (2\pi\hbar^2/mk_B T)^{1/2}$ . So we have

$$\rho = n\lambda_{dB}^3 = 2.612 \quad (1.8)$$

as the condition for BEC. But what happens if we cool atoms below  $T_c$ ? Einstein realized that as long as  $\mu$  becomes zero, the number of particles in the lowest quantum state becomes infinite. So we assume a macroscopic number of atoms  $N_0$  occupy the ground state, and we rewrite Eq. 1.3 by

$$N = N_0 + \sum_{k \neq 0} \frac{1}{e^{\beta\epsilon_k} - 1}. \quad (1.9)$$

Again, replace summation to integration we would obtain the fraction of particles in the condensate as

$$\frac{N_0}{N} = 1 - \left(\frac{T}{T_c}\right)^{3/2}, \quad (1.10)$$

a remarkable formula of BEC as illustrated in Fig. 1.6.

Another important quantity is the heat capacity. By definition  $C_V = \partial\mu/\partial T|_n$ . From the calculation of total internal energy

$$U = V \int d\epsilon \frac{\epsilon}{e^{\beta(\epsilon-\mu)} - 1} g(\epsilon)$$

with  $\mu = U/N$ , we obtain

$$\begin{aligned} C_V &\sim 3k_B T/2 && \text{for } T \gg T_c \\ C_V &= \frac{15}{4} \frac{g_{5/2}(1)}{g_{3/2}(1)} \left(\frac{T}{T_c}\right)^{3/2} k_B && \text{for } T < T_c. \end{aligned} \quad (1.11)$$

This is sketched in Fig. 1.7. At  $T_c$  the heat capacity has a cusp, or a discontinuity in the slope. We say that a first-order phase transition occurs at  $T_c$ . At any nonzero temperature below  $T_c$ , we have a mixture of the normal and condensate phases.

### 1.3 The Gross-Pitaevskii Equation

After the creation of a condensate, next, we will ask: How to describe it theoretically? Practically, there are weakly interactions between cold atoms, and the Hamiltonian of the system can be written as

$$H = \sum_i \frac{\mathbf{p}_i^2}{2m} + \sum_i V_{ext}(\mathbf{r}_i) + \sum_{i<j} V_{int}(\mathbf{r}_i - \mathbf{r}_j), \quad (1.12)$$

where  $V_{ext}$  is the confining potential and  $V_{int}$  denotes interactions between atoms. According to the experimental setup,  $V_{ext}$  is the average potential generated from the time dependent magnetic field and is usually in the parabolic form[9]. For dilute gases,  $na_s^3 \ll 1$ , where  $n$  is the particle density and  $a_s$  is the s-wave scattering length. In the case, the probability of three body collision is too small to be neglected, and interactions can be considered from only two-body collisions. Atoms can see each other only when they approach closely enough so  $V_{int}$  can be interpreted in terms of the Dirac-delta function from a hard-sphere model. The exact potential derived from the classical scattering theory can be seen in Appendix A.

In order to solve the above equation we set the many-body trial function:

$$\Psi(\mathbf{r}_1, \mathbf{r}_2, \dots, \mathbf{r}_N) = \prod_i^N \psi(\mathbf{r}_i), \quad (1.13)$$

where the total wave function is symmetric against the permutation operator  $P$ , namely,

$$P\Psi(\mathbf{r}_1, \mathbf{r}_2, \dots, \mathbf{r}_j, \mathbf{r}_k, \dots, \mathbf{r}_N) = \Psi(\mathbf{r}_1, \mathbf{r}_2, \dots, \mathbf{r}_k, \mathbf{r}_j, \dots, \mathbf{r}_N). \quad (1.14)$$

If we assume BEC occurs when all atoms fall into the same single-particle state, then  $\psi(\mathbf{r}_i) = \psi(\mathbf{r})$  fulfills the symmetry constraint automatically. With the normalization condition

$$\int d\mathbf{r} |\psi(\mathbf{r})|^2 = 1, \quad (1.15)$$

the equation of motion of the condensate can be derived through minimization of energy functional

$$E = \int d\mathbf{r} \left[ \frac{\hbar^2}{2m} |\nabla\psi(\mathbf{r})|^2 + V_{ext}(\mathbf{r}) + \frac{4\pi\hbar^2 a_s}{2m} |\psi(\mathbf{r})|^4 \right] \quad (1.16)$$

, where we have replaced  $\psi(\mathbf{r})$  with  $\sqrt{N}\psi(\mathbf{r})$  such that  $\int d\mathbf{r} |\psi(\mathbf{r})|^2 = N$ . Therefore we have the chemical potential  $\mu$  as the Lagrange multiplier to ensure the



conservation of particle number while we minimize the quantity  $E - \mu N$  at fixed  $\mu$ . So the zero of the variation  $E - \mu N$  with respect to  $\psi^*$  gives

$$-\frac{\hbar^2}{2m}\nabla^2\psi(\mathbf{r}) + V_{ext}(\mathbf{r})\psi(\mathbf{r}) + \frac{4\pi\hbar^2 a_s}{m}|\psi(\mathbf{r})|^2\psi(\mathbf{r}) = \mu\psi(\mathbf{r}). \quad (1.17)$$

This is the time-independent Gross-Pitaevskii (GP) equation and the mean field approach gives the self-trapping nonlinear potential.

The sign of the scattering length can be tunned by the magnetic field near the Feshbach resonant regimes[10]. Determination of scattering length in alkali atoms are reported in [2, 12, 13, 14, 15]. When  $a_s < 0$  the interaction is attractive and it is possible for atomic cloud to be unstable. While  $a_{osc} = (\hbar/m\omega)^{1/2}$  denotes the characteristic quantum mechanical length scale for the harmonic oscillator, the critical particle number can be estimated through

$$\frac{N_c a_s}{a_{osc}} \simeq 0.67. \quad (1.18)$$

We have more interested in the stable regime where  $a_s > 0$  and the cloud is extended in function of particle number  $N$  by the repulsive interaction. For sufficient large clouds, an accurate description of the GP equation can be obtained by neglecting the kinetic energy term. From Eq. 1.17 and set  $U = 4\pi\hbar^2 a_s/m$  we have

$$[V_{ext}(\mathbf{r}) + U|\psi(\mathbf{r})|^2]\psi(\mathbf{r}) = \mu\psi(\mathbf{r}). \quad (1.19)$$

There is an analytical solution

$$\psi(\mathbf{r}) = \sqrt{\frac{\mu - V_{ext}}{U}}, \quad (1.20)$$

where  $\mu$  is obtained through the normalization condition

$$\int d\mathbf{r}|\psi(\mathbf{r})|^2 = N. \quad (1.21)$$

In the following we show the numerical solution of the GP equation by using Fourier-Grid-Hamiltonian method[20]. In simplification, we show the simulation for a condensate in the spherical trap for  $N = 100, 1000, 10000$ . We consider the repulsive case only. Also we show the noninteracting wave function in comparison.

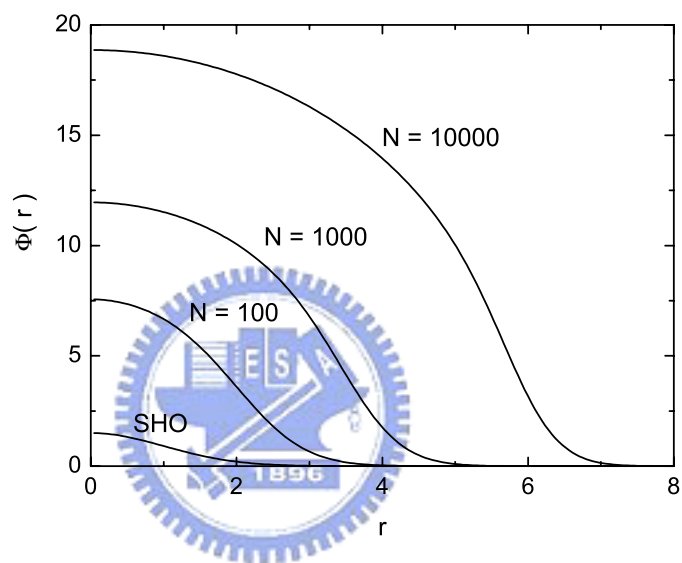


Figure 1.8: Ground state wave function of a condensate in the isotropic magnetic trap. Consider repulsive interactions between two atoms, we plot  $N = 100$ , 1000, and 10000. Also, the profile of a noninteracting particle is shown as a comparison.

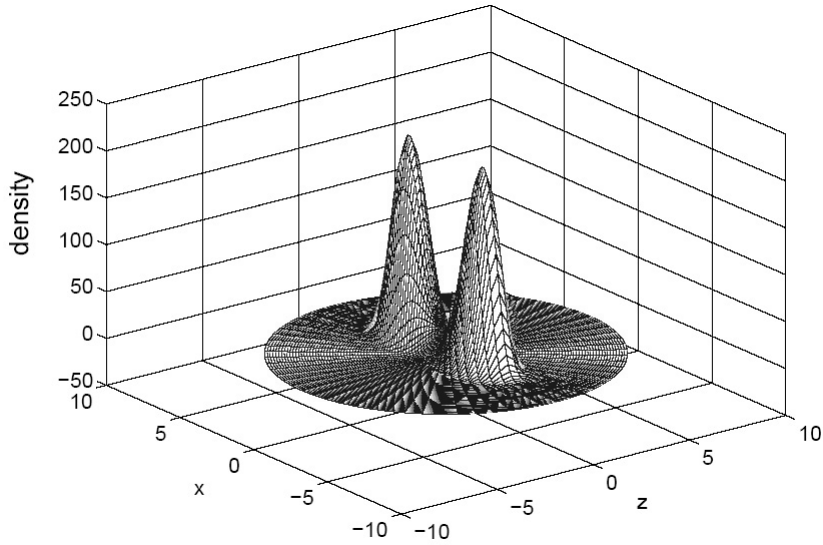


Figure 1.9: Density profile of a condensate in the axial-symmetric double well. Here the particle number  $N = 10000$  and the dimensionless barrier height is 8.

## 1.4 Summary

In this chapter we have a brief introduction of the route to BEC. The statistic property gives the microscopic criterion for BEC and determine the relation between particle number and the temperature. The phase space density should be larger than order of one when  $T \leq T_c$ . There are normal particles due to the presence of thermal fluctuations. However, while we consider a repulsive interaction between atoms, there are particles out of the condensate even at  $T = 0$ . This is the evidence of the quantum fluctuation. Finally, in the Hartree approximation, we derive the GP equation for the condensate. The many-body system can be just regarded as a one-particle system. Since the condensate, by definition, occupies the lowest quantum state, only the ground state solution of the GP equation is valid. Due to the presence of the nonlinear potential, the GP equation must be solved self-consistently. In each step, a constraint of conservation of particle number should be fulfilled. Start with the GP equation we can investigate dynamical behaviors of the condensate.



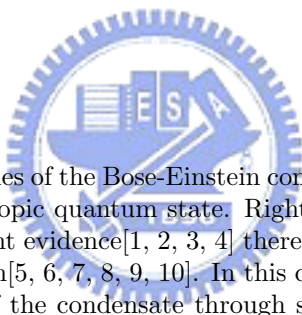
# Bibliography

- [1]  $Rb^{87}$ , June 1995. E. Cornell *et al.*, Jila.
- [2]  $Li^7$ , July 1995. R. Hulet *et al.*, Rice Univ..
- [3]  $Na^{23}$ , Sep. 1995. W. Ketterle *et al.*, MIT.
- [4]  $H^1$ , June 1998. D. Kleppner *et al.*, MIT.
- [5]  $He^4$ , Feb. 2001. A. Aspect *et al.*, ENS.
- [6] H. J. Metcalf and P. van der Straten, *Laser cooling and trapping*, Springer 1999.
- [7] B. P. Anderson, *Experimental research with dilute-gas Bose Einstein condensates*, unpublished note.
- [8] Kerson Huang, *Statistic Mechanics*, Wiley 1987.
- [9] M. H. Anderson, J. R. Ensher *et al.*, *Science* **269**, 198(1995).
- [10] H. Feschbach, *Ann. Phys.* **19**, 287(1962).
- [11] E. R. I. Abraham, W. I. McAlexander *et al.*, *Phys. Rev. A* **55**, 3299(1997).
- [12] E. Tiesinga, C. J. Williams *et al.*, *J. Res. Nat. Inst. Stand. Technol.* **101**, 505(1996). F. A. van Abeelen and B. J. Verhaar, *Phys. Rev. A* **59**, 578(1999).
- [13] J. L. Bogn, J. P. Burke *et al.*, *Phys. Rev. A* **59**, 3660(1999).
- [14] P. S. Julienne, F. H. Mies *et al.*, *Phys. Rev. Lett.* **78**, 1880(1997).
- [15] C. Chin, V. Vuletic *et al.*, *Phys. Rev. Lett.* **85**, 2717(2000).
- [16] F. Brau and C. Semay, *J. Comp. Phys.* **139**, 127(1998).



## Chapter 2

# The Measurement of the Phase of Bose-Einstein Condensates by Interference of Matter Waves



One of the fascinating properties of the Bose-Einstein condensation is the nature of the coherence in a macroscopic quantum state. Right after the experiments performed to show the coherent evidence [1, 2, 3, 4] there are also many theoretical works on this phenomenon [5, 6, 7, 8, 9, 10]. In this chapter we focus on the determination of the phase of the condensate through some fundamental concepts and the results in experiments. Extended by controls of time-dependent processes we design a model for simulations such that the phase difference of condensates can be directly read out from interference patterns.

### 2.1 Why Can We Measure the Phase Between Condensates?

#### 2.1.1 A Definite Phase of the Giant Matter Wave

A gas of bosonic atoms are defined as atoms composed of an even number of constituents with half-integer spin. As Fig. 2.1 shows: if one cools the gas below a critical temperature  $T_c$  such that atoms exhibit wavelike properties, they will become densely enough so that the average distance between atoms is comparable to their "de Broglie wavelength." Below  $T_c$  individual atoms become impossible to distinguish. If the atoms are bosons, they fall collectively into the

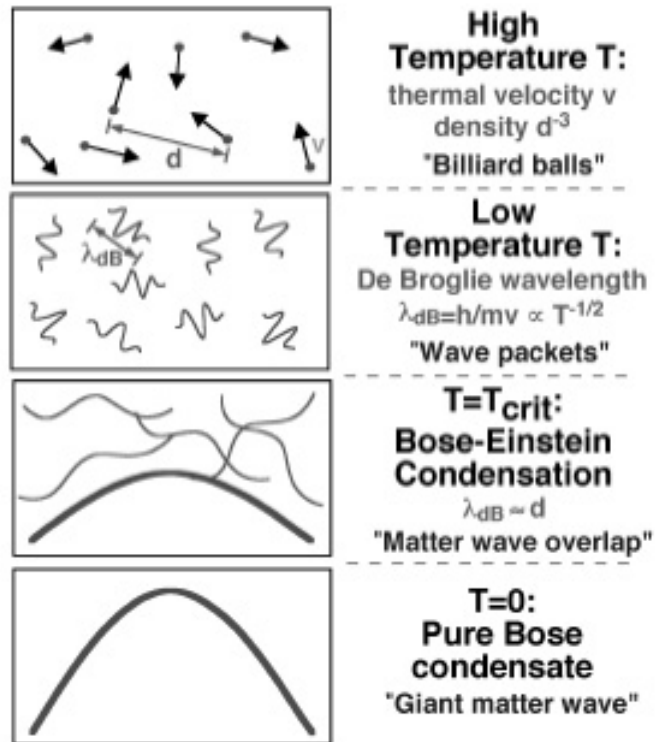


Figure 2.1: At high temperatures atoms behave as billiard balls. When the temperature is lowed enough the quantum wave characters reveal. Atoms can be regarded as wavepackets with an extension  $\lambda_{dB}$ , the de Broglie wave length. At BEC transition temperature,  $\lambda_{dB}$  is comparable with distance between atoms. And when  $T$  approaches zero, the thermal cloud disappear leaving a pure condensate. *From Rev. Mod. Phys.* **74**, 1131(2002).



lowest-energy state to form a Bose-Einstein condensate, a weakly interacting gas. We say that as the system undergoes the phase transition it turns out to be an ordered quantum state and in real space the many-body system can be described through a macroscopic order parameter  $\psi(\mathbf{r})$ . Since it's the wave behavior that characterizes the quantum system the complex order parameter acquires a common phase of all atoms in the condensate indicating the existence of the phase coherence for a condensate. Namely, we can rewrite

$$\psi(\mathbf{r}) = \sqrt{n(\mathbf{r})}e^{i\theta(\mathbf{r})}, \quad (2.1)$$

where  $\sqrt{n(\mathbf{r})} = |\psi(\mathbf{r})|$  is the modulus and  $\theta(\mathbf{r})$  is its phase. And we say the coherence length roughly equals to the size of the condensate.

In analogy of the optical field the matter wave behaviors of a condensate stimulate lots of interests to characterize its coherent behaviors[11, 12]. By means of the quantum coherent many-particle state, the nature of the non-vanishing off diagonal long range order parameter associated with the coherence can be linked.

### 2.1.2 The Coherent State

It's well known the system of a quantum harmonic oscillator can be described in terms of the bosonic ladder operators  $\hat{a}$  and  $\hat{a}^\dagger$ [13]. The energy levels can be written as

$$E_n = \hbar\omega(\hat{a}^\dagger\hat{a} + \frac{1}{2}) = \hbar\omega(n + \frac{1}{2}), \quad (2.2)$$

and the eigenvectors  $\psi_n(x)$  can be represented as

$$\psi_n(x) = \frac{1}{(n!)^{1/2}}(\hat{a}^\dagger)^n\psi_0(x), \quad (2.3)$$

which constitute a complete set. Therefore we can define a coherent state by

$$|\alpha\rangle = C(\psi_0(x) + \alpha\psi_1(x) + \frac{\alpha^2}{2!^{1/2}}\psi_2(x) + \frac{\alpha^3}{3!^{1/2}}\psi_3(x) + \dots) \quad (2.4)$$

$$= e^{-|\alpha|^{1/2}}(1 + \alpha\hat{a}^\dagger + \frac{(\alpha\hat{a}^\dagger)^2}{2!} + \frac{(\alpha\hat{a}^\dagger)^3}{3!} + \dots)|0\rangle, \quad (2.5)$$

where  $|0\rangle = \psi_0(x)$  is the ground state and also a coherent state with  $\alpha = 0$ . One important property of the coherent state is that  $|\alpha\rangle$  has a definite phase  $\theta$ , namely we can write

$$\alpha = |\alpha|e^{i\theta}. \quad (2.6)$$

Then Eq. 2.4 can be written as

$$|\alpha\rangle = C(\psi_0(x) + e^{i\theta}|\alpha|\psi_1(x) + e^{2i\theta}\frac{|\alpha|^2}{2!^{1/2}}\psi_2(x) + \dots). \quad (2.7)$$

Coherent states were first used in the theory of the laser. The ladder operators are usually written as  $\hat{a}^\dagger_{ks}$  and  $\hat{a}_{ks}$  to represent the creation and annihilation of

a photon with momentum  $k$  and polarization  $s$ . The many particle system can be in convenient to be represented in terms of the occupation number

$$|n_{k_0 s_0}, n_{k_1 s_1}, n_{k_2 s_2}, n_{k_3 s_3}, \dots \rangle, \quad (2.8)$$

and obeys

$$\begin{aligned} \hat{a}_{ks}^\dagger |\dots n_{ks} \dots \rangle &= \sqrt{n_{ks} + 1} |\dots n_{ks} + 1 \dots \rangle \\ \hat{a}_{ks} |\dots n_{ks} \dots \rangle &= \sqrt{n_{ks}} |\dots n_{ks} \dots \rangle. \end{aligned} \quad (2.9)$$

Of course the ladder operators obey the bosonic commutation relations but we omit to show here. And we can write a general coherent state in the form of

$$|\alpha_{k_0 s_0}, \alpha_{k_1 s_1}, \alpha_{k_2 s_2}, \dots \rangle = e^{-\sum |\alpha_{ks}|^2 / 2} \exp(\sum \alpha_{ks} a_{ks}^\dagger) |0 \rangle. \quad (2.10)$$

In practical lasers, there are usually few macroscopically occupied modes through nonlinear optical pumping processes[14]. Due to the similarities on the existences of the nonlinear media and the macroscopic wave behaviors, we can borrow the language in lasers to describe the BEC system. In the following paragraphs we are going to show how to connect the order parameter with the coherent state.

### 2.1.3 Quantum Fields and the Long Range Order Parameter

In conventional quantum field language the Hamiltonian can be expressed in terms of the field operators  $\hat{\psi}(\mathbf{r})$  and  $\hat{\psi}^\dagger(\mathbf{r})$ [15], namely

$$\begin{aligned} \hat{H} &= \int d\mathbf{r} \hat{\psi}^\dagger(\mathbf{r}) \left[ -\frac{\hbar^2}{2m} \nabla^2 + V_{ext}(\mathbf{r}) \right] \hat{\psi}(\mathbf{r}) \\ &+ \frac{1}{2} \int d\mathbf{r} d\mathbf{r}' \hat{\psi}^\dagger(\mathbf{r}) \hat{\psi}^\dagger(\mathbf{r}') V(\mathbf{r} - \mathbf{r}') \hat{\psi}(\mathbf{r}') \hat{\psi}(\mathbf{r}), \end{aligned} \quad (2.11)$$

where the field operators obey

$$\begin{aligned} [\hat{\psi}(\mathbf{r}), \hat{\psi}^\dagger(\mathbf{r}')] &= \delta(\mathbf{r} - \mathbf{r}'), \\ [\hat{\psi}(\mathbf{r}), \hat{\psi}(\mathbf{r}')] &= 0, \\ [\hat{\psi}^\dagger(\mathbf{r}), \hat{\psi}^\dagger(\mathbf{r}')] &= 0. \end{aligned} \quad (2.12)$$

In simplification, we consider a homogeneous gas and ignore the external potential. Then the field operator can be expanded in basis of the plane wave, namely,

$$\begin{aligned} \hat{\psi}(\mathbf{r}) &= \frac{1}{\sqrt{V}} \sum_{\mathbf{k}} e^{i\mathbf{k} \cdot \mathbf{r}} a_{\mathbf{k}}, \\ \hat{\psi}^\dagger(\mathbf{r}) &= \frac{1}{\sqrt{V}} \sum_{\mathbf{k}} e^{-i\mathbf{k} \cdot \mathbf{r}} a_{\mathbf{k}}^\dagger. \end{aligned} \quad (2.13)$$

So we have the kinetic energy term in Eq. 2.11 as

$$\begin{aligned}
\hat{T} &= \int d\mathbf{r} \hat{\psi}^\dagger(\mathbf{r}) \left[ -\frac{\hbar^2}{2m} \nabla^2 \right] \hat{\psi}(\mathbf{r}) \\
&= \frac{1}{V} \sum_{\mathbf{k}\mathbf{k}'} \int d\mathbf{r} (a_{\mathbf{k}'}^\dagger e^{-i\mathbf{k}'\cdot\mathbf{r}} \frac{\hbar^2 k^2}{2m} a_{\mathbf{k}} e^{i\mathbf{k}\cdot\mathbf{r}}) \\
&= \sum_{\mathbf{k}} a_{\mathbf{k}}^\dagger a_{\mathbf{k}} \frac{\hbar^2 k^2}{2m}.
\end{aligned} \tag{2.14}$$

The potential energy term is

$$\begin{aligned}
\hat{V} &= \frac{1}{2V^2} \sum_{\mathbf{k}_1\mathbf{k}_2\mathbf{k}_3\mathbf{k}_4} \int d\mathbf{r} d\mathbf{r}' V(\mathbf{r}-\mathbf{r}') a_{\mathbf{k}_1}^\dagger a_{\mathbf{k}_2}^\dagger a_{\mathbf{k}_3} a_{\mathbf{k}_4} \times e^{i(-\mathbf{k}_1\cdot\mathbf{r}-\mathbf{k}_2\cdot\mathbf{r}'+\mathbf{k}_3\cdot\mathbf{r}'+\mathbf{k}_4\cdot\mathbf{r})} \\
&= \frac{1}{2V^2} \sum_{\mathbf{k}_1\mathbf{k}_2\mathbf{k}_3\mathbf{k}_4} a_{\mathbf{k}_1}^\dagger a_{\mathbf{k}_2}^\dagger a_{\mathbf{k}_3} a_{\mathbf{k}_4} \delta_{\mathbf{k}_1+\mathbf{k}_2,\mathbf{k}_3+\mathbf{k}_4} \int d\mathbf{r} V(\mathbf{r}) e^{i(-\mathbf{k}_1+\mathbf{k}_4)\cdot\mathbf{r}}.
\end{aligned} \tag{2.15}$$

If we set  $-\mathbf{k}_1 + \mathbf{k}_4 = \mathbf{q}$ ,  $\mathbf{k}_1 = \mathbf{k}$  and  $\mathbf{k}_3 = \mathbf{k}'$ , the Hamiltonian can be rewritten as

$$\hat{H} = \sum_{\mathbf{k}} a_{\mathbf{k}}^\dagger a_{\mathbf{k}} \frac{\hbar^2 k^2}{2m} + \frac{1}{2} \sum_{\mathbf{k}\mathbf{k}'\mathbf{q}} V_{\mathbf{q}} a_{\mathbf{k}}^\dagger a_{\mathbf{k}'+\mathbf{q}}^\dagger a_{\mathbf{k}'} a_{\mathbf{k}+\mathbf{q}}. \tag{2.16}$$

The coherent property of the condensate atoms can be viewed through the *correlation function* between any two particles[16, 17]. In other words we are going to consider the *one-body density matrix* of the system,

$$\rho(\mathbf{r}-\mathbf{r}') = \langle \hat{\psi}^\dagger(\mathbf{r}) \hat{\psi}(\mathbf{r}') \rangle. \tag{2.17}$$

Use the Fourier transformations of Eq. 2.13 we have

$$\rho(\mathbf{r}-\mathbf{r}') = \frac{1}{V} \sum_{\mathbf{k}\mathbf{k}'} e^{i(\mathbf{k}'\cdot\mathbf{r}'-\mathbf{k}\cdot\mathbf{r})} \langle a_{\mathbf{k}}^\dagger a_{\mathbf{k}'} \rangle. \tag{2.18}$$

For a translational invariant system the total momentum operator  $\mathbf{P}$  commutes with the Hamiltonian such that by using  $Tr(AB) = Tr(BA)$  we have

$$\begin{aligned}
\langle [\mathbf{P}, a_{\mathbf{k}}^\dagger a_{\mathbf{k}'}] \rangle &= \hbar(\mathbf{k}-\mathbf{k}') \langle a_{\mathbf{k}}^\dagger a_{\mathbf{k}'} \rangle \\
&= 0,
\end{aligned} \tag{2.19}$$

therefore Eq. 2.18 becomes diagonal in  $\mathbf{k}$ :

$$\rho(\mathbf{r}-\mathbf{r}') = \frac{1}{V} \sum_{\mathbf{k}} e^{i\mathbf{k}\cdot(\mathbf{r}'-\mathbf{r})} \langle a_{\mathbf{k}}^\dagger a_{\mathbf{k}} \rangle. \tag{2.20}$$

If the ensemble average is taken over the coherent state the above equation is just the Fourier transformation of the occupation of  $|\alpha_{\mathbf{k}}\rangle$  state. Namely, according to Eq. 2.10 we have

$$\langle a_{\mathbf{k}}^\dagger a_{\mathbf{k}} \rangle = \langle \hat{n}_{\mathbf{k}} \rangle = |\alpha_{\mathbf{k}}|^2, \tag{2.21}$$

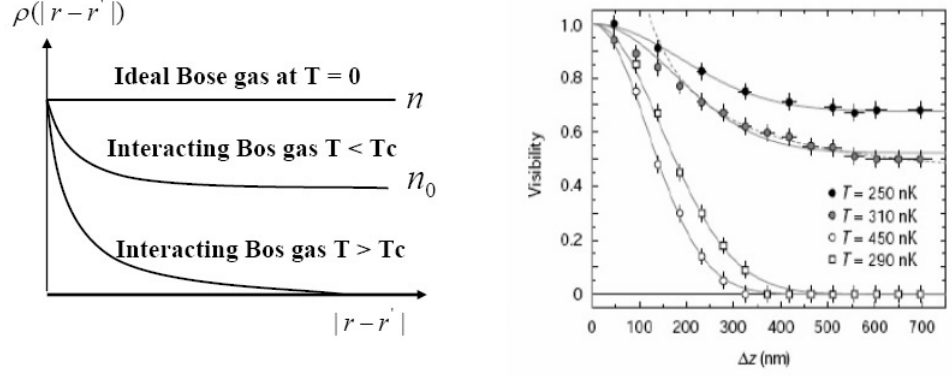


Figure 2.2: One particle density matrix  $\rho(\mathbf{r} - \mathbf{r}')$ . For the ideal Bose gas at  $T = 0$  it is the total density  $n$ . For the interacting Bose gas at  $T < T_c$ ,  $\rho(\mathbf{r} - \mathbf{r}')$  approaches an appreciable large value  $n_0$  for atoms separating at long distances. However if  $T \geq T_c$ , the condensate density  $n_0$  is zero; there is no long range correlation between atoms. The experimental data of spatial correlation is measured by Bloch *et al.*, published on Nature **403**, 166(2000). While  $T_c$  is  $430 \text{ nK}$  the dark mark data are correlations of condensed atoms and the hollow mark data are correlations of thermal atoms. Obviously, spatial correlation of a condensate is much larger than the thermal atoms and is almost equal to the size of the condensate.

then

$$\begin{aligned}
 n \equiv \rho(\mathbf{r} - \mathbf{r}') &= \frac{1}{V} \sum_{\mathbf{k}} e^{i\mathbf{k} \cdot (\mathbf{r}' - \mathbf{r})} |\alpha_{\mathbf{k}}|^2 \\
 &\simeq n_0 + \frac{2}{(2\pi)^3} \int d\mathbf{k} e^{i\mathbf{k} \cdot (\mathbf{r}' - \mathbf{r})} f(\mathbf{k}). \quad (2.22)
 \end{aligned}$$

The expression in Eq. 2.22 means that we have a macroscopic occupied state with  $\mathbf{k} = \mathbf{k}_0$  giving the density of  $n_0$  and all other states  $|\alpha_{\mathbf{k}_i}|$  are small and would vanish as  $|\mathbf{r} - \mathbf{r}'| \rightarrow \infty$ . Therefore

$$\langle \hat{\psi}^\dagger(\mathbf{r}) \hat{\psi}(\mathbf{r}') \rangle \rightarrow n_0 \quad (2.23)$$

as  $|\mathbf{r} - \mathbf{r}'| \rightarrow \infty$ . As shown in Fig. 2.2 for  $T \geq T_c$ , there is no long range coherence for thermal atoms. But for  $T < T_c$  atoms in the condensate located at  $\mathbf{r}$  and  $\mathbf{r}'$  are correlated even when they are separated apart. In random phase approximation, we can write the correlation function as the product of

two individual ensemble averaged mean field, namely, by writing

$$\langle \hat{\psi}^\dagger(\mathbf{r})\hat{\psi}(\mathbf{r}') \rangle \rightarrow \langle \hat{\psi}^\dagger(\mathbf{r}) \rangle \langle \hat{\psi}(\mathbf{r}') \rangle . \quad (2.24)$$

So, by choosing a basis of coherent states, we will obtain a nonzero expectation of the field operator  $\psi(\mathbf{r}) = \langle \hat{\psi}^\dagger(\mathbf{r}) \rangle$ , which just can be written in the form of  $\sqrt{n_0}e^{i\theta}$ . Therefore cold atoms are coherent and can be described via a long range order parameter.

## 2.2 Evidence of Coherence - Manifestation by Interference Patterns

In order to demonstrate the coherent property we have to probe the condensate to get the phase information. However, the phase of the condensate is the argument of the complex wave function and is not an observable. Only the relative phase of condensates can be measured. Through famous experiments in MPQ[18] and MIT[1] the observation of interference patterns manifest the evidence of the spatial coherence for condensates. Analogous to Young's double slit experiment, Bloch *et al.* in MPQ created a double slit for BEC by using a radio wave with two different frequencies. The measured interference patterns show spatial correlation between two condensates for  $T < T_c$  even when the separation of two slits is in order of the size of the condensate. The experiment then give the evidence of so called spontaneous broken symmetry and validity in description of the condensate by a giant order parameter.

The spatial coherence between two condensates is verified by Andrews *et al.*. Fig. 2.3 shows clear interference fringes for different laser powers. When cold atoms are transformed into a double well above  $T_c$ , two condensates are formed after evaporation cooling. Depends on the laser power, two condensates can be divided into weakly linking or isolated clouds. For the former, the interference patterns directly imply dc Josephson effect for atoms. By setting condensates with wave functions of  $\psi_1 e^{i\phi_1}$  and  $\psi_2 e^{i\phi_2}$ , the overlap of two clouds can be calculated from the density correlation by setting wave packets located at  $x = \pm d/2$ :

$$\hat{\psi}(x) = \hat{\psi}(-d/2)e^{ikx} + \hat{\psi}(d/2)e^{ik'x}. \quad (2.25)$$

The average spatial density is then

$$\begin{aligned} \langle \hat{\psi}^\dagger(x)\hat{\psi}(x) \rangle &= \langle \hat{\psi}^\dagger(-d/2)\hat{\psi}(-d/2) \rangle + \langle \hat{\psi}^\dagger(d/2)\hat{\psi}(d/2) \rangle \\ &+ \langle \hat{\psi}^\dagger(-d/2)\hat{\psi}(d/2) \rangle + e^{i(k-k')x} + c.c. \end{aligned} \quad (2.26)$$

The coherence function  $\langle \hat{\psi}^\dagger(-d/2)\hat{\psi}(d/2) \rangle$  gives the interference fringes. Contradictory to an naive image, two independent condensates also show interference patterns. The interference fringes show strong correlations between two condensates whether they are initially prepared within relative coherence or not. But rather than the robust phase obtained from two condensates in initial coherent state, the phase measured from two independent condensates changes

in each repetition of experiments. Therefore, in average, we have an *incoherent* pattern. In order to explain the observation, we have to compute a second-order correlation function.

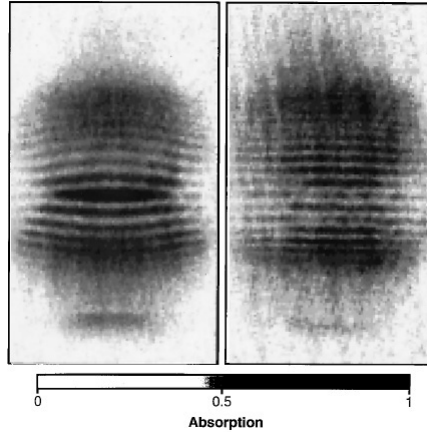


Figure 2.3: Interference patterns of two expanding condensates for different laser powers. In the weakly linked condition, the experiment demonstrates dc Josephson effect, and the induced Josephson frequency can be derived from overlapping of two Gaussian wave packets. And the fringe period is just the de Broglie wavelength associated with a free particle travelling between to central peaks within time  $t$ . *From Science* **275**, 637(1997).

Soon after MIT's work, Anderson and Kasevich realized macroscopic interference from atomic tunnel arrays. As shown in the top of Fig. 2.4, tunneling was induced by acceleration due to gravity. If the wells are populated with identical relative phase, the continuous emission of atomic waves interfere constructive to form a pulse that was shown in the lower part of the figure. The pulse frequency  $\omega = mg\lambda/2\hbar$  can be determined by the gravitational energy difference between adjacent wells. Nearly constant time interval of successive pulses in the experiment directly shows the evidence of a definite relative phase of each pulse. The effect is closely to ac Josephson effect in superconductors. While Josephson effect play an important role to determine the flux  $\Phi = 2e/h$ . It is the gravitation constant  $g$  in Anderson's experiment to be determined. And this can be achieved by carefully measurement of pulse timing.

So through many interference experiments we learn that:

1. The intrinsic coherent property of the condensate stimulates lots of interesting researches on its phase. In order to extract the phase information, interference experiments must be performed. All of them show a large coherence length of the condensate. But the relative coherence can not be determined from one-to-shot experiment. Repetition of experiments

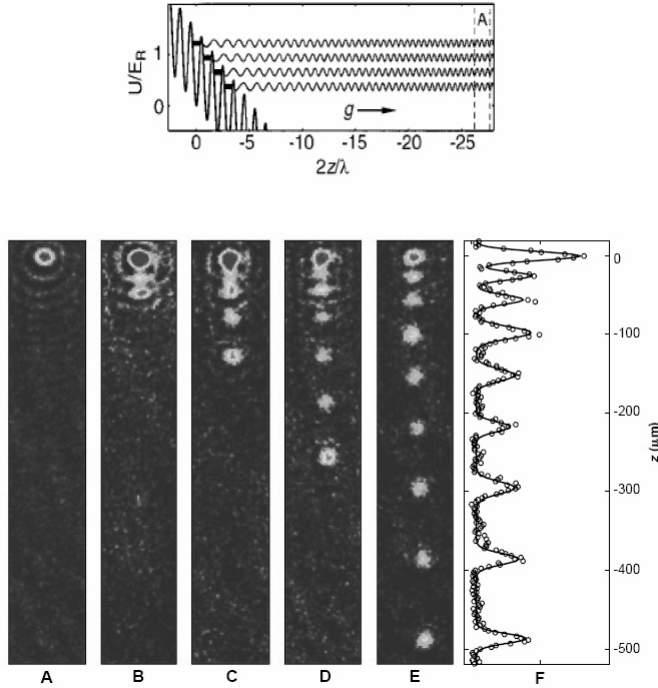


Figure 2.4: *Up*: The effective optical-pulse-gravitational potential  $U/E_R$ , where  $E_R$  is photon recoil energy. The oscillation curves indicate the de Broglie waves tunneling out from each wells. In region A, pulses interfere constructively to form pulses. *Down*: (A) Absorption images of a BEC in the TOP trap. From (B) to (E): absorption images after fixed holding times in the optical lattice showing the time development of pulse trains. (F) The integrated absorption profile for (E), obtained from summing over horizontal cross sections. The solid curve shows a nonlinear least square fits to a series of Gaussian pulses constrained to be separated by a fixed time interval. *From Science* **282**, 1686(1998).

will tell the truth. In order to analyze the interference effects, we have to compute high-order correlation functions.

2. While the Josephson effect in superconductors is molded as the paradigm of phase coherence manifestation in a macroscopic quantum system, it is important that in neutral atomic system the spatial coherent property can be observed through interference experiments of condensates.
3. Practically, it's meaningful to design these experiments. The application of the emission of coherent matter waves is realized in atomic lasers. Both the successful of BEC on a microelectronic chip[19] indicate that manipulation of atomic waves with such an atom-optical integrated system can be applied to such as interferometry, holography, microscopy, atomic lithography, quantum information processing, and so on.

## 2.3 The Read-Out Phase Measurement by Simulation of Interference of Two Condensates

With inspiration from MIT's experiment, We present in this section a way to produce an additional phase to the matter wave by adding a loop change of an additional optical dipole potential to the double-well trap. The *value* of phase difference of a double-well BEC can be found through the interference pattern. Different from MIT's experiment, the relative phase in our work is *robust* defined by adiabatically producing two identical condensates. Experimentally, the comparison of free expansion density patterns *with* and *without* the optical potential will provide the information for the phase of matter wave. This is one of the realistic cases that the quantum mechanical phase can be studied in a quantum system.

### 2.3.1 The Model

First, consider  $N$  cold atoms in a magnetic harmonic trap. The Bose-Einstein condensate (BEC) can be described by the mean-field Gross-Pitaevskii equation (GPE):

$$\left( -\frac{\hbar^2}{2m} \nabla^2 + \frac{1}{2}m(\omega_{\perp}^2 x^2 + \omega_{\perp}^2 y^2 + \omega^2 z^2) + \frac{4\pi\hbar^2 N a_s}{m} |\Psi|^2 \right) \Psi(x, y, z) = \mu \Psi(x, y, z), \quad (2.27)$$

where  $a_s$  is the s-wave scattering length. For the cigar-shaped trap,  $\omega_{\perp} \gg \omega$ . The transverse motion can be approximated as frozen in the ground state of the 2-dimensional simple harmonic oscillator. Define the transverse length scale  $L_{\perp} = \sqrt{\hbar/m\omega_{\perp}}$ , and integrate out the transverse part, the system is approximated by a one-dimensional nonlinear equation. Further use the energy unit  $\hbar\omega$ , length unit  $L = \sqrt{\hbar/M\omega}$ , and time unit  $\tau = 2\pi/\omega$ , and denote  $g = 8N(a_s/L)(L/L_{\perp})^2$ , the GPE becomes :

$$\left( -\frac{1}{2} \frac{d^2}{dz^2} + \frac{1}{2} z^2 + g |\Psi(z)|^2 \right) \Psi(z) = \mu \Psi(z). \quad (2.28)$$

Now  $\mu$  is the chemical potential in unit of  $\hbar\omega$  and is related to the number of atoms in the condensate. The normalization is

$$N \int_{-\infty}^{\infty} |\Psi(z)|^2 dz = \int_{-\infty}^{\infty} \rho(z) dz = N. \quad (2.29)$$

In the following numerical calculations, we use  $10^4$  sodium atoms in the trap of  $\omega_{\perp} = 2\pi \times 250 \text{ Hz}$ ,  $\omega = 2\pi \times 20 \text{ Hz}$ , and  $a_s = 3 \text{ nm}$ . To solve the ground state of the nonlinear equation, we employ the Fourier-Grid-Hamiltonian method[20] iteratively until accuracy criterion is satisfied. The coordinates range from -12 to 12 is set to evenly spaced 401 grid points. The calculated chemical potential



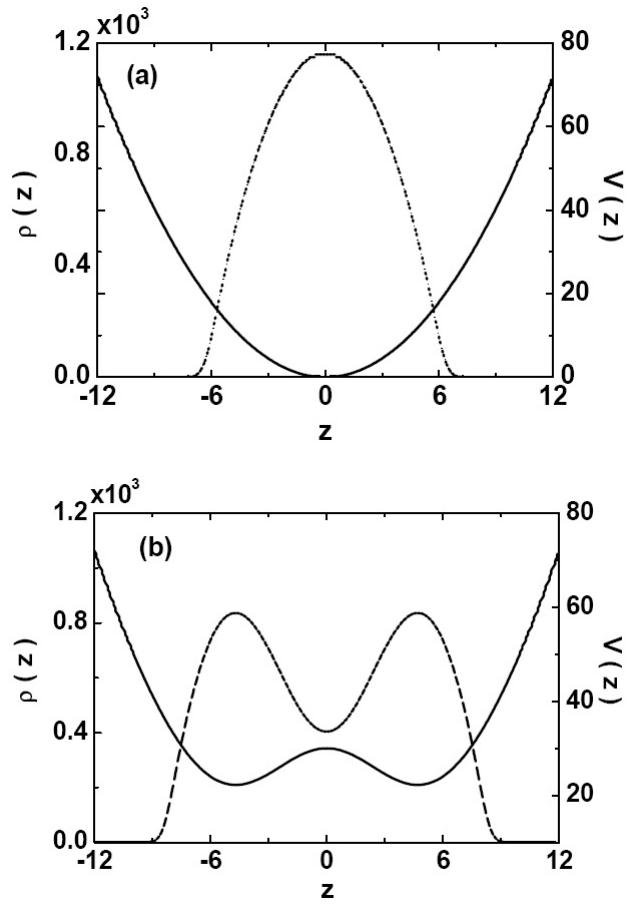


Figure 2.5: Potential  $V(z)$  (solid line) and density profile  $\rho(z)$  (dotted line) of  $10^4$  sodium atoms in a cigar-shaped harmonic trap of frequency  $\omega = 2\pi \times 20\text{Hz}$ . (a) The condensate; (b) the condensate with a central barrier in the form of Eq. 2.30 at maxima barrier height of 30.

is  $\mu = 20.78$  for the condensate with described parameters. The density decays to  $10^{-6}$  at distance 8.6 from the trap center as shown in Fig. 2.5a.

According to the experimental setup[1] the double well trap can be created by focusing blue-detuned far-off-resonant laser light into the magnetic trap, generating a repulsive optical dipole potential on the long axis of the condensate. We thus simulate the potential within the Gaussian profile:

$$V(z) = V_0 \exp\left[-\frac{z^2}{2\sigma^2}\right]. \quad (2.30)$$

Moreover, we simulate a time dependent process to create the potential. In dimensionless calculations we replace  $V(z)$  with

$$V(t) = V_g \times t/T_e \exp\left[-\frac{z^2}{2\sigma^2}\right], \quad (2.31)$$

where  $T_e$  is characteristic time of the external field and  $V_g$  is the strength parameter tunable by the laser field. In this work, the external field strength is designed to increase linearly in time. The barrier height  $V(t)$  ranges from 0 to 30 and is turned-on and -off linearly with time. The height is much smaller than trap barrier but large enough to affect the condensate behavior. In Fig. 2.5b, we plot the condensate density profile for the double-well at  $V(t) = 30$ . At the maximum height of perturbing potential, the density at central barrier position is about one half of the peak density so that the two separated condensates are correlated with each other.

## 2.3.2 Generation of an Additional Phase

### A. The Adiabatic and Nonadiabatic Processes[21]

Consider a system, for example, a perfect pendulum oscillating back and forth in a vertical plane. Its period  $T_z$  would be the characteristic time of the system. Now we have some actions on the holder. If we shake the holder with heavy force, the motion of the pendulum may have possible to react chaotically. However, if we shake it tenderly, the pendulum will continuous swing smoothly with the same amplitude. So we can define the characteristic time of the external force  $T_e$ , over which some correspondent quantities of the system change appreciably. We say when  $T_z \ll T_e$  it satisfies the adiabatic condition, and when  $T_z \gg T_e$ , the system undergoes a fast modulation by the field. If  $T_z$  is comparable with  $T_e$ , we call it the nonadiabatic process.

We take another example from view points of quantum mechanics as shown in Fig. 2.6. The ground state wave function of a particle in the box of dimension  $a$  is plotted at the top of the figure. When we pull the wall of the box smoothly, the eigenstates will follow the step of the moving. It will become the ground state of the new box of dimension  $2a$ . However, if we pull the box too fast to be detected by the particle, it will keep its own look but turn out to be the excited state in the new box.

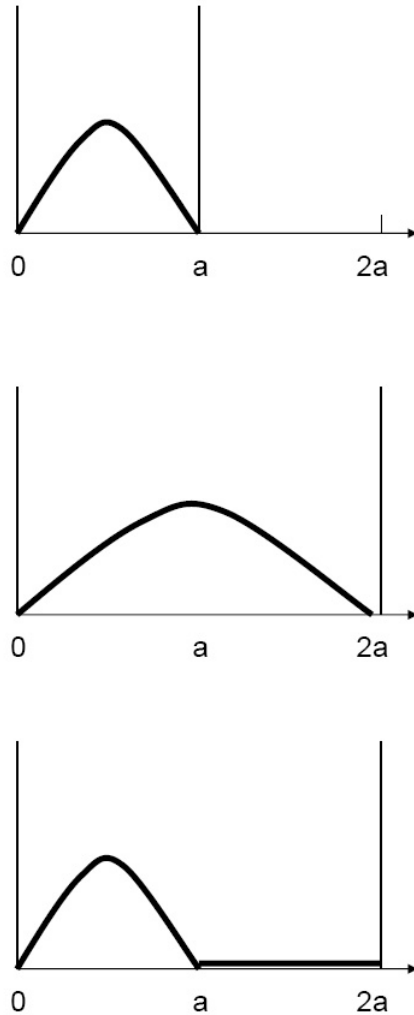


Figure 2.6: *Top:* The ground state wave function of a particle in a box of dimension  $a$ . *Middle:* If we adiabatically pull the wall of the box the particle will follow the expansion step and the wave function will stay in the ground state of the new system. *Bottom:* If the wall is pulled too fast to be detected by the particle, the original wave function would be kept but becomes the excited state wave function in the new box.

Now, we will describe the adiabatic process more precisely. Consider a general eigenvalue equation

$$H\psi_n(x) = E_n\psi_n(x), \quad (2.32)$$

the time evolution of the stationary state follows

$$\Psi_n(x, t) = \psi_n(x)e^{-iE_nt/\hbar}. \quad (2.33)$$

If the Hamiltonian changes gradually in the presence of an external field, the Schrödinger equation can be written as

$$H(t)\psi_n(x, t) = E_n(t)\psi_n(x, t), \quad (2.34)$$

and

$$\Psi_n(x, t) = \psi_n(x, t)e^{-i/\hbar \int_0^t E_n(t')dt'} e^{i\gamma_n(t)}. \quad (2.35)$$

in addition to the *dynamical phase*

$$\theta_n(t) = -1/\hbar \int_0^t E_n(t')dt', \quad (2.36)$$

there would be an extra geometrical phase  $\gamma_n(t)$ . Since Eq. 2.35 satisfies  $i\hbar\partial\Psi/\partial t = H\Psi$ , we have

$$\begin{aligned} i\hbar\left[\frac{\partial\psi_n}{\partial t}e^{i\theta}e^{i\gamma_n} - \frac{i}{\hbar}E_n(t)\psi_n e^{i\theta}e^{i\gamma_n} + i\frac{d\gamma_n}{dt}\psi_n e^{i\theta}e^{i\gamma_n}\right] \\ = E_n\psi_n e^{i\theta}e^{i\gamma_n}. \end{aligned} \quad (2.37)$$

Eq. 2.37 implies that

$$\frac{\partial\psi_n}{\partial t} + i\frac{d\gamma_n}{dt}\psi_n = 0, \quad (2.38)$$

and therefore

$$\gamma_n(t) = \int_0^t i \langle \psi_n | \frac{\partial\psi_n}{\partial t'} \rangle dt'. \quad (2.39)$$

From the general treatment in quantum mechanics, we know the eigen wave function would accumulate time dependent dynamical and geometrical phases through the adiabatic dynamical processes. While on the other hand, the non-adiabatical evolution would generate both time dependent and spatial dependent phase.

## B. Global Phase and Local Phase

We apply the above concept to our BEC system. While  $T_z = 2\pi/\omega = 50 \text{ ms}$ , we set  $T_e = 39.5 \text{ s}$ ,  $50 \text{ ms}$  and  $0.5 \text{ ms}$  for adiabatic, nonadiabatic and fast processes, over which the barrier constructed by laser sheet grows appreciably. Next, we will justify that the adiabatic condition can be reached by the way of turning on the optical potential slowly enough. *To speed up the calculations* we raise the intensity of  $V_g$  such that the barrier will spend time less than  $T_e$  to reach the

peak value. At the same time,  $V_g$  is tuned such that the growth of the barrier in each time step is slow enough to guarantee the adiabatic process. We turn on and off the optical dipole barrier within a time interval of 60 s at time step 50  $\mu$ s. The turned-on and -off time interval for the fast process is reduced to 0.5 ms and at time step 5  $\mu$ s. For a given initial BEC in a cigar-shaped trap, the condensate is subject to evolve under the trap and the added optical potential at the designed switching ways.

The initial value problem of time-dependent Gross-Pitaevskii equation

$$i \frac{\partial \Psi(z, t)}{\partial t} = \int dz' \langle z | \frac{\hat{p}^2}{2} | z' \rangle \Psi(z', t) + \left\{ \frac{z^2}{2} + V_b(z, t) + g|\Psi|^2 \right\} \Psi(z, t) \quad (2.40)$$

is again discretized by the Fourier-Grid-Hamiltonian method and then integrated by error controlled routine[22]. In Fig. 2.7 we plot the density profiles of the adiabatic process at the initial time, the moment of maximum barrier height and the final time. The density profile at the moment of maximum barrier height is identical to that of Fig. 2.5b. At the other time, we double checked and found that the density calculated by solving the stationary Gross-Pitaevskii equation with additional optical potential, and calculated by the corresponding time-evolving Eq. 2.40 are identical with each other. It shows the system changes adiabatically and always stays at the new ground state from time to time. On the other hand, if the external field changes too fast to be detected by the atoms, the condensate would be left in its initial state and therefore the density profile of the fast process is always identical with the initial one. The results imply that the modelled adiabatic and fast conditions are satisfactory respectively.

During the time-dependent process, if the adiabatic condition is satisfied, or the process is fast, the accumulated phase will be global after a cycle of parameter change. Otherwise, it will produce a position dependent phase function (that is, a local phase). In Fig. 2.8, we plot the phase with respect to the initial state for the adiabatic, and the nonadiabatic processes at the moment of optical barrier vanishes. The switching ways of the adiabatic and fast cases are described above. For the nonadiabatic case, the turned-on and -off time interval is changed to 50 ms. Thus, the pulse duration ratio of adiabatic, nonadiabatic and the fast case is  $1.2 \times 10^5 : 100 : 1$ . We see that well-defined global phases are shown for the adiabatic cases, while the phase function for the nonadiabatic case is local. Furthermore, in the adiabatic process, the additional global phase to the matter wave is equal to the difference of the total phase and the dynamic phase  $\int \mu(t) dt$  over the loop. Also shown in Fig. 2.8 is the additional phase for the adiabatic process with perturbing potential with the form of Eq. 2.31.

### 2.3.3 The Method to Produce a Relative Phase Between Condensates

In the above calculation, we have settled down numerically the condition of the adiabatic process and obtained the global phase. However, the so obtained

phase is unmeasurable. We propose in the following a mechanism to produce a measurable phase for verification.

First we start with a double-well condensate which is built by adding a stationary optical barrier to the central region of a cigar-shaped trap as described above. Here we model the central barrier as

$$V_b = V_0 e^{-\frac{1}{2}\left(\frac{z}{\sigma}\right)^2}, \quad (2.41)$$

with  $V_0 = 50, \sigma = 18$ . The higher barrier is to reduce the effect of the upcoming perturbation in the left well on the right-hand side condensate, so that an additional phase will appear in the left well condensate only when we add a perturbing optical potential to the left well. The exact values of related parameters are not critical actually. In the next step, we add a time-dependent smaller Gaussian potential barrier only to the left well. The form is just like  $V_b$  above but with potential maximum equal to 4,  $\sigma = 0.5$ , and duration 8.04 s. After the adiabatic evolution of the system, the calculated additional phase is 0.763 rad. as shown in Fig. 2.9. Since the central barrier is much higher than the barrier added to the left well, the additional phase will appear only in the order parameter of the left side condensate of the double well.

Next, to measure this additional phase, we remove all the trap potential and barrier potential after the disturbance to the left well. The condensates start to expand freely. Before the time of overlap, two individual condensates are shown in Fig. 2.10. When the two condensates overlap with each other, the interference pattern of matter waves shows up. It was discussed that the interference fringe period is the de Broglie wavelength and is proportional to the temporal distance from the moment of potential relaxation[8]. This is a common phenomenon for waves and was reported for double-well condensates[1]. Specially in the case that there is a further difference of the additional phase in the right and left condensates, the pattern is different from that of purely double-well BEC free expansion. In Fig. 2.10 we depict the free expansion interference patterns of pure double-well BEC and those with an additional phase. At  $t = 30.2 ms$ , two separate condensates are shown in both cases. At  $t = 65.3 ms$ , both cases show interferences pattern but they are displaced from each other due to the additional phase. At later time,  $t = 80.4 ms$ , the fringe period is larger than that of  $t = 65.3 ms$ .

Since the interference pattern of the pure double-well condensates was known[1], the measurement of similar interference of double-well condensates with an additional phase would be feasible. Comparison of the two interference patterns will provide an experimental result of the additional quantum phase.

Through the time-dependent integration of the nonlinear GPE, we investigate the adiabatic condition to obtain the global additional quantum phase for matter waves in a double-well condensate under a cycle of perturbed optical potential. We then propose a way to measure it. Next, our result of the obtained quantum phase can be estimated below. Consider the simple case of two colliding sinusoidal waves *with* and *without* a relative phase difference  $\phi$ , the two interference patterns will show displaced patterns and the phase  $\phi$  can

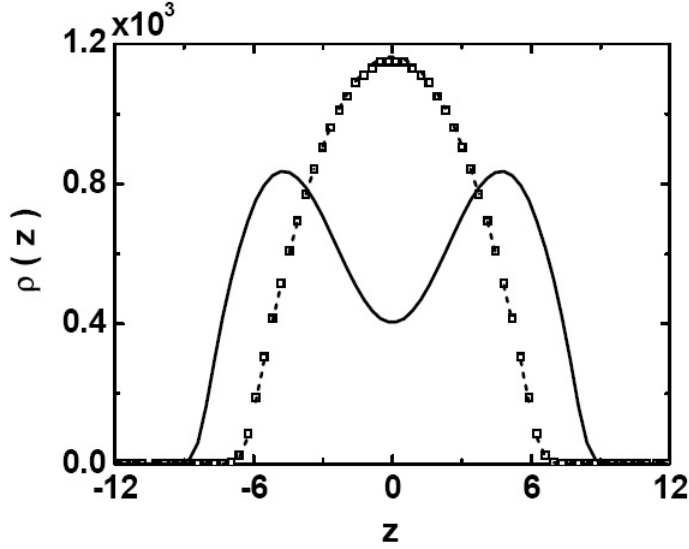


Figure 2.7: Density profiles at the initial time (dotted line), the moment of maximum barrier height (solid line), and at the final moment of the perturbing potential (squared curve).

be read out by the interference pattern. The method was used to show that the coherence of two condensates extend in the double-well trap [1]. Similarly, from the displacement of interference patterns described in Fig. 2.10, we can estimate their phase difference through  $\phi = 2\pi\Delta z/\lambda$ , where  $\Delta z$  is the displacement of corresponding interference peaks in pure double-well condensate and BEC with the additional quantum phase, and  $\lambda$  is the wavelength of interference pattern. The estimated value is about  $0.78 \text{ rad}$ . The estimation fits quite well to the calculated additional phase obtained from the numerical integration of the time-dependent GPE. Finally, the parameters we used in our modelling is not critical, with some changes to fit the experimental environments will give the same qualitative conclusion. The proposed way would provide a method to measure the phase in quantum mechanics.

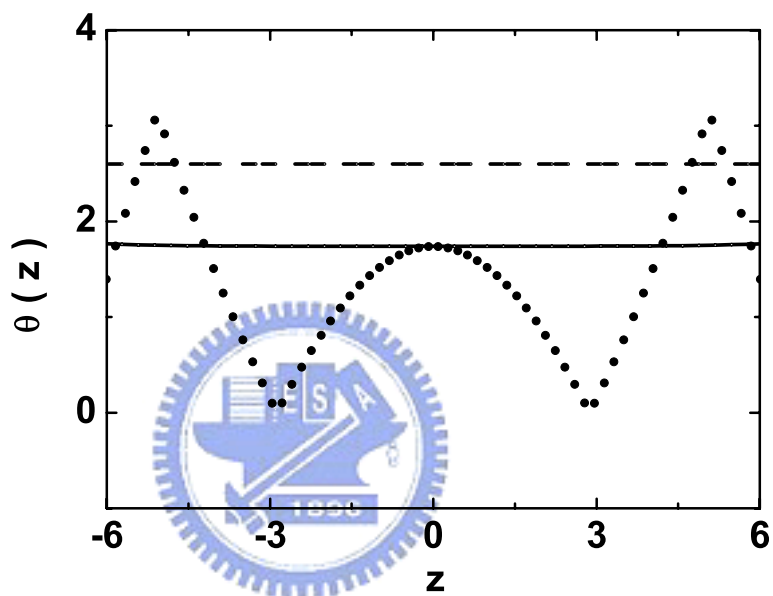


Figure 2.8: The additional phase of the condensate accumulated after a loop of perturbation for adiabatic (dashed line), nonadiabatic (dotted line) cases respectively, also shown is the additional phase (solid line) of the adiabatic process.



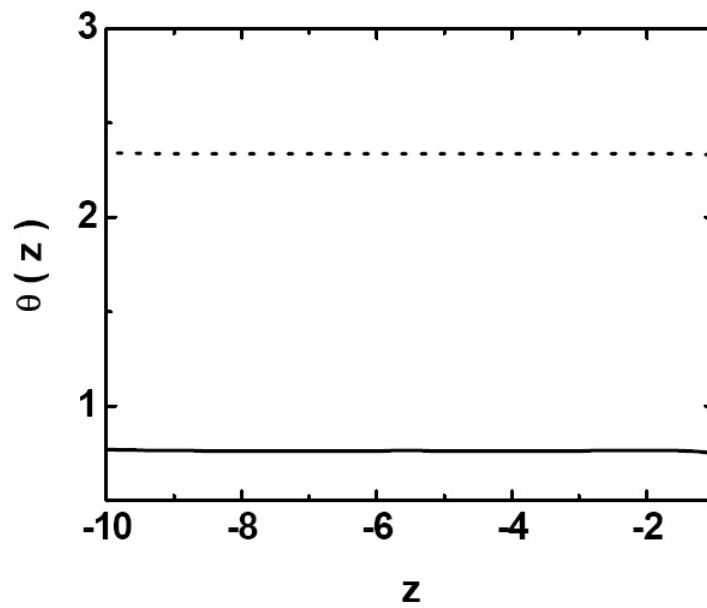


Figure 2.9: The phase functions at the end of adiabatically added perturbing potential to the left well. Since the central barrier of the double-well trap is much higher than the left-well perturbation, the additional phase (solid line) appears only in the left-well order parameter. The dashed line is the corresponding total phase

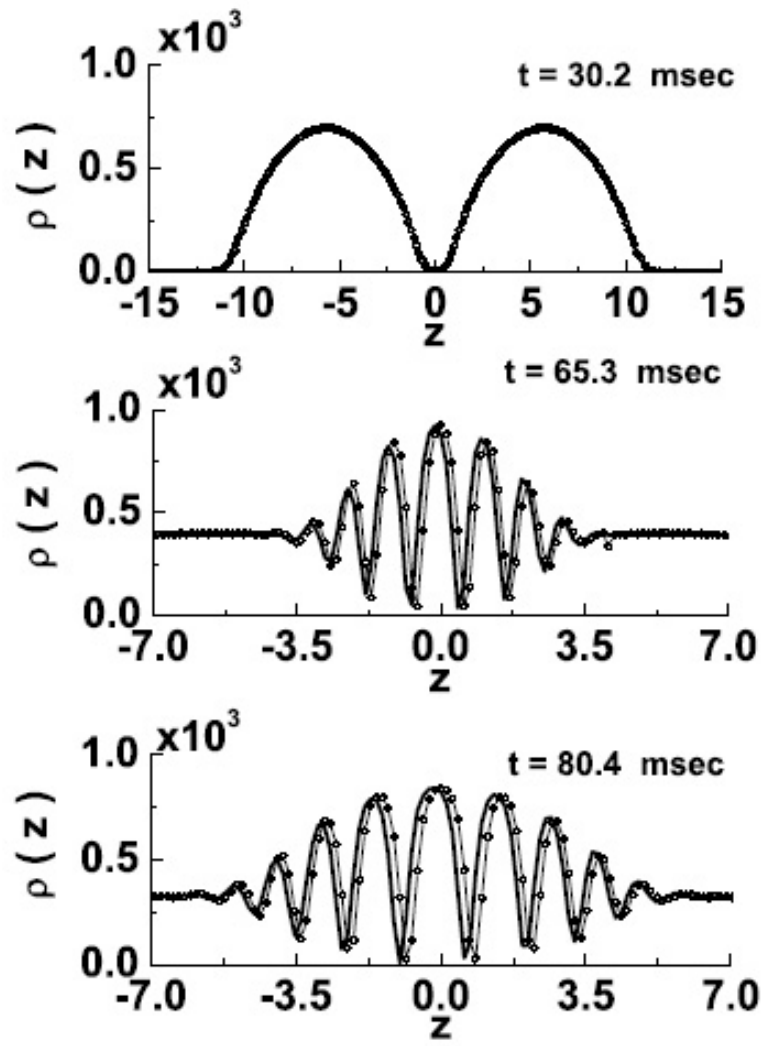


Figure 2.10: Free expansion interference patterns for the pure double-well BEC (dotted line) and the two condensates with a difference of the additional phase (solid line).

## 2.4 Summary

In this chapter we introduce the nature of the condensate, coherence, through theoretical descriptions and experimental verifications. We use many-body formulations to show the long-range order parameter of the condensate is a coherent state with a definite phase. To extract the phase information, interference experiments are performed. Through the double-slit experiment we observe the long-range spatial correlation between condensates. Moreover, if there is a definite relative phase between condensates in an optical lattice, an atomic laser can be created. By changing the lattice height, cold atoms can be manipulated through superfluid to insulator states and the system can be modelled to be a memory chip.

Inspired by MIT's experiment, we design an interesting model to measure an additional phase of the condensate imprinted by the adiabatically switched-on loop field. Verification of adiabatic degree is examined numerically through the generation of the global phase in the time-dependent process. After that, we compare interference patterns with and without adding the external field. The value of the read-out phase matches quite well with calculations of two sinusoidal waves. Basically, we design an available experiment to be easily carried out. Up to now, we don't include the noise effect in the experiment which, in fact, varies in every repetitions and would destroy the robustness of the measurements. Actually, the set-up should be modified such that we can measure two sets of data in one shot[23]. By imposing a standing wave upon a double-well, experimentalists can create a four-pieces condensate with same atom numbers. Again, we add a small loop field in one of the well. Then the measurement of interference patterns between two groups will give us the precise accumulated phase. It's interesting that the set-up can be designed to be a photon capacitance which plays an important role in creation of a super computer.



# Bibliography

- [1] M. R. Andrews, C. G. Townsend, H.-J. Miesner, D. S. Durfee, D. M. Kurn, and W. Ketterle, *Science* **275**, 637(1997).
- [2] E. A. Burt, R. W. Ghrist, C. J. Myatt, M. J. Holland, E. A. Cornell, and C. E. Wieman, *Phys. Rev. Lett.* **79**, 337(1997).
- [3] E. W. Hagley, L. Deng, M. Trippenbach, Y. B. Bandet *al.*, *Phys. Rev. Lett.* **83**, 3112(1999).
- [4] B. P. Anderson and M. A. Kasevich, *Science* **282**, 1686(1998).
- [5] J. Javanainen and Sung Mi Yoo, *Phys. Rev. Lett.* **76**, 161(1996).
- [6] A. Röhrl, M. Naraschewski, A. Schenzle, and H. Wallis, *Phys. Rev. Lett.* **78**, 4143(1997).
- [7] J. I. Cirac, C. W. Gardiner, M. Naraschewski, and P. Zoller, *Phys. Rev. A* **54**, R3714(1996).
- [8] H. Wallis, A. Röhrl, M. Naraschewski, and A. Schenzle *Phys. Rev. A* **55**, 2109(1997).
- [9] M. Naraschewski, and R. J. Blauber, *Phys. Rev. A* **59**, 4595(1999).
- [10] Y. Castin and J. Dalibard, *Phys. Rev. A* **55**, 4330 (1997).
- [11] E. V. Goldstein and P. Meystre, *Phys. Rev. Lett.* **80**, 5036(1998).
- [12] E. V. Goldstein, O. Zobay, and P. Meystre, *Phys. Rev. A* **58**, 2373(1998).
- [13] Stephen Gasiorowicz, *Quantum physics*, Wiley 1995.
- [14] R. Loudon, *The Quantum Theory of Light*, 1979.
- [15] J. F. Annett, *Superconductivity, Superfluids, and Condensates*, (Oxford 2003).
- [16] Kerson Kuang, *statistical Mechanics*, Wiley 1987.
- [17] W. Ketterle and H.-J. Miesner, *Phys. Rev. A* **56**, 3291(1997).

- [18] I. Bloch, T. W. Hänsch, and T. Esslinger, *Nature* **403**, 166(2000).
- [19] W. Hänsel, P. Hommelhoff, T. W. Hänsch, and J. Reichel, *Nature* **413**, 498(2001).
- [20] Shih-I Chu, *Chem. Phys. Lett.* **167**, 155 (1990); C.C. Marston and G.G. Balint-Kurti, *J. Chem. Phys.* **91**, 3571(1989).
- [21] David Griffith, *Introduction to quantum mechanics*, Prentice Hall 1995.
- [22] *NAG Fortran Library Mark 17*, NAG Ltd., Oxford, UK, 1995.
- [23] Thank you for suggestions of Prof. Ite Yu of Physics department in National Tsin-Hua university.



## Chapter 3

# Instabilities of a Bose-Einstein Condensate in an Optical Lattice

### 3.1 Introduction

The realization of BEC provides noiseless and coherence atomic sources to investigate some fundamental phenomena. Exchange the probing role with photons, cold atoms in an optical lattice demonstrate phenomena of solid state physics such like band structures[1], Bloch oscillations[2], Wannier-Stark ladder[3] and Josephson effect[4]. For deeper lattice wells the creation of squeezed states[5] and the superfluid-to-Mott insulator phase transition are also observed[6]. For shallow wells, studies on tunneling of BEC out of the traps in the presence of gravity[7], and the superfluid[8] phenomena have open another window in the field. By using Bragg scattering[9], a sensitive probe for atomic localization, the coherent and incoherent wave dynamics can be measured. BEC in an optical lattice offers great opportunities for quantum information processing, and a dream to realize an atomic chip.

Superfluid phenomenon is an another manifestation of phase coherence of BEC. This can be observed through experiments in shallow optical lattices as atoms move freely from one site to another by quantum tunneling. Practically, it is easily to induce instabilities to observe dissipation behaviors[8]. In this chapter we are going to simulate dynamics of the condensate in an optical lattice to investigate the mechanism of instabilities. Based on the GP equation, we can further calculate the linear response of the external perturbation. Then from collective excitation spectra we found the presence of quasiparticles would destroy the superfluid. We prove Landau's idea about the existence of the critical velocity[10]. Beyond the critical velocity, phonons can be generated and the system goes into the Landau instability regime. Moreover, the presence of an

optical lattice serves as a viscous medium to destroy the superfluid. Whenever the group velocity of the flow increases to a critical value beyond that the correspondent effective mass of the condensate becomes negative, it costs no pay to induce quasiparticles and the model of superfluid would breakdown.

In this chapter we give a brief introduction of how a condensate moves in an optical lattice. First, we have to know how to construct an optical lattice and why the condensate would stay there. This is the question about cooling and trapping. Next, we review the history about the discovery of the superfluid. Then we will ask what's the nature of the BEC for itself to perform the superfluid behavior. And finally we come into the topic of how is the superfluid destroyed in the presence of quantum fluctuations and thermal atoms.

## 3.2 How Does an Optical Lattice Work?

The idea to confine atoms in the wavelength size of a standing wave was first suggested by V. S. Letokhov in 1968[11] and was first realized in 1987 in one dimension with atomic channelling by standing waves[12]. By superposition of electric fields of a pair of counterpropagating beams, an optical lattice is constructed effectively in the form of an array of light-shifted potential wells[13], as shown in Fig. 3.1. With more laser beams an egg-crate potential of a 2D optical lattice can be constructed as shown in Fig. 3.2. And the crate provides a good arrangement for Greiner's group to carry out the superfluid to Mott-insulator phase transition in cold atoms. A good optical lattice can cool and trap atoms in low-lying quantum states with center-of-mass motion in individual wells. The mechanism is just like what atoms being in the Sisyphus cooling processes[14]. In the optical lattice atoms would experience spatial dependent *dipole force* exerted on them due to coherent redistribution of photons after the encounters with laser beams. By definition, the force proportional to the gradient of the light shift is associated with the Rabi frequency  $\Omega$  and the detuning  $\delta$ . By solving optical Bloch equations for a two-level atom[15], the dipole force in a standing wave propagating along  $z$ - axis can be approximately written as

$$F_{dip} \propto \frac{A}{\delta} \sin 2kz. \quad (3.1)$$

For  $\delta < 0$  the force drives atoms to positions with maxima intensity, whereas for  $\delta > 0$ , atoms are attracted to the intensity minima. Therefore atoms in any case can be confined in antinodes or nodes of standing waves. Better than the conventional focusing[16, 17], the confinement by standing waves would be more focused to the order of a half wavelength. Therefore we need only lasers in weaker power to achieve the trapping.



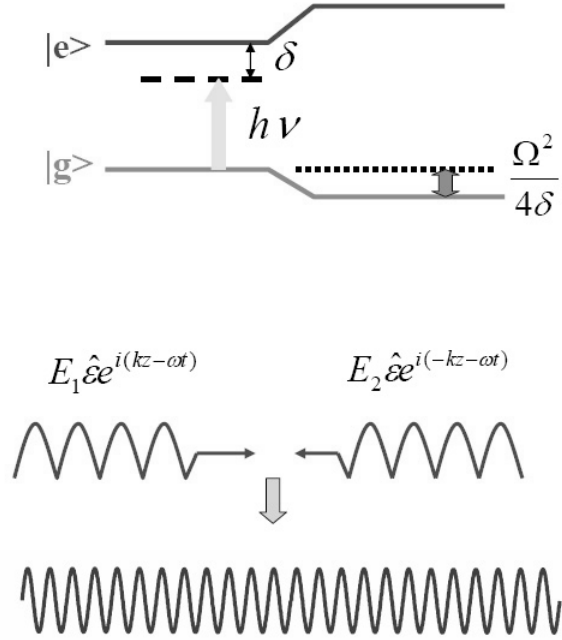


Figure 3.1: An 1D optical lattice can be constructed via superposition of two counter-propagating laser beams with same frequency and different polarization. The periodic potential seen by an atom is resulted from light shift of the ground state. Depends on the detuning of the laser atoms can be trapped at the nodes or antinodes of the standing wave.

### 3.3 Superfluidity and Dissipations of the BEC

#### 3.3.1 Historical Review of Superfluidity: From $He^4$ to BEC

Although the successful of realization of creating a BEC in dilute gases in 1995 being 70 years late after the prediction of Bose and Einstein, the progress was proceeding and motivated by the study of  $He^4$ [18, 19, 20].

Under atmospheric pressure, gases  $He^4$  forms a liquid when the temperature is reduced below to  $4.2 K$ . At this stage the liquid and the residual vapor coexist. Maintain the coexistence phase but slowly reduce the temperature, in the 1920s Keesom[21] and his co-workers obtained an exciting result on measurement of heat capacity  $C_v$  as the function of temperature  $T$ . As Fig. 3.3 shows that at  $T = 2.17 K$  there is a sharp variation and discontinuity of  $C_v$ . Below  $2.17 K$ , the liquid can flow without viscosity and becomes a *superfluid*.

In 1938, London[22] suggested that the  $\lambda$  transition in liquid  $He^4$  may be

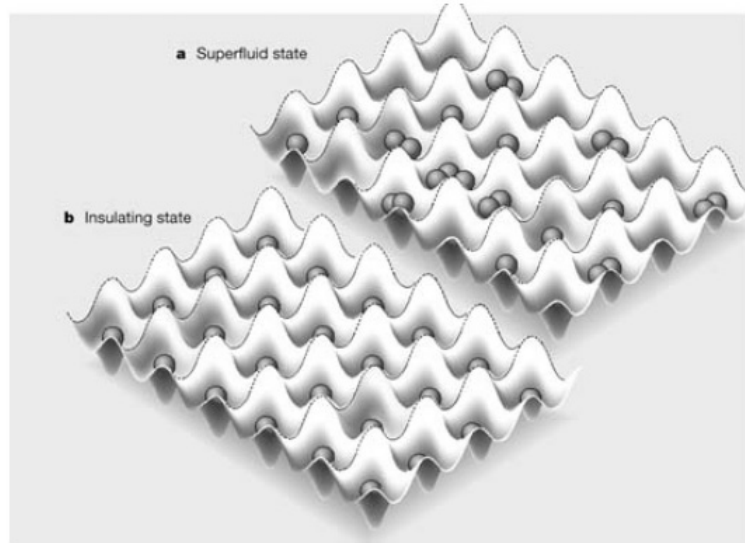


Figure 3.2: An egg-crate potential of a two dimensional optical lattice is shown. The potential wells are separated by half wave length  $\lambda/2$ . By changing the lattice height, experimentalists can control the flow of atoms from a superfluid to an insulator phase. *From Nature 415, 39(2002)*.

a manifestation of BEC. Since at  $\lambda$  point the experimental mass density of the liquid helium is

$$\frac{mN}{V} = 0.146 \times 10^3 \text{ kg/m}^3, \quad (3.2)$$

one needs to do is to compute the Bose temperature  $T_B$  of an ideal Bose gas at the same number density  $N/V$ . According to the formula that BEC occurs when

$$kT_B = \frac{1}{\pi(2.612)^{2/3}} \frac{h^2}{2m} (N/V)^{2/3}, \quad (3.3)$$

we obtain  $T_B \sim 3.15 \text{ K}$ . This result seems to fit quite good with  $T_\lambda$  and makes London's theory in a plausible success. Shortly after, Tisza used the notation of BEC in his two-fluid model[23] describing the co-existence of the thermal and the condensed phase in the fluid. He considered that "*the atoms belonging to the lowest energy state do not take part in the dissipation. Thus the viscosity comes entirely from atoms in excited states*". His model qualitatively explained the fountain effect that the superfluid component moves in the direction of the hot side where the pressure increases and predicts the existence of *the second sound*, the temperature waves, when the superfluid and normal components move out of phase. Nearly all the predictions by Tisza were proved correct in experiments.

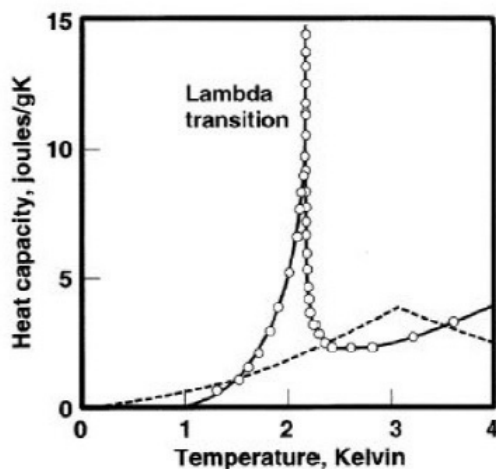


Figure 3.3: Heat capacity of  $He^4$ . At  $T = 2.17 K$  there is a sharp variation and discontinuity of  $C_v$ . Below  $2.17 K$ , the liquid can flow without viscosity and becomes a superfluid. From file of R. Roth, GSI theory group.

However in 1941, Landau[10] introduced a phenomenological point of view and stated that *the superfluid is a weakly interacting mixture of excitations* such as phonons and rotons. He rejected London's and Tisza's theories based on the argument that *in the highly interacting system like liquid helium the use of description of the ideal gas is inadequate*. He considered energy states of the liquid instead of individual atoms. After years the measurement of the excitation spectrum did show the disagreeable result with the parabolic spectrum in Tisza's theory. London's theory turns out to be correct.

While the superfluid is the collective motion of the condensed atoms Landau assumed the properties of the normal component is related to the elementary excitations of the superfluid. Fig. 3.4 shows that for small momenta the excitations in liquid helium are sound waves like *phonons*. The dispersion relation is linear and the energy can be written as

$$\epsilon = v_s p, \quad (3.4)$$

where  $v_s$  is velocity of sound. On the other hand, for larger momenta the dispersion relation shows an upward curvature and passes a point of local maximum and before it raises again there forms a point of local minimum at  $p = p_0$ . Therefore in the vicinity of  $p_0$  the dispersion relation can be approximated by

$$\epsilon(p) = \epsilon(p_0) + (p - p_0)^2/2m^*, \quad (3.5)$$

where  $m^*$  is a fitting parameter in dimension of mass. Excitations with  $p$  closed to  $p_0$  are called *rotons*. So, there are no excitations with phase velocities less

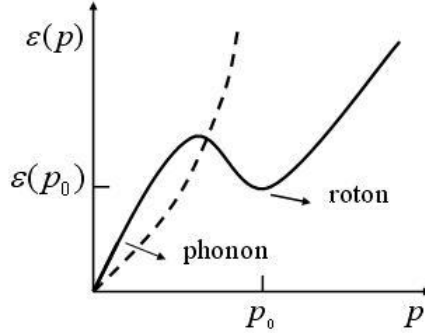


Figure 3.4: Dispersion relation of  $He^4$ . At small momenta the dispersion is linear indicating the creation of phonons. At  $p = p_0$  there is an energy minimum of roton. The parabolic dashed-line is the dispersion of the ideal Bose gas.

than a critical velocity  $v_c = \min(\epsilon/p)$ , and in the absence of rotons  $v_c$  is the sound velocity  $v_s$ . Namely, the motion of the superfluid can not slow down by exciting collective modes if  $v < v_c$ .

To understand Landau's excitation spectrum, in 1947 Bogoliubov[24] used the field theory method to present a basis in which the Hamiltonian of a weakly interacting Bose system can be diagonalized. His basis describes excitations that exhibit a phonon like, linear dispersion in low momentum regime, which is consistent with Landau's theory. From his theory the dispersion relation of a uniform gas can be written as

$$\epsilon(p) = \sqrt{2nU_0\epsilon_p^0 + (\epsilon_p^0)^2} \quad (3.6)$$

, where  $U_0$  is the short range interaction potential,  $n$  is atomic density, and  $\epsilon_p^0$  is the free particle energy. Then  $\epsilon(p) \sim v_s \hbar p$  for small  $p$ , and the spectrum is sound-like. There is non-zero velocity  $v_s$  due to the collective motion from atoms in excited states, which is

$$v_s = \sqrt{nU_0/m}. \quad (3.7)$$

This agrees with the expression of the sound velocity from the hydrodynamic result. Therefore Bogoliubov gave a theoretic support that the excitation spectrum in long wave length regime provides the key to superfluid behavior.

Despite the fact that the theory is valid only for weakly interacting systems, Bogoliubov's theory did explain qualitatively the features of superfluid  $He^4$  with strong interactions among atoms. But the experimental verification of these theories were not available until the realization of BEC.

The collective excitations in the inhomogeneous dilute gases are well studied by several groups[25, 26] soon after the successful creation of the BEC in

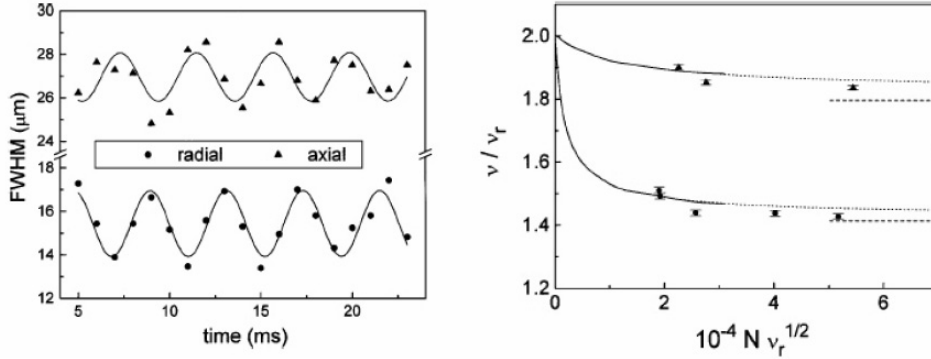


Figure 3.5: *Left*: A weak driving of  $m = 0$  collective excitations. The freely evolving response of the condensate shows the radial oscillation. The response of the axial width shows  $180^\circ$  out of phase. The excitation frequency is determined from a sine wave fit to the freely oscillation cloud's width. *Right*: Frequency of  $m = 0$ (triangles) and  $m = 2$ (circles) excitation modes as a function of interaction strength. Solid lines are mean-field calculations by Edwards group[1]. Dashed lines are predictions in Thomas-Fermi regime by Stringari[28]. From *Phys. Rev. Lett.* **77**, 420(1996) and *Phys. Rev. Lett.* **77**, 420(1996)

1995. By applying a small sinusoidal current to the coils responsible for the rotating field of the TOP trap, and by appropriately setting the phase of the current, the experimentalists can excite the condensate in different symmetries. The measurement of the absorption images of the expanded cloud's center-of-mass positions and widths in function of evolution time as shown in will return the oscillation frequency of certain modes. The peculiar nonlinear features of the system can also be detected through the excitation spectra by varying the trapping frequency or the number of atoms. Fig. 3.5 is one of the examples that shows compatible results of both the measurements and the theoretical calculations.

The studies of the development of the superfluid behavior from  $He^4$  to BEC as yet do give us evidences that the collective excitation spectrum plays an important role in understanding fundamental properties of Bose systems.

### 3.3.2 Bose-Einstein Condensation and Superfluidity

It's well known the wave function of the condensate acquires a definite phase. But what is the significance of the phase  $\theta$ ? How can it relate with the superfluid velocity? From quantum mechanics we know the velocity  $\mathbf{v}$  of the particle flow can be derived from the continuity equation of the particle density. Consider a time dependent Schrödinger equation

$$i\hbar \frac{\partial \psi(\mathbf{r}, t)}{\partial t} = -\frac{\hbar^2}{2m} \nabla^2 \psi(\mathbf{r}, t) + V(\mathbf{r}, t) \psi(\mathbf{r}, t), \quad (3.8)$$

and its conjugate equation for  $\psi^*$ . By using  $\partial|\psi|^2/\partial t = \psi^* \partial\psi/\partial t + \psi \partial\psi^*/\partial t$  we obtain

$$i\hbar \left( \psi^* \frac{\partial \psi}{\partial t} + \psi \frac{\partial \psi^*}{\partial t} \right) = -\frac{\hbar^2}{2m} (\psi^* \nabla^2 \psi - \psi \nabla^2 \psi^*). \quad (3.9)$$

The Eq. 3.9 can be rewritten as

$$\frac{\partial |\psi|^2}{\partial t} + \nabla \cdot \left[ \frac{\hbar}{2mi} (\psi^* \nabla \psi - \psi \nabla \psi^*) \right] = 0. \quad (3.10)$$

Obviously Eq. 3.10 is similar to the continuity equation

$$\frac{\partial n}{\partial t} + \nabla \cdot (n\mathbf{v}) = 0. \quad (3.11)$$

Therefore we have the current density  $\mathbf{J} = n\mathbf{v}$  and

$$\mathbf{v} = \frac{\hbar}{2mi} \frac{\psi^* \nabla \psi - \psi \nabla \psi^*}{|\psi|^2}. \quad (3.12)$$

The formulations above are also valid for the condensate even though there is a nonlinear potential in the Schrödinger equation. Since the wave function for a condensate can be written as  $\psi(\mathbf{r}, t) = \sqrt{n_c(\mathbf{r}, t)} e^{i\theta(\mathbf{r}, t)}$ , we have the velocity of the flow

$$\mathbf{v} = \frac{\hbar}{2mi} (-2in_c(\mathbf{r}, t)) \nabla \theta(\mathbf{r}, t) / n_c(\mathbf{r}, t) = \frac{\hbar}{m} \nabla \theta(\mathbf{r}, t) \quad (3.13)$$

proportional to the gradient of the phase.

We can demonstrate the relation between the phase and velocity of the *flow* more clearly if we observe the motion of the condensate *at side*. If we define the condensate in a frame  $\mathbf{F}$  moving with the velocity  $-\mathbf{v}$  relative to another frame  $\mathbf{F}'$  where we stand in. We want to know how the physical quantities related to what we are measured in the rest frame of the condensate. So we can ask the question that what is the property of the wave function under Galilean transformation? We then find that the wave function in the  $\mathbf{F}'$  frame moving with  $\mathbf{v}$  satisfies Eq. 3.8 can be written as

$$\psi'(\mathbf{r}, t) = \psi(\mathbf{r} - \mathbf{v}t, t) \exp\left[\frac{i}{\hbar} (m\mathbf{v} \cdot \mathbf{r} - \frac{1}{2} m v^2 t)\right]. \quad (3.14)$$

While in stationary state the condensate wave function can be written as  $\psi(\mathbf{r}, t) = \sqrt{n_0(\mathbf{r})}e^{-i\mu t}$ , now the phase of the condensate becomes

$$\theta(\mathbf{r}, t) = \frac{1}{\hbar}[m\mathbf{v} \cdot \mathbf{r} - (\frac{1}{2}mv^2 + \mu)t]. \quad (3.15)$$

Using the vector formula

$$\nabla(\mathbf{a} \cdot \mathbf{b}) = (\mathbf{a} \cdot \nabla)\mathbf{b} + (\mathbf{b} \cdot \nabla)\mathbf{a} + (\mathbf{a} \times \nabla)\mathbf{b} + (\mathbf{b} \times \nabla)\mathbf{a}, \quad (3.16)$$

we would obtain the gradient of the phase

$$\nabla\theta(\mathbf{r}, t) = \frac{m}{\hbar}\mathbf{v}, \quad (3.17)$$

that links with velocity of the motion of the condensate.

The additional phase in Eq. 3.14 implies the condensate as a whole moves at the velocity  $\mathbf{v}$ . We can understand it via a point of the view that at extremely low temperatures there are small perturbations in momentum  $\hbar\mathbf{k} = m\mathbf{v}$  giving every particle of the condensate a small boost, and the whole quantum state moves *rigidly* with a constant velocity. Therefore we define the superfluid velocity  $\mathbf{v}$  of a macroscopic system as

$$\mathbf{v} = \frac{\hbar\mathbf{k}}{m}. \quad (3.18)$$

### Landau's Fluid Model and the Excitation Spectrum

After we know the superfluid velocity of the condensate is associated with its phase, next, we have to know the velocity of flow should be limited otherwise the superfluid model would breakdown. From Landau's Bose fluid model, we can obtain the simple picture of the excitation spectrum and we can path the scattering processes to know why the existence of the phonos would induce viscosity to dissipate the superfluid phenomenon. We can explicitly determine the criterion for the velocity of the superfluid and show that the ideal Bose gas is not a superfluid.

Consider a fluid flowing in a pipe. Let the fluid at a velocity  $-\mathbf{v}$  relative to the pipe. In the rest frame  $\mathbf{F}$  in which the fluid is stationary and in its ground state, the fluid feels the pipe moving at  $\mathbf{v}$ . If there are  $N$  bosons then in the  $F'$  frame the momentum is

$$\mathbf{P}' = \mathbf{P} - Nm\mathbf{v}, \quad (3.19)$$

and the total energy in the absence of the external potential is

$$E' = \sum_i^N \frac{(\mathbf{p}_i - m\mathbf{v})^2}{2m} + \sum_{i \neq j} V(\mathbf{r}_i - \mathbf{r}_j) = E - \mathbf{P} \cdot \mathbf{v} + \frac{1}{2}Nm v^2. \quad (3.20)$$

In the previous section we mentioned the excitation spectrum is close related to the superfluid behavior. To describe it more clearly we set the energy of an excited state with momentum  $\mathbf{q}$  in the  $\mathbf{F}$  frame is

$$E_q = E_0 + \Delta E_q, \quad (3.21)$$

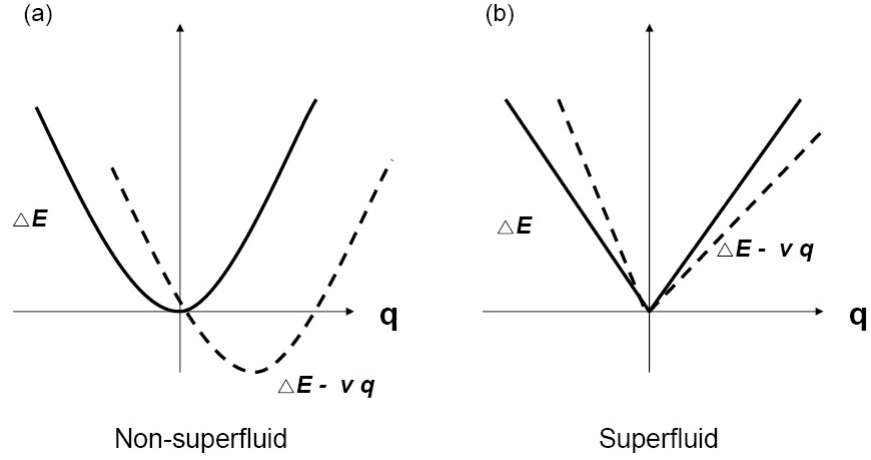


Figure 3.6: Galilean transformation for the excitation spectrum. Superfluid requires ground state of the fluid at rest remains the ground state in the moving frame.

then in the  $F'$  frame it is

$$\begin{aligned} E'_q &= E_q - \mathbf{v} \cdot \mathbf{q} \\ \Delta E'_q &= E'_q - E_0 = \Delta E_q - \mathbf{v} \cdot \mathbf{q}. \end{aligned} \quad (3.22)$$

If the pipe wall is not smooth enough it will always exerts forces on the moving particles and the viscosity is induced in the scattering processes. For elastic scattering, the wall can scatter the particle into any final state without any cost of energies. For inelastic scattering, however, the particle can be scattered into a lower energy state. As shown in Fig. 3.6a, for an ideal Bose gas, a simple way to create excitations is to take off a particle out of the condensate and put it in a state with momentum  $\mathbf{q}$ , so in the rest frame  $\Delta E_q = \mathbf{q}^2/2m$ . Therefore, in the pipe frame we have

$$\Delta E' = \mathbf{q}^2/2m - \mathbf{v} \cdot \mathbf{q} < 0. \quad (3.23)$$

So from here we obtain Landau's critical velocity  $v_c = \min(\Delta E_q/q)$ . And we come to the conclusion that the ground state of the ideal Bose gas is unstable against the excitation of particles since the critical velocity is zero! The flow can be dragged by the wall and the wall can impart momentum into the flow leading to viscous friction.

On the other hand, a superfluid requires the ground state of the fluid in the rest frame remains the lowest energy state in the moving frame. So we require that

$$\Delta E' = \mathbf{q}^2/2m - \mathbf{v} \cdot \mathbf{q} > 0 \quad (3.24)$$



for all excitations. Therefore the excitation spectrum can't be as the ideal Bose case and we show in Fig. 3.6b a post-sight sketch from Landau's intuitive theory. The ingenious idea of implying the spectrum as the quantized collective modes instead of a single particle excitation was verified by the experiments. At small momenta, the excitation energy is linear in  $\mathbf{q}$ , and the critical velocity is just the sound velocity. When the velocity of the flow  $\mathbf{v}$  is smaller than  $\mathbf{v}_s$ , it's impossible to create quasiparticles and the flow would be the superfluid.

### 3.3.3 Summary

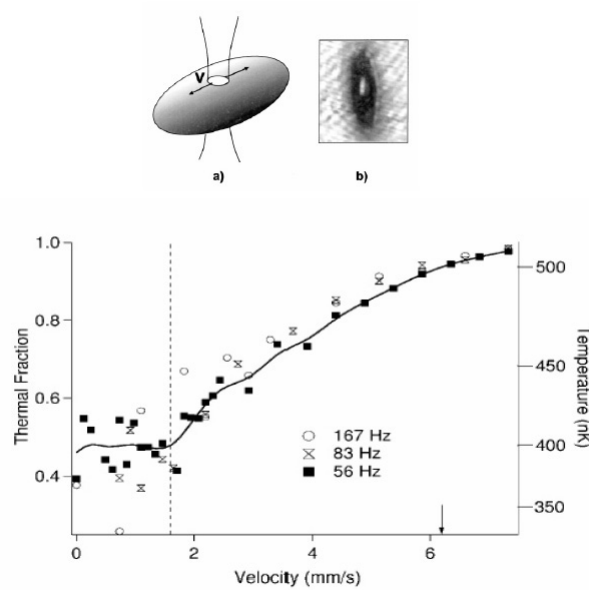


Figure 3.7: Evidence for a critical velocity in BEC. *Up*: Stirring the condensate with a blue detuned laser beam. (A) Atoms are repelled from the region where laser passes through. (B) The absorption image of a condensate with a scanning hole. *Down*: At  $v > 1.6 \text{ mm/s}$  the thermal fraction increases obviously. The right axis indicate the temperature  $T = (1 - N_0/N)^{1/3}T_c$ . From *Phys. Rev. Lett.* **83**, 2502(1999).

In the above paragraphs we describe the history of researches on superfluids. Calculations on collective excitation spectra based on Bogoliubov's approach do explain the experimental data and verify Landau's prediction. From the spectrum, he also derived the critical velocity which denoted as the velocity of sound, the criterion to excite quasiparticles. Therefore we know as the flow of a condensate is slower than the sound, it will remain the superfluid. Experimentally we do observe the the evidence of the critical velocity in BEC[29]. MIT

group studied dissipation when an object is moved through the fluid. They used a blue-detuned laser beam to repel atoms from its focus to create moving boundaries. As shown in Fig. 3.7, there are no atoms in the region that laser passes through. And atoms nearby the hole out-move at the velocity  $v$ . The scanning velocity  $v = 2df$  is controlled by varying the scanning frequency  $f$  and the range  $d$ . Different from the criterion to generate phonons, the stir of the cloud generates vortex lines. Fig. 3.7 shows that when  $v > 1.6 \text{ mm/s}$ , the thermal fractional atoms increase abruptly, and the superfluid flow becomes unstable against the formation of quantized vortex lines that signals the onset of the dissipation region.

The authors also do simulations by solving the nonlinear Schrödinger equation. Theoretical calculations matches very well with experimental observations. This indicate Bogoliubov's approach does work in calculation of thermal excitations. And in the next section we can apply the recipe in simulation of dissipation processed for a condensate in an optical lattice.



## 3.4 Landau and Dynamical Instability of a Bose-Einstein Condensate in an Optical Lattice

### 3.4.1 Motivation

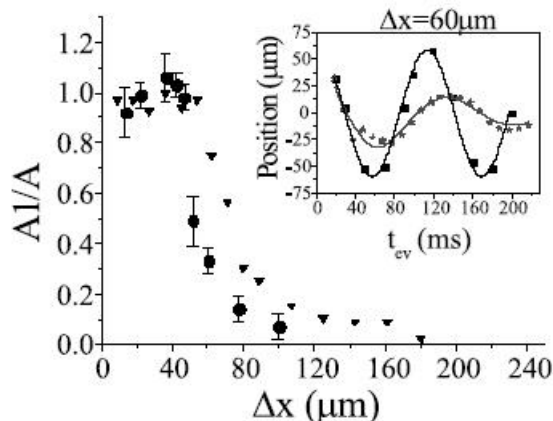


Figure 3.8: Ratio of the first peak amplitude of the oscillation to the free oscillation amplitude as a function of displacement. The inset shows the oscillation with (stars) and without (squares) the lattice.

In 2001 Burger, Cataliotti and their co-workers[8] created the BEC of  $Rb^{87}$  in a static magnetic trap with a superimposed blue-detuned 1D optical lattice. The main purpose of their work is to investigate the superfluid phenomenon of a condensate by studying its center-of-mass oscillations. Experimentally, they identify different dynamical regimes by varying the initial displacement of the BEC from the bottom of the trap. In the absence of an optical lattice, the condensate oscillates in frequency of the magnetic trap. While the lattice is switched on and in small displacement conditions the condensate oscillates undamped but the frequency shifts due to the renormalization of atomic mass in the band states. However the condensate enters the dissipative regime by increasing the initial displacement and hence the velocity of the condensate as shown in Fig. 3.8. *Superfluidity can be expected to disappear when the velocity is sufficient for the spontaneous emission of elementary excitations.* They measured the fraction of atoms in the condensate as a function of the velocity. In Fig. 3.9 we see that for  $v \geq 4.1 \text{ mm/s}$  the condensate disperses indicating the superfluid vanishes. And the critical velocity is just the sound velocity theoretically defined in an inhomogeneous system by  $v_s = \sqrt{(n(r)/m)(\delta\mu/\delta n)}$ [30]. Experiments so claimed to observe Landau instability and they observed the dissipation occurs at higher velocities for decreasing lattice height  $V_0$  and the

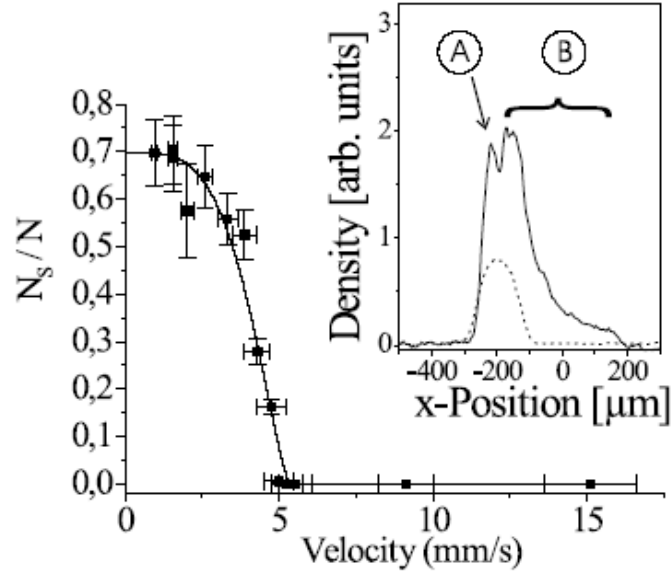


Figure 3.9: The fraction of atoms remains in the condensate as the function of velocity reached during the evolution in the optical lattice. At about  $v = 2.5 \text{ mm/s}$  there is a suddenly decrease of  $N_0$ . In the inset in the case of  $v = 4 \text{ mm/s}$ , the density distribution obtained from absorption images shows only central part of the fluid is moving without retardation.

condensate propagates without dissipation in a regime with very few particles.

However Wu and Niu[31] claimed that the observation should be the dynamical instability rather than Landau instability since the dissipation would become more severe with low densities of BEC. They also claimed GP equation can only simulates the dynamical instability, while the description of energy dissipation due to emission of phonons in the Landau instabilities can't be accounted by the GP equation.

In order to simulate these phenomena and to investigate the underlying mechanisms we start our work by solving an effective 1D GP equation and then we calculate the collective excitation spectra based on the Bogoliubov's approach. Meanwhile, the  $\mathbf{k} \cdot \mathbf{p}$  method is applied to demonstrate the superfluid property in the shallow potential wells. We found that:

1. When the group velocity of the condensate is larger than the sound velocity the excitation of quasiparticles is initiated, and the flow enters the *Landau instability* regime.
2. When the group velocity goes on increasing to a certain value where the

corresponding effective mass becomes negative, indicating the presence of *nonreal* excitation energy, the model of superfluid breakdowns in this *dynamical instability* regime due to the exponential growth of the number of quasiparticles.

### 3.4.2 The Effective 1D Gross-Pitaevskii Equation

The evolution of a Bose condensate in an optical lattice obeys the Gross-Pitaevskii (GP) equation. In the mean-field approximation it is

$$i\hbar \frac{\partial \Psi}{\partial t} = -\frac{\hbar^2}{2m} \nabla^2 \Psi + V(\mathbf{r})\Psi + g|\Psi|^2\Psi, \quad (3.25)$$

where  $g = 4\pi\hbar^2 a_s/m$ , and  $a_s$  is s-wave scattering length. In Eq. 3.25,

$$V(\mathbf{r}) = E_0 \sin^2\left(\frac{\pi X}{L}\right) + \frac{1}{2}m[\omega_X^2 X^2 + \omega_\perp^2(Y^2 + Z^2)] \quad (3.26)$$

describes the optical lattice potential of period  $L$  and the parabolic magnetic trapping well. If the trap is tuned such that  $\omega_\perp^2 \gg \omega_X^2$  the wave function can be expressed as  $\Psi(X, Y, Z, T) = U(Y, Z)\mathcal{X}(X, T)$ , and the potential can be decomposed as  $V(X, Y, Z) = V_X(X) + V_\perp(Y, Z)$ . Then we will approximately obtain the analytical solutions in Y-Z plane

$$U = \sqrt{\frac{m\omega_\perp}{\pi\hbar}} \exp\left[-\frac{m\omega_\perp}{2\hbar}(Y^2 + Z^2)\right]. \quad (3.27)$$

Therefore by integrating Eq. 3.27 into Eq. 3.25 and setting  $\omega_X \gg 2\pi/L$ , we have

$$i\hbar \frac{\partial \mathcal{X}}{\partial T} = -\frac{\hbar^2}{2m} \nabla_X^2 \mathcal{X} + E_0 \sin^2\left(\frac{\pi X}{L}\right) \mathcal{X} + 2\hbar\omega_\perp a_s |\mathcal{X}|^2 \mathcal{X}. \quad (3.28)$$

By setting

$$\begin{aligned} t &= T/T_0 \\ x &= X/(L/2) \\ \mathcal{X} &= \psi/L_1^{1/2} \\ V_0 &= E_0/E_r, \end{aligned}$$

where

$$\begin{aligned} T_0 &= \frac{mL^2}{4\hbar} \\ L_1 &= \omega_\perp |a_s| mL^2 / 2\hbar \\ E_r &= 4\hbar^2 / mL^2, \end{aligned}$$

the dimensionless GP equation becomes

$$i \frac{\partial \psi}{\partial t} = -\frac{1}{2} \frac{\partial^2 \psi}{\partial x^2} + V_0 \sin^2\left(\frac{\pi}{2}x\right) \psi + \sigma |\psi|^2 \psi, \quad (3.29)$$

where  $\sigma = \text{sign}(a_s)$ . In the absence of an external force the evolution of the condensate wave function follows its ground state energy  $\mu$  and can be written as  $\varphi(x, t) = \varphi(x)e^{-i\mu t}$ . So Eq. 3.29 becomes

$$\mu\varphi(x) = -\frac{1}{2}\frac{\partial^2\varphi}{\partial x^2} + V_0 \sin^2\left(\frac{\pi}{2}x\right)\varphi(x) + \sigma|\varphi(x)|^2\varphi(x). \quad (3.30)$$

### 3.4.3 k·p Method and 1-band Approximation

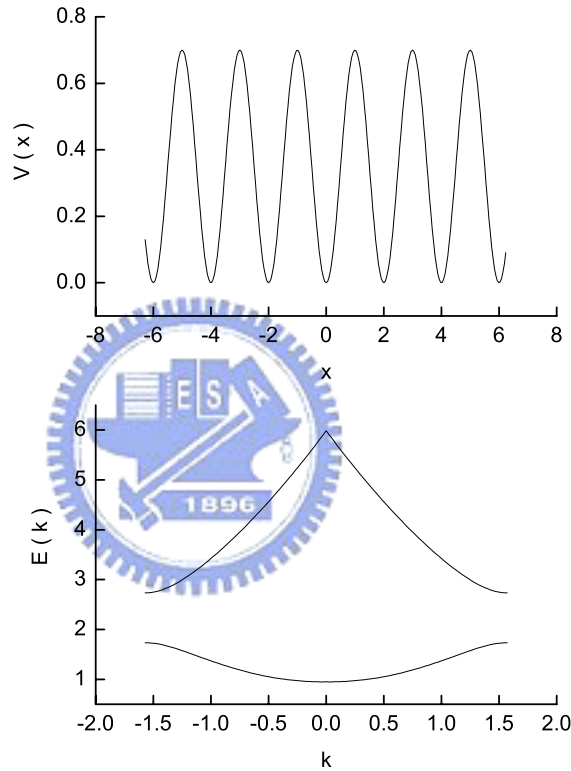


Figure 3.10: Periodic potential and lowest two band structures of  $V = 0.7 \sin^2(\pi x/2)$ .

While we set  $\sigma = 0$ , Eq. 3.30 reduces to a general, widely studied eigenvalue problem in the solid state physics. By using plane wave method the Bloch wave functions and the band structures can be expressed in an analytic manner [see Appendix B]. And the complete Bloch states turn out to be the good basis in solving the nonlinear Eq. 3.30. So we expand  $\varphi(x)$  in basis of Bloch states

$\varphi_{nk}(x)$

$$\varphi(x) = \sum_n \int_{-\pi/2}^{\pi/2} A_n(k) \varphi_{nk}(x) dk, \quad (3.31)$$

where  $n$  is the band index and the integral is taken over the first Brillouin zone. The k·p method applied that in the vicinity of a certain  $k_0$ , the Bloch wave function is approximated to

$$\varphi_{nk}(x) \simeq e^{i(k-k_0)x} \varphi_{nk_0}(x). \quad (3.32)$$

Then under 1-band approximation ( $n = 0$ ), the condensate wave function of the infinite large system can be written as

$$\begin{aligned} \varphi(x) &\simeq \int A_n(k) e^{i(k-k_0)x} \varphi_{nk_0}(x) dk = \varphi_{nk_0}(x) \int A_n(k) e^{i(k-k_0)x} dk \\ &= \varphi_{nk_0}(x) F_{nk_0}(x). \end{aligned} \quad (3.33)$$

The expression is valid in the assumption of slow varying envelope function  $F_{nk_0}(x)$  in coordinate space.

Substitute Eq. 3.33 in to Eq. 3.30, the linear part of the equation becomes

$$\begin{aligned} &-\frac{1}{2} \frac{\partial^2 \varphi}{\partial x^2} + V_0 \sin^2\left(\frac{\pi}{2}x\right) \varphi(x) \\ &= \int A_n(k) \left[-\frac{1}{2} \frac{\partial^2}{\partial x^2} + V_0 \sin^2\left(\frac{\pi}{2}x\right)\right] \varphi_{nk}(x) dk \end{aligned} \quad (3.34)$$

$$= \int A_n(k) E_n(k) \varphi_{nk}(x) dk \quad (3.35)$$

$$\begin{aligned} &\simeq \varphi_{nk_0}(x) \int A_n(k) [E_n(k_0) + V_g(k_0)(k - k_0) \\ &+ \frac{1}{2m_{eff}}(k - k_0)^2] e^{i(k-k_0)x} dk \end{aligned} \quad (3.36)$$

$$= E_n(k_0) \varphi_{nk_0}(x) F_{nk_0}(x) + \varphi_{nk_0}(x) [V_g(k_0) \hat{p} + \frac{\hat{p}^2}{2m_{eff}}] F_{nk_0}(x). \quad (3.37)$$

Thus, in the k·p approximation the expansion of the band structure around  $k = k_0$  changes the problem to another scenario. We are no longer dealing with the system containing a periodic potential with infinite number of wells. Rather, the dynamics of the particle can be described in terms of an envelope wave packet with the effective mass  $m^*$  and the group velocity  $V_g$  moving in the free space. Extend the approach to the interacting condensate, the GP equation becomes

$$\varphi_{nk_0}(x) [V_g(k_0) \hat{p} + \frac{\hat{p}^2}{2m_{eff}} + \sigma |\varphi_{nk_0} F_{nk_0}|^2] F_{nk_0} = [\mu - E_n(k_0)] \varphi_{nk_0}(x) F_{nk_0}(x). \quad (3.38)$$

Integrate Eq. 3.38 by  $\varphi_{nk_0}^*(x)$  we obtain

$$[-iV_g(k_0)\frac{\partial}{\partial x} - \frac{1}{2m_{eff}}\frac{\partial^2}{\partial x^2} + \sigma'|F_{nk_0}|^2]F_{nk_0}(x) = [\mu - E_n(k_0)]F_{nk_0}(x), \quad (3.39)$$

where

$$\begin{aligned} \sigma' &= \int |\varphi_{nk_0}(x)|^4 dx = \frac{2\pi}{2} \sigma \int_{-1}^1 |\varphi_{nk_0}(x)|^4 dx \\ &= \frac{\sigma}{2\pi} \left[ 1 + \frac{8}{V_0^2} \frac{(k_0^2 + V_0 - 2E(k_0))^2}{\left[1 + \frac{4}{V_0^2}(k^2 + V_0^2 - 2E(k_0))^2\right]^2} \right]. \end{aligned} \quad (3.40)$$

In Eq. 3.40 we have used the analytic expression derived in Appendix D. The 3rd order derivative term  $ic_3 \frac{\partial^3}{\partial x^3}$  would be included in Eq. 3.39 for points close to the one with infinite mass and  $c_3$  is in the form of

$$c_3 = \frac{1}{6} \frac{-6\pi^4(-2k_0 + \pi)V_0}{\left[(-2k_0\pi + \pi^2)^2 + V_0^2\right]^{5/2}}. \quad (3.41)$$

### 3.4.4 Collective Excitations

Following the history of investigation of superfluid phenomenon of liquid helium that we briefly introduced in the previous section we know the concept of elementary excitations plays an important role to explain the properties of the Bose liquid. The elementary excitation spectrum for  $He^4$  has been directly observed by neutron scattering[32], and we know the low frequency excitation are phonons, long-wavelength collective modes of the superfluid. However a satisfactory microscopic theory is only valid in explanation of behaviors for dilute quantum gases. It is until the realization of BEC that the theory can be tested experimentally.

The observation of collective excitations of the Bose-Einstein condensation in the magnetic-optical trap (MOT) stimulates a lot of calculations[33]. The oscillation spectra of the low-lying states give us the information about the dilute atomic gas at extremely low temperatures. A complete derivation of formulas to obtain excitation spectra in Bogoliubov's approach is in Appendix D. Spectra for a condensate in the harmonic magnetic trap and double well are also shown there.

Let's come back to the optical lattice system. To investigate the superfluid behavior we have to find out if the system remains in energy minimum against external perturbations. In second quantization language the grand canonical, many-body hamiltonian can be written in terms of the boson field operator  $F_{nk_0}(x) \equiv \langle F(\hat{x}) \rangle$  as

$$H = \int dx \{ F(\hat{x})^\dagger \left( -iV_g \frac{\partial}{\partial x} - \frac{1}{2m_{eff}} \frac{\partial^2}{\partial x^2} + E \right) F(\hat{x}) + \frac{\sigma'}{2} |F(\hat{x})|^4 - \mu |F(\hat{x})|^2 \}. \quad (3.42)$$



The boson field operators  $F^\dagger(x)$  and  $F(x)$ , respectively, create and destroy an atom at position  $x$  and satisfy the commutation relations

$$\begin{aligned} [F(x), F^\dagger(x')] &= \delta(x - x') \\ [F(x), F(x')] &= [F^\dagger(x), F^\dagger(x')] = 0. \end{aligned} \quad (3.43)$$

Under Bogoliubov's approach the condensate is assumed to contain most of atoms such that  $N - N_0 \ll N_0$ , where  $N_0$  denotes the macroscopic occupation of the condensate and  $N$  is the total number of atoms in the system. In the case, the field operator can be written as the condensate wave function  $A(x)$  plus a small correction  $\hat{\phi}(x)$

$$F(x) = A(x) + \hat{\phi}(x), \quad (3.44)$$

where

$$\begin{aligned} \hat{\phi}(x) &= \sum_q [u_q(x)e^{iqx}\hat{a}_q + v_q^*(x)e^{-iqx}\hat{a}_q^\dagger] \\ \hat{\phi}^\dagger(x) &= \sum_q [u_q^*(x)e^{-iqx}\hat{a}_q^\dagger + v_q(x)e^{iqx}\hat{a}_q] \end{aligned} \quad (3.45)$$

are represented in term of quasi-particle and quasi-hole amplitudes in the exploitation of so-called Bogoliubov transformation.

From Eq. 3.42 we have zero order term  $H_0$  as

$$H_0 = \int dx A^*(x) \left( -iV_g \frac{\partial}{\partial x} - \frac{1}{2m_{eff}} \frac{\partial^2}{\partial x^2} + E \right) A(x) + \frac{\sigma'}{2} |A(x)|^4 - \mu |A(x)|^2, \quad (3.46)$$

where  $E \equiv E_n(k_0)$  and  $\mu = E + \sigma' A(x)^2$ , and the first order perturbation  $\delta H$  as

$$\begin{aligned} \delta H &= a_q^\dagger a_q \int dx [u_q^*(x)e^{-iqx} + v_q(x)e^{iqx}] \left( -iV_g \frac{\partial}{\partial x} - \frac{1}{2m_{eff}} \frac{\partial^2}{\partial x^2} \right) \\ &\quad [u_q(x)e^{iqx} + v_q^*(x)e^{-iqx}] + \frac{\sigma'}{2} [4A^2(x)(|u_q(x)|^2 + |v_q(x)|^2) \\ &\quad + 2A^2(x)(u_q^*(x)v_q(x) + v_q^*(x)u_q(x))]. \end{aligned} \quad (3.47)$$

Then in matrix form, Eq. 3.47 is equivalent to

$$\delta H = a_q^\dagger a_q \int dx \begin{pmatrix} u^*(x) & v(x) \end{pmatrix} B \begin{pmatrix} u(x) \\ v^*(x) \end{pmatrix} \quad (3.48)$$

where  $B$  is a  $2 \times 2$  matrix

$$\begin{pmatrix} c_{11} & c_{12} \\ c_{21} & c_{22} \end{pmatrix} \quad (3.49)$$

in which

$$c_{11} = -\frac{1}{2m_{eff}}\left[\frac{\partial}{\partial x} + i(q + m_{eff}V_g)\right]^2 - \frac{1}{2}m_{eff}V_g^2 + E - \mu + 2\sigma'A^2(x),$$

$$c_{22} = -\frac{1}{2m_{eff}}\left[\frac{\partial}{\partial x} + i(q - m_{eff}V_g)\right]^2 - \frac{1}{2}m_{eff}V_g^2 + E - \mu + 2\sigma'A^2(x),$$

and

$$c_{12} = c_{21} = \sigma'A^2(x). \quad (3.50)$$

Since the envelope function is slow varying in coordinate space, in convenience, it is to be assumed as a constant in our work and so do amplitudes of quasiparticles. Under the assumption and including the 3rd order correction, the matrix becomes

$$B = \begin{pmatrix} \frac{q^2}{2m_{eff}} + qV_g + c_3q^3 + \sigma'A^2 & \sigma'A^2 \\ \sigma'A^2 & \frac{q^2}{2m_{eff}} - qV_g - c_3q^3 + \sigma'A^2 \end{pmatrix}. \quad (3.51)$$

Minimizing the energy functional of Eq. 3.48 gives us the stationary eigen solutions and they are

$$\lambda = \left(\frac{q^2}{2m_{eff}} + \sigma'A^2\right) \pm \sqrt{(qV_g + c_3q^3)^2 + \sigma'^2A^4}. \quad (3.52)$$

Therefore we obtain the criterion to excite quasiparticles, namely when

$$V_g > \sqrt{\frac{q^2}{4m_{eff}^2} + \frac{\sigma'A^2}{m_{eff}}} - c_3q^2, \quad (3.53)$$

and when  $q \rightarrow 0$ ,  $V_g > C_s = \sqrt{\frac{\sigma'A^2}{m_{eff}}}$ , the first sound velocity, in the case that Landau instability occurs.

To investigate the dynamics of the condensate, a small displacement on the magnetic trapping potential is performed to drive the system. Then start with the time dependent GP equation

$$i\frac{\partial \hat{F}}{\partial t} + iV_g\frac{\partial \hat{F}}{\partial x} - ic_3\frac{\partial^3 \hat{F}}{\partial x^3} = -\frac{1}{2m_{eff}}\frac{\partial^2 \hat{F}}{\partial x^2} + E\hat{F} + \sigma'|\hat{F}|^2\hat{F}, \quad (3.54)$$

with  $\hat{F} = (A + u_q(t)e^{i(qx - E_q t)}\hat{a}_q + v_q^*(t)e^{-i(qx - E_q t)}\hat{a}_q^\dagger)e^{-i\mu t}$ , the equations of motion of the quasiparticles are

$$i\frac{\partial}{\partial t} \begin{pmatrix} u \\ v \end{pmatrix} = \begin{pmatrix} \frac{q^2}{2m_{eff}} + qV_g + c_3q^3 + \sigma'A^2 & \sigma'A^2 \\ -\sigma'A^2 & -\frac{q^2}{2m_{eff}} + qV_g + c_3q^3 - \sigma'A^2 \end{pmatrix} \times \begin{pmatrix} u \\ v \end{pmatrix}. \quad (3.55)$$

The quasiparticles will oscillate in multiple frequency of the external field with excitation energies

$$\begin{aligned} E_q &= qV_g + c_3q^3 \pm \sqrt{\frac{q^4}{4m_{eff}^2} + \frac{q^2\sigma'A^2}{m_{eff}}} \\ &= qV_g + c_3q^3 \pm \varepsilon_q. \end{aligned} \quad (3.56)$$

While the motion of atoms is unidirectional with group velocity  $V_g$ , the two excitation branches manifest the phenomenon in analogy of the *Doppler effect*. With amplified excitation energies the high energy branch bringing *particles* obeying Bose commutation relation

$$[a_q, a_k^\dagger] = \delta_{qk}, \quad (3.57)$$

results in the normalization condition

$$|u_q|^2 - |v_q|^2 = 1. \quad (3.58)$$

Therefore we obtain the amplitudes of particles

$$\begin{aligned} |u_q|^2 &= \frac{1}{2} \left( \frac{\xi_q}{\varepsilon_q} + 1 \right) \\ |v_q|^2 &= \frac{1}{2} \left( \frac{\xi_q}{\varepsilon_q} - 1 \right), \end{aligned} \quad (3.59)$$

where  $\xi_q = \varepsilon_q^0 + \sigma'A^2$  and  $\varepsilon_q^0 = \frac{q^2}{2m_{eff}}$ .

On the other hand, the low energy branch, which we assert to be constructed by *antiparticles* obeying *anti-Bose* commutation relation[34]

$$[b_q^\dagger, b_k] = [a_q, a_k^\dagger] = \delta_{qk}, \quad (3.60)$$

and the *anti-normalization* condition

$$|u_q|^2 - |v_q|^2 = -1. \quad (3.61)$$

Then the amplitudes of antiparticles are

$$\begin{aligned} |u_q|^2 &= \frac{1}{2} \left( \frac{\xi_q}{\varepsilon_q} - 1 \right) \\ |v_q|^2 &= \frac{1}{2} \left( \frac{\xi_q}{\varepsilon_q} + 1 \right). \end{aligned} \quad (3.62)$$

In mean field approximation, the depletion of the condensate by ensemble average of the excitation field operator  $\langle \tilde{\phi}^\dagger \tilde{\phi} \rangle$  is given as

$$\tilde{N} = \sum_q [|u_q|^2 + |v_q|^2] f(q) + |v_q|^2, \quad (3.63)$$

where  $f(q) = \langle a_q^\dagger a_q \rangle = \langle b_q b_q^\dagger \rangle = [e^{E_q/k_B T} + 1]^{-1}$ . For  $m_{eff} > 0$ , the low energy excitation is initiated if  $V_g > C_s$  which gives us an estimation for the occurrence of Landau instability. While for  $m_{eff} < 0$  the spectra become complex indicating the exponential growth of the number of the quasiparticles. The superfluid phenomenon vanishes due to the rise of dynamical instability.

### 3.5 Numerical Results and Discussions

We simulate an 1D optical lattice model with shallow dimensionless potential of  $V_0 = 2$ . As a typical value we take the total number of lattice site  $I = 250$ .

In Fig. 3.11 we show  $m_{eff}^{-1}$ ,  $V_g$  and  $C_s$  in function of quasimomentum  $k$ . For  $k \geq 1.13581$   $m_{eff}$  becomes negative indicating the cutoff while afterwards that superfluid behavior vanishes. In Fig. 3.11(b) we have  $C_s = \sqrt{\frac{\sigma' A^2}{m_{eff}}}$ , where  $A^2$  is the condensate density defined as

$$A = \sqrt{N_0 \pi / R_{max}}. \quad (3.64)$$

Eq. 3.63 is constructed from the normalization condition

$$N = A^2 \int_{-R_{max}}^{R_{max}} |\varphi_{nk}(x)|^2 dx = N_0 + \tilde{N}. \quad (3.65)$$

While we set  $N = 750$  and  $R_{max} = 250$ , the self-consistent calculations return  $736.025 \leq N_0(k) \leq 748.221$  at  $T = 0$  K. For  $k \geq 1.03914$  the low energy excitations are stimulated and the Landau instability occurs.

In Fig. 3.12 we plot  $N_0/N$  for  $N = 750$  and  $900$  at  $T = 0$  K and  $30$  nK. Different from the smooth curve of the condensate fraction vs. temperature in the absence of the lattice, there is a kink in the fraction of the condensate accelerated by the lattice even at  $T = 0$  K. For  $T > 0$  the kink becomes sharp. The sudden decrease of atoms in the condensate attributes to the creation of *anti*-quasiparticles of the low excitation energy branch. We assert that Landau instability occurs in company with the superfluid. Before the collapse of the condensate our calculations show two plateaus in good matched with that observed in the experiment data. The two regions are separated by the appearance of Landau and dynamical instabilities. With the increase of the total number of particles, the region of the second plateau diminishes. It takes more energy to excite anti-particles according to Eq. 3.51 and for  $N > N_c \sim 1200$  in our work, it is no longer to excite atoms in low energy branch. While the velocity unit is about  $3.613$  mm/s, Landau instability occurs at  $v_L = 2.9$  mm/s and dynamical instability occurs at  $v_d = 3.1$  mm/s. However the correspondent data in the experiment are  $v_L = 2.5$  mm/s and  $v_d = 4.0$  mm/s. Obviously there are some differences between the results. The error in  $v_d$  might arise from the two-band approximation. And practically, a comparison between 1D simulation and 3D experimental set-up might cause errors too, even we have made some reductions of experimental parameters to 1D case. But actually, via calculations of excitation spectra, we do prove that both Landau and dynamical instability occur to destroy the superfluid.

In order to explore the physics of strange phenomena behind Fig. 3.12 we plot dispersion relations of the quasiparticle in various quasimomentum  $k$ . Fig. 3.13 shows the low excitation energy spectra for  $N = 750$  at  $T = 30$  nK. First, we choose  $k = 0.55582$  lying in the first plateau and we see clearly that excitation is allowed only for few momenta  $q$ . Therefore for  $k < 1.03914$  most atoms are

in condensed state. For  $k = 1.03914, 1.06331$  and  $1.08747$ ,  $E_q$  almost linearly increase with  $q$ . Since  $E_q(k = 1.03914) < E_q(k = 1.06331) < E_q(k = 1.08747)$ , it explains the sharp kink at  $k = 1.03914$  and afterwards the fraction arises. As we come to the point at  $k = 1.11164$  where  $E_q$  is nonlinear of  $q$ , instability appears when  $q \geq 0.7$ . And for  $k > 1.11164$ , the positive assurance of Eq. 3.51 is not fulfilled. By Fig. 3.13 our results confirm the existence of the critical velocity over which the superfluid vanishes.

Fig. 3.14 shows spectra of the high energy branch. In comparison with the spectra in Fig. 3.13, there are no forbidden excitations for  $k < 1.03491$ . Except the dispersion curve of  $k = 1.11164$ , all spectra are linear in  $q$ , and the number of thermal atoms of various of  $k$  come in order of 10 at  $T = 30$  nK. The excitation energy for  $k = 1.11164$  however is lower such that there are about 50 thermal atoms in this case.



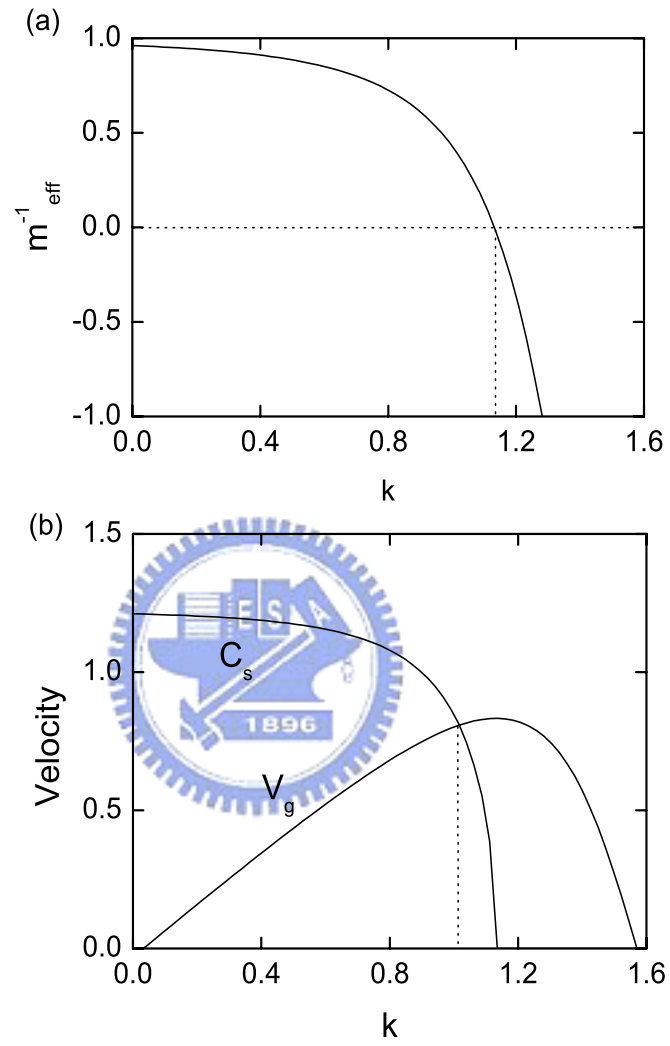


Figure 3.11: In (a) we show  $m_{\text{eff}}^{-1}(k)$ . For  $k \geq 1.13581$   $m_{\text{eff}}$  becomes negative and the damping occurs in the system. In (b) we show  $V_g(k)$  and  $C_s(k)$ .  $V_g$  is zero at  $k = 0$  and  $\pi/2$ . For  $k \geq 1.03914$   $V_g > C_s$  and for  $k \geq 1.03581$   $C_s$  is not defined.

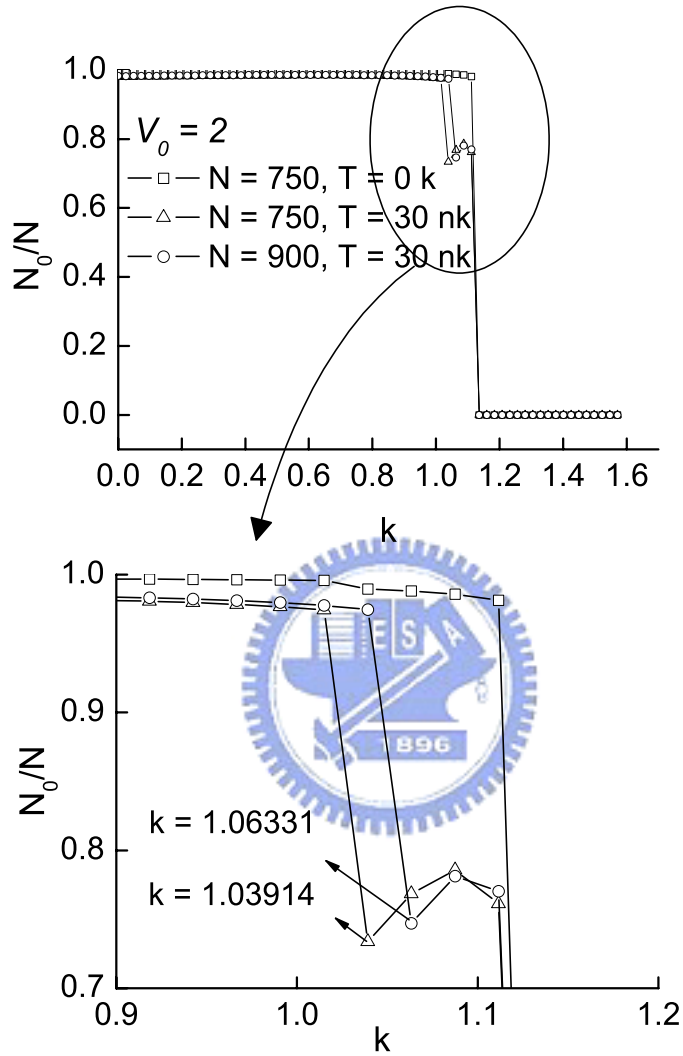


Figure 3.12: Fraction  $N_0/N$  of  $k$  at  $V_0 = 2$ ,  $T = 0$  K, 30 nK. At  $T = 0$  K, very few quasiparticles are excited due to the quantum fluctuations. When  $T > 0$  the kink around some  $k$  indicates the onset of Landau instability. For  $k > 1.1164$  the superfluid breakdowns due to the occurrence of dynamical instability.

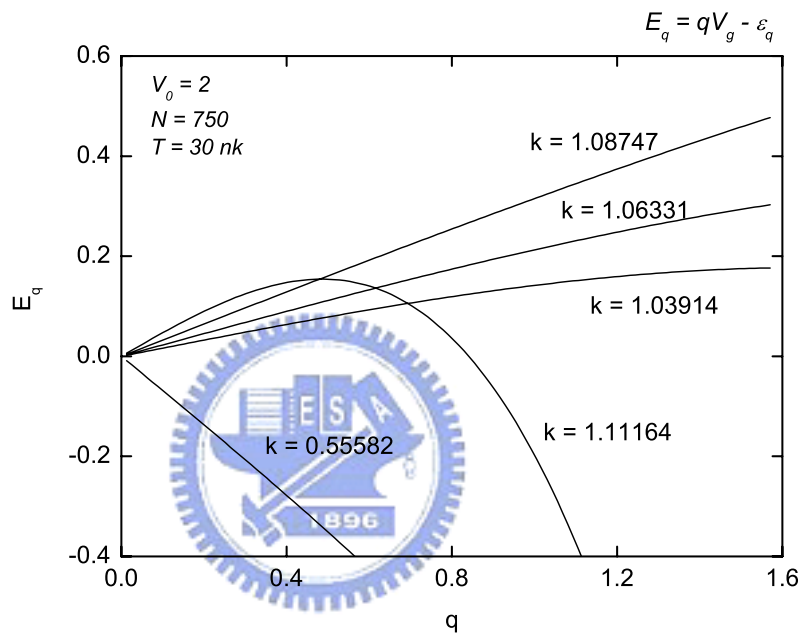


Figure 3.13: Low energy branch of the excitation energy spectra at  $V_0 = 2$ ,  $N = 750$ ,  $T = 30nK$ . For smaller  $k$ ,  $E_q < 0$  for all  $q$  indicates the group velocity is too small to excite quasiparticles. Since it is easier to excite quasiparticles for smaller  $E_q$ , the figure explain the kink of fraction at  $k = 1.03914$ .



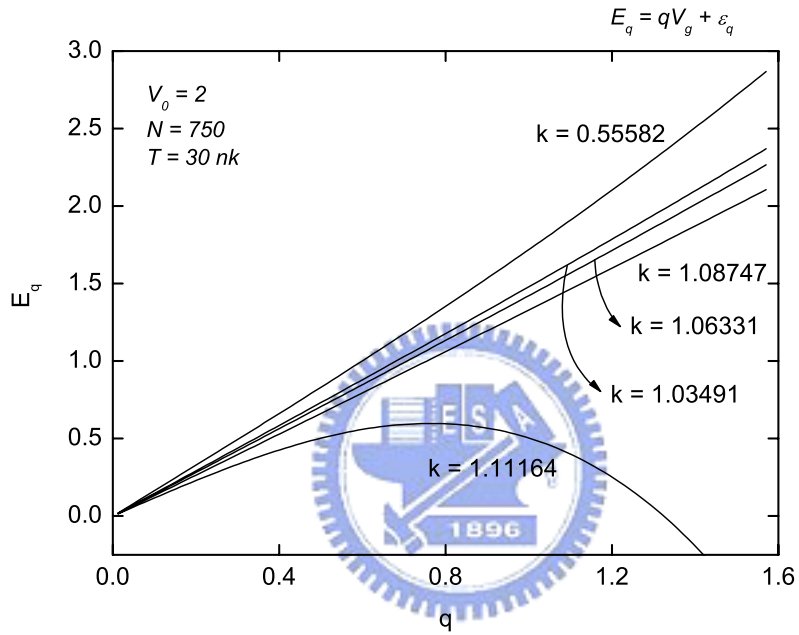


Figure 3.14: Low energy branch of the excitation energy spectra at  $V_0 = 2$ ,  $N = 750$ ,  $T = 30 \text{ nK}$ . In comparison with the spectra in Fig.2.8, there are no forbidden excitations for  $k < 1.03491$ . Except the dispersion curve of  $k = 1.11164$ , all spectra are linear in  $q$ , and the number of thermal atoms of various of  $k$  come in order of 10 at  $T = 30 \text{ nK}$ .

### 3.6 Summary

In this chapter we report theoretical study of the instability phenomenon of a condensate in an optical lattice. While the frequencies of two laser beams are controlled to have a detuning  $\delta\nu$  the lattice is constructed moving at velocity  $v = \lambda\delta\nu/2$ . In other words the condensate can be regarded to move in the opposite direction with the group velocity  $v = \hbar k/m$ , where  $k$  is the quasimomentum and is well defined as the condensate is loaded into an adiabatically switched-on lattice.

Distinct from the localized motion in deep traps usually described via the Bose-Hubbard model[35], We use  $\mathbf{k} \cdot \mathbf{p}$  method to describe condensate's motion in the shallow traps by directly solving time- dependent GP equation. Under this approximation we construct a wave packet extended broadly in real space. Therefore we may say the coherence length of the condensate is much larger than the size of several lattice sites. This also implies the superfluid nature of the system. But the existence of the optical lattice serves as the roughness to be able to destroy the superfluid. Instabilities take place if the relative velocity between the condensate and the lattice exceeds the sound velocity and if the effective mass of the condensate becomes an undefined negative value wherein the condensate itself is unstable to against the creation of thermal atoms.

While Burger *et al.* claimed their observation of destruction of the superfluid as the occurrence of Landau instability, but we propose in our work a different point of view that in addition to Landau instability there is also a regime of dynamical instability. From theoretical calculations, the analyses of excitation spectra based upon Bogoliubov's approach clearly explain reasons of the occurrence of instabilities. We are glad that the study on superfluid phenomenon of the BEC provides a successful touchstone to verify theories on superfluids.

# Bibliography

- [1] M. Raizen, C. Salomon, and Q. Niu, *Phys. Today* **50**, 30(1997).
- [2] M. B. Dahan, E. Peik, J. Reichl, Y. Castin, and C. Salomon, *Phys. Rev. Lett.* **76**, 4508(1996).
- [3] S. R. Wilkinson, C. F. Bharucha, K. W. Madison, Q. Niu, and M. G. Raizen, *Phys. Rev. Lett.* **76**, 4512(1996). Q. Niu, X. G. Zhao, G. A. Geogarkis, and M. G. Raizen, *Phys. Rev. Lett.* **76**, 4504(1996).
- [4] F. S. Cataliotti *et al.*, *Science* **293**, 843(2001).
- [5] C. Orzel *et al.*, *Science* **231**, 2386(2001).
- [6] D. Jaksch, C. Bruder, J. I. Cirac, C. W. Gardiner, and P. Zoller, *Phys. Rev. Lett.* **81**, 3108(1998). M. Greiner, O. Mandel, T. Esslinger, T. W. Hänsch, and I. Bloch, *Nature* **415**, 39(2002).
- [7] B. P. Anderson, and M. A. Kasevich, *Science* **282**, 1686(1998).
- [8] S. Burger, F. S. Cataliotti, C. Fort *et al.*, *Phys. Rev. Lett.* **86**, 4447(2001).
- [9] G. Birkl, M. Gatzke, I. H. Deutsch, S. L. Roston, and W. D. Phillips, *Phys. Rev. Lett.* **75**, 2823(1995). G. Raithel, G. Birkl, A. Katsberg, W. D. Phillips, and S. L. Roston, *Phys. Rev. Lett.* **78**, 630(1997). M. Weidemüller, A. Hemmerich *et al.*, *Phys. Rev. Lett.* **75**, 4583(1995).
- [10] L. Landau, *J. Phys. USSR* **5**, 71 (1941).
- [11] V. S. Letokhov, *JETP Lett.* **7**, 272(1968).
- [12] C. Salomon, J. Dalibard, A. Aspect, H. Metcalf, and C. N. Cohen-Tannoudji, *Phys. Rev. Lett.* **59**, 1659(1987).
- [13] W. D. Phillips, *Rev. Mod. Phys.* **70**, 721(1998). C. N. Cohen-Tannoudji, *Rev. Mod. Phys.* **70**, 707(1998).
- [14] J. Dalibard and C. N. Cohen-Tannoudji, *J. Opt. Soc. Am. B* **6**, 2023(1989).
- [15] *Atom Optics*. P. Meystre, Springer 2001. *Laser Cooling and Trapping*. H. J. Metcalf and P. van der Straten, Springer 1999.

- [16] J. F. Bjorkholm, R. E. Freeman, A. Ashkin, D. B. Pearson, Phys. Rev. Lett. **41**, 1361(1978).
- [17] J. F. Bjorkholm, R. E. Freeman, A. Ashkin, D. B. Pearson, Opt. Lett. **5**, 111(1980).
- [18] R. Ozeri, N. Katz, *et. al.*, Rev. Mod. Phys. **77**, 187 (2005).
- [19] S. Balibar, *arXiv: cond-mat/0303561* v1 26 Mar 2003.
- [20] C. Pethick and H. Smith, *Bose-Einstein condensation in dilute gases*, Cambridge 2002.
- [21] W. Keesom, *Helium*, Elsevier, Amsterdam 1942.
- [22] F. London, Nature **141**, 643 (1938).
- [23] L. Tisza, Nature **141**, 913 (1938).
- [24] J. Phys. USSR. **11**, 23(1947).
- [25] D. S. Jin, J. R. Ensher, M. R. Matthews, C. E. Wieman, and E. A. Cornell, Phys. Rev. Lett. **77**, 420(1996).
- [26] M.-O. Mewes, M. R. Andrews, N. J. van Druten, D. M. Kurn, D. S. Durfee, C. G. Townsend, W. Ketterle, Phys. Rev. Lett. **77**, 988(1996).
- [27] M. Edwards, P. A. Ruprecht, K. Burnett *et al.*, (to be published).
- [28] S. Stringari, cond-matt/9603126.
- [29] C. Raman, M. Köhl, R. Onofrio, D. S. Durfee *et al.*, Phys. Rev. Lett. **83**, 2502(1999).
- [30] M. R. Andrews *et al.*, Phys. Rev. Lett. **79**, 533 (1997); **80**, 2967(1998).
- [31] Biao Wu and Qian Niu, Phys. Rev. Lett. **89**, 088901(2002).
- [32] V. F. Sears, E. C. Svensson, P. Martel, and A. D. B. Woods, Phys. Rev. Lett. **49**, 279(1982).
- [33] S. Stringari, Phys. Rev. Lett. **77**, 2360(1996). K. G. Singh, and D. S. Rokhsar, Phys. Rev. Lett. **77**, 1667(1996). M. Edwards, P. A. Ruprecht, K. Burnett *et al.*, Phys. Rev. Lett. **77**, 1671(1996). F. Dalfovo, S. Giorgini *et al.*, Phys. Rev. A **56**, 3840(1997).
- [34] N. Ullah and D. J. Rowe, *Nuclear Physics A* **163**, 257 (1971).
- [35] A. M. Ray, K. Burnett, R. Roth *et al.*, J. Phys. B **36**, 825(2003). C. Menotti, A. Smerzi, A. Trombettoni, New Journal of Physics **5**, 112.1(2003).

## Appendix A

# Derivation of Interaction Potential in Terms of Scattering Length

Consider the scattering of two *distinguishable* particles of mass  $m_1$  and  $m_2$ , the wave function of the center-of-mass motion is a plane wave while the relative motion satisfies the Schrödinger equation with the mass equal to the reduced mass  $\mu = m_1 m_2 / (m_1 + m_2)$ . If the particle is incident in the  $z$  direction, the wave function far from the scattering target can be written as

$$\psi(\mathbf{r}) = e^{ikz} + \psi_{sc}(\mathbf{r}), \quad (\text{A.1})$$

where  $\psi_{sc}$  is the scattered wave function. If the scattering between particles is spherical symmetric, the scattered wave function can be expressed in the form of the spherical wave with the scattering amplitude  $f(\theta)$  depends only on the angle of the relative momentum before and after scattering. Then the wave function at large distance is

$$\psi(\mathbf{r}) = e^{ikz} + f(\theta) \frac{e^{ikr}}{r}, \quad (\text{A.2})$$

and the energy of the system is

$$E = \frac{\hbar^2 k^2}{2\mu}. \quad (\text{A.3})$$

To explicitly determine the scattering amplitude we expand the wave function in terms of the Legendre polynomials  $P_l(\cos \theta)$ ,

$$\psi(\mathbf{r}) = \sum_l A_l P_l(\cos \theta) R_{kl}(r). \quad (\text{A.4})$$

Substitute Eq. (4) into Schrödinger equation with central potential  $U(r)$ , the radial part  $R_{kl}(r)$  satisfies

$$\left[\frac{1}{r} \frac{d^2}{dr^2} r - \frac{l(l+1)}{r^2} + k^2 - \frac{2\mu}{\hbar^2} U(r)\right] R_{kl}(r) = 0. \quad (\text{A.5})$$

In the far field where  $U(r) \rightarrow 0$ , the asymptotic solution is Bessel function  $j_l(kr)$  for the free particle,

$$R_{kl}(r) \sim \frac{1}{kr} \sin(kr - \frac{\pi l}{2} + \delta_l), \quad (\text{A.6})$$

with the phase shift  $\delta_l$  provided  $U(r)$  decrease faster than  $r^{-1}$ .

To compare the asymptotic wave function of Eq. (4) with Eq. (2), we expand the plane wave as

$$e^{ikz} = \sum_l (2l+1) i^l j_l(kr) P_l(\cos \theta) \sim \sum_l (2l+1) i^l \frac{\sin(kr - \pi l/2)}{kr} P_l(\cos \theta). \quad (\text{A.7})$$

Then

$$\begin{aligned} \psi(\mathbf{r}) &= e^{ikz} + f(\theta) \frac{e^{ikr}}{r} \\ &= \sum_l (2l+1) P_l(\cos \theta) e^{il\pi/2} \frac{(e^{i(kr-l\pi/2)} - e^{-i(kr-l\pi/2)})}{2ikr} + f(\theta) \frac{e^{ikr}}{r} \\ &= \sum_l (2l+1) P_l(\cos \theta) \frac{(e^{ikr} - e^{-i(kr-l\pi)})}{2ikr} + f(\theta) \frac{e^{ikr}}{r} \end{aligned} \quad (\text{A.8})$$

$$\begin{aligned} &= \sum_l A_l P_l(\cos \theta) \frac{1}{2ikr} (e^{i(kr-l\pi/2+\delta_l)} - e^{i(kr-l\pi/2+\delta_l)}) \\ &= \sum_l A_l P_l(\cos \theta) \frac{1}{2ikr} e^{-i\delta_l} e^{-il\pi/2} (e^{i(kr+2\delta_l)} - e^{-i(kr-l\pi)}). \end{aligned} \quad (\text{A.9})$$

Compare Eq. (8) and Eq. (9), we obtain

$$A_l = (2l+1) i^l e^{i\delta_l}, \quad (\text{A.10})$$

and

$$f(\theta) = \frac{(2l+1)}{2ik} P_l(\cos \theta) (e^{2i\delta_l} - 1). \quad (\text{A.11})$$

## A.1 Relative Magnitude of Phase Shifts

In order to determine the phase shifts we make simplifying assumptions in calculations. In *classical* scattering one introduces impact parameter  $b$  which is given by

$$L = bP, \quad (\text{A.12})$$

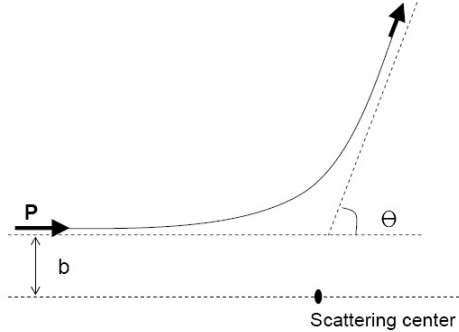


Figure A.1: Classical scattering between two particles.

where  $L$  and  $P$  are incident parameter's angular momentum and linear momentum. Therefore if the interacting potential is appreciable over the range  $a$ , the scattering effect is negligible for  $b > a$ . For the incident particle with momentum  $P = \hbar k$  and angular momentum  $L = \sqrt{l(l+1)}\hbar \sim l\hbar$ , the criterion of non-interaction is

$$l > ak. \quad (\text{A.13})$$

For low energy scattering with  $ka \ll 1$ , only  $l = 0$  phase shift will differ appreciably from zero. Then the so called s-wave scattering amplitude becomes

$$\begin{aligned} f(\theta) &= \frac{1}{k} e^{i\delta_0} \sin \delta_0 \\ &\sim \frac{\delta_0}{k} \\ &\equiv -a, \end{aligned} \quad (\text{A.14})$$

and  $a$  is defined to be the s-wave scattering length.

## A.2 Viewpoints From Quantum Mechanics

In low temperature dilute gases interactions among atoms are weak except when they approach each other. Consider only two-body elastic scattering between identical particles, it is convenient to introduce an effective interaction to simplify simulations of the interacting processes.

Since the state of the particle can be specified by momentum  $k$ , it is suitable to deal the many-body system in momentum space. Then the wave function of Eq. (1) in momentum representation is written as

$$\psi(\mathbf{k}) = \int d\mathbf{r} e^{-i\mathbf{k}\cdot\mathbf{r}} [e^{i\mathbf{k}'\cdot\mathbf{r}} + \psi_{sc}(\mathbf{r})]$$

$$= (2\pi)^3 \delta(\mathbf{k} - \mathbf{k}') + \psi_{sc}(\mathbf{k}). \quad (\text{A.15})$$

The Schrödinger equation in momentum space would be derived through the Fourier transform. From  $H\psi = E\psi$  we have

$$\int d\mathbf{r} e^{-i\mathbf{k}\cdot\mathbf{r}} \left[ -\frac{\hbar^2 \nabla^2}{m} + V(\mathbf{r}) \right] (e^{i\mathbf{k}'\cdot\mathbf{r}} + \psi_{sc}(\mathbf{r})) \quad (\text{A.16})$$

$$= \int d\mathbf{r} e^{-i\mathbf{k}\cdot\mathbf{r}} \left[ \frac{\hat{P}^2}{m} + V(\mathbf{r}) \right] (e^{i\mathbf{k}'\cdot\mathbf{r}} + \psi_{sc}(\mathbf{r})) \quad (\text{A.17})$$

$$= \frac{\hbar^2 k^2}{m} [(2\pi)^3 \delta(\mathbf{k} - \mathbf{k}') + \psi_{sc}(\mathbf{k})] + V(\mathbf{k}' - \mathbf{k}) + \int d\mathbf{r} e^{-i\mathbf{k}\cdot\mathbf{r}} V(\mathbf{r}) \int d\mathbf{k}'' e^{i\mathbf{k}''\cdot\mathbf{r}} \psi_{sc}(\mathbf{k}'') \quad (\text{A.18})$$

$$= \frac{\hbar^2 k^2}{m} [(2\pi)^3 \delta(\mathbf{k} - \mathbf{k}') + \psi_{sc}(\mathbf{k})] + V(\mathbf{k}' - \mathbf{k}) + \int d\mathbf{k}'' V(\mathbf{k}, \mathbf{k}'') \psi_{sc}(\mathbf{k}'') \quad (\text{A.19})$$

$$= \frac{\hbar^2 k'^2}{m} [(2\pi)^3 \delta(\mathbf{k} - \mathbf{k}') + \psi_{sc}(\mathbf{k})]. \quad (\text{A.20})$$

Therefore Eq. (15) satisfies

$$\left( \frac{\hbar^2 k'^2}{m} - \frac{\hbar^2 k^2}{m} \right) \psi_{sc}(\mathbf{k}) = V(\mathbf{k}' - \mathbf{k}) + \int d\mathbf{k}'' V(\mathbf{k}, \mathbf{k}'') \psi_{sc}(\mathbf{k}''). \quad (\text{A.21})$$

Then the scattered wave function is given by

$$\psi_{sc}(\mathbf{k}) = \left( \frac{\hbar^2 k'^2}{m} - \frac{\hbar^2 k^2}{m} + i\xi \right)^{-1} [V(\mathbf{k}, \mathbf{k}') + \int d\mathbf{k}'' V(\mathbf{k}, \mathbf{k}'') \psi_{sc}(\mathbf{k}'')] \quad (\text{A.22})$$

$$= \left( \frac{\hbar^2 k'^2}{m} - \frac{\hbar^2 k^2}{m} + i\xi \right)^{-1} T(\mathbf{k}, \mathbf{k}'; E). \quad (\text{A.23})$$

For low energy incident wave and at large distances we have  $\psi_{sc}(\mathbf{r})$  by Fourier transform from Eq. (22), namely,

$$\psi_{sc}(r) \sim -\frac{mT(0, 0; 0)}{4\pi\hbar^2 r}. \quad (\text{A.24})$$

From Eq. (2), (14) and (23) we obtain

$$T(0, 0; 0) = \frac{4\pi\hbar^2 a}{m} \quad (\text{A.25})$$

In the Born approximation,  $T$  matrix is obtained by taking only  $V(\mathbf{k}, \mathbf{k}')$  term and the scattering length becomes

$$a_{Born} = \frac{m}{4\pi\hbar^2} V(0) = \frac{m}{4\pi\hbar^2} \int d\mathbf{r} V(\mathbf{r}), \quad (\text{A.26})$$



corresponding to  $|\mathbf{k}' - \mathbf{k}| = 0$ . Therefore we obtain that the effective interaction between two particles at low energies is a constant  $V(0) = 4\pi\hbar^2 a/m$  in the momentum representation. Then in coordinate space the effective interaction turns out to be  $\frac{4\pi\hbar^2 a}{m}\delta(\mathbf{r} - \mathbf{r}')$ .





# Bibliography

- (1) R. L. Liboff, *quantum mechanics*, Addison-Wesley 1991.
- (2) C. J. Pethick and H. Smith, *Bose-Einstein Condensation in Dilute Gases*, Cambridge 2002.





## Appendix B

# Analytical Expressions for Band Structures by Plane Wave Method

The plane wave method [1] provides a generic algorithm for eigenvalue problems with periodic potentials [1] such as

$$E\varphi(x) = -\frac{1}{2}\frac{\partial^2\varphi}{\partial x^2} + V(x)\varphi(x). \quad (\text{B.1})$$

To solve Eq. B.1 we expand the periodic potential in terms of the plane wave basis:

$$V(x) = \sum_G U_G e^{iGx}, \quad (\text{B.2})$$

where  $G$  is the reciprocal lattice vector. Also we set

$$\varphi(x) = \sum_k C_k e^{ikx}, \quad (\text{B.3})$$

where wave vectors  $k$  is taken over all values allowed by the Born-von Karman boundary condition. Substitute above equations in to Eq. B.1 we would obtain

$$V(x)\varphi(x) = \sum_{Gk} U_G C_k e^{i(k+G)x} = \sum_{Gk'} U_G C_{k'-G} e^{ik'x}, \quad (\text{B.4})$$

and therefore the Schrödinger equation becomes

$$\left(\frac{k^2}{2} - E\right)C_k + \sum_G U_G C_{k-G} = 0. \quad (\text{B.5})$$

It is convenient to write  $k = q - G$  so that  $q$  lies in the first Brillouin zone. Then Eq. B.5 becomes

$$\left(\frac{(q-G)^2}{2} - E\right)C_{q-G} + \sum_{G'} U_{G'} C_{q-G-G'} = 0, \quad (\text{B.6})$$

or if we make the change of variables  $G' \rightarrow G' - G$ ,

$$\left(\frac{(q-G)^2}{2} - E\right)C_{q-G} + \sum_{G'} U_{G'-G} C_{q-G'} = 0. \quad (\text{B.7})$$

For fixed  $q$  in the first Brillouin zone the set of Eq. B.7 for all reciprocal lattice vectors  $G$  couples only coefficients of  $C_q, C_{q-G}, C_{q-G'}, C_{q-G''} \dots$ . Then the original problem has separated into  $N$  independent problems: one for each allowed  $q$  in the first Brillouin zone.

The band structure and the corresponding Floquet-Bloch modes can be obtained by solving Eq. B.7. The accuracy of modes depends on the number of plane wave basis taken in expansion. For the case of a Bose condensate in an optical lattice, the potential is usually in the form of  $V(x) = \sin^2(\pi x/D)$  which implies non zero terms in Eq. B.2 to  $U_0 = V/2$  and  $U_{G_1} = U_{-G_1} = -V/4$ . So when the potential is rather *shallow* in which only few bound states exist, we can approximately use the two band approach for  $G = 0$  and  $G = G_1$ :

$$\begin{aligned} \frac{(q^2 - E + U_0)}{2} C_q + U_{G_1} C_{q-G_1} &= 0 \\ \frac{((q-G_1)^2 - E + U_0)}{2} C_{q-G_1} + U_{-G_1} C_q &= 0. \end{aligned} \quad (\text{B.8})$$

For simplicity, we have  $D = 2$  and the corresponding  $G_1 = 2\pi/D = \pi$  in our work. Then we obtain the band structure

$$E(q) = \frac{V}{2} + \frac{q^2 + (q-\pi)^2}{4} \pm \frac{\sqrt{(q^2 - (q-\pi)^2)^2 + V^2}}{4}. \quad (\text{B.9})$$

On the other hand, the normalization condition  $\frac{2\pi}{2} \int_{-1}^1 |\varphi(x)|^2 dx = 1$  implies that  $|C_q|^2 + |C_{q-G_1}|^2 = \frac{1}{2\pi}$ . So we can rewrite the wave function as

$$\varphi(x) = C_q e^{iqx} \left(1 + \frac{2}{V}(q^2 + V - 2E)e^{-i\pi x}\right), \quad (\text{B.10})$$

where  $C_q = 1/\sqrt{2\pi}(1 + \frac{4}{V^2}(q^2 + V - 2E)^2)^{-1/2}$ , and  $C_{q-G_1} = (q^2 + V - 2E)2C_q/V$ . Therefore, by definition the effective mass and the group velocity can be written as

$$\frac{1}{m_{eff}} = \frac{\partial^2 E}{\partial q^2} = 1 \pm \frac{\pi^2 V^2}{[(q^2 - (q-\pi)^2)^2 + V^2]^{3/2}} \quad (\text{B.11})$$

$$V_g = \frac{\partial E}{\partial q} = \left(q - \frac{\pi}{2}\right) \left(1 \pm \frac{\pi^2}{\sqrt{(q^2 - (q-\pi)^2)^2 + V^2}}\right). \quad (\text{B.12})$$

# Bibliography

- [1] N. K. Efremidis and D. N. Christodoulides, *Phys. Rev. A* 67, 063608 (2003)
- [2] Ashcroft and Mermin, *Solid state physics*, Australia ;Brooks/Cole,c1976, Singapore .







## Appendix C

# Bloch Theorem and k·p Method

Consider an electron in a potential  $U(\mathbf{r})$  with the perfect *periodicity* of the underlying Bravais lattice[1]; ie,

$$U(\mathbf{r} + \mathbf{R}) = U(\mathbf{r}), \quad (\text{C.1})$$

for all Bravais lattice vector  $\mathbf{R}$ . Then eigenstates of the electron  $\psi$  that satisfies the Schrödinger equation

$$H\psi = \left(-\frac{\hbar^2 \nabla^2}{2m} + U(\mathbf{r})\right)\psi = E\psi \quad (\text{C.2})$$

would be written in the form as

$$\psi_{n\mathbf{k}}(\mathbf{r}) = e^{i\mathbf{k}\cdot\mathbf{r}} u_{n\mathbf{k}}(\mathbf{r}), \quad (\text{C.3})$$

where  $u_{n\mathbf{k}}(\mathbf{r})$  is the Bloch wave function with the same periodicity of the potential. Then the *Bloch theorem* states that the eigenstate of  $H$  can be chosen so that associated with each  $\psi$  is a wave vector  $\mathbf{k}$  such that

$$\psi(\mathbf{r} + \mathbf{R}) = e^{i\mathbf{k}\cdot\mathbf{R}}\psi(\mathbf{r}). \quad (\text{C.4})$$

### C.1 General Remarks About Bloch's Theorem

1. Bloch theorem introduces a wave vector  $\mathbf{k}$  and the *crystal momentum*  $\hbar\mathbf{k}$  to the electron in the periodic potential. However unlike wave vector  $\mathbf{k}$  of a free electron is associated with its momentum by  $\mathbf{P} = \hbar\mathbf{k}$ , the eigenstates  $\psi_{n\mathbf{k}}(\mathbf{r})$  are not eigenstates of the momentum operator due to the incomplete translational invariance of the Hamiltonian in the presence of the nonconstant potential; ie,

$$-i\hbar\nabla\psi_{n\mathbf{k}} = -i\hbar\nabla(e^{i\mathbf{k}\cdot\mathbf{r}}u_{n\mathbf{k}}(\mathbf{r})) = \hbar\mathbf{k}\psi_{n\mathbf{k}} - i\hbar e^{i\mathbf{k}\cdot\mathbf{r}}\nabla u_{n\mathbf{k}}(\mathbf{r}). \quad (\text{C.5})$$

Therefore  $\mathbf{k}$  is only viewed as a quantum number characteristic of the translational symmetry of a periodic potential.

2. The Bloch wave function  $u_{n\mathbf{k}}(\mathbf{r})$  satisfies the eigenvalue equation

$$H_{\mathbf{k}}u_{n\mathbf{k}}(\mathbf{r}) = \left(\frac{\hbar^2}{2m}\left(\frac{1}{i}\nabla + \mathbf{k}\right)^2 + U(\mathbf{r})\right)u_{n\mathbf{k}}(\mathbf{r}) = E_{n\mathbf{k}}u_{n\mathbf{k}}(\mathbf{r}), \quad (\text{C.6})$$

with the boundary condition

$$u_{n\mathbf{k}}(\mathbf{r}) = u_{n\mathbf{k}}(\mathbf{r} + \mathbf{R}). \quad (\text{C.7})$$

3. The wave  $\mathbf{k}$  can be restricted in the first Brillouin zone and for any  $\mathbf{k}'$  not in the region can be written as

$$\mathbf{k}' = \mathbf{k} + \mathbf{K}, \quad (\text{C.8})$$

where  $\mathbf{K}$  is the reciprocal lattice vector of the Bravais lattice. Then for any given  $n$ , we have

$$\begin{aligned} \psi_{n,\mathbf{k}+\mathbf{K}}(\mathbf{r}) &= \psi_{n,\mathbf{k}}(\mathbf{r}), \\ E_{n,\mathbf{k}+\mathbf{K}} &= E_{n,\mathbf{k}}, \end{aligned} \quad (\text{C.9})$$

and  $E_{n,\mathbf{k}}$  is referred to as the *band structure* of the system.

4. We'll show in the next section that from  $\mathbf{k}\cdot\mathbf{p}$  theorem an electron in a level specified by  $n$  and  $\mathbf{k}$  has a nonvanishing mean velocity

$$\mathbf{v}_n(\mathbf{k}) = \frac{1}{\hbar}\nabla_{\mathbf{k}}E_{n\mathbf{k}}. \quad (\text{C.10})$$

It asserts that in spite of interactions between the electron and ions an electron in a periodic potential moves without any degradation of its mean velocity.

## C.2 $\mathbf{k}\cdot\mathbf{p}$ Perturbation, Group Velocity, and Effective Mass

Instead of solving the whole band structure of Eq. (6), the  $\mathbf{k}\cdot\mathbf{p}$  method is used to explore the band structure in the vicinity of some  $\mathbf{k}_0$ [2]. Setting  $\mathbf{k} = \mathbf{k}_0 + \mathbf{q}$ , and by perturbation theory we set

$$\begin{aligned} E_{n\mathbf{k}} &= E_{n\mathbf{k}_0} + \frac{\partial E_{n\mathbf{k}}}{\partial \mathbf{k}}\Big|_{\mathbf{k}_0} \cdot \mathbf{q} + \frac{1}{2} \frac{\partial^2 E_{n\mathbf{k}}}{\partial \mathbf{k}^2}\Big|_{\mathbf{k}_0} \cdot \mathbf{q}^2 + \dots \\ &= E_{n\mathbf{k}}^{(0)} + E_{n\mathbf{k}}^{(1)} + E_{n\mathbf{k}}^{(2)} + \dots \\ u_{n\mathbf{k}} &= u_{n\mathbf{k}}^{(0)} + u_{n\mathbf{k}}^{(1)} + u_{n\mathbf{k}}^{(2)} + \dots, \end{aligned} \quad (\text{C.11})$$

Eq. (6) can be rewritten as

$$\begin{aligned} & \left[ \frac{\mathbf{p}^2}{2m} + \frac{\hbar}{m} \mathbf{k}_0 \cdot \mathbf{p} + \frac{\hbar^2 \mathbf{k}_0^2}{2m} + U(\mathbf{r}) + H' \right] [u_{n\mathbf{k}}^{(0)} + u_{n\mathbf{k}}^{(1)} + u_{n\mathbf{k}}^{(2)} + \dots] \\ & = [E_{n\mathbf{k}}^{(0)} + E_{n\mathbf{k}}^{(1)} + E_{n\mathbf{k}}^{(2)} + \dots] [u_{n\mathbf{k}}^{(0)} + u_{n\mathbf{k}}^{(1)} + u_{n\mathbf{k}}^{(2)} + \dots], \end{aligned} \quad (\text{C.12})$$

where

$$H' = \frac{\hbar^2}{m} \mathbf{q} \cdot \left( \frac{\mathbf{p}}{\hbar} + \mathbf{k}_0 \right) + \frac{\hbar^2 \mathbf{q}^2}{2m} = H'_1 + H'_2. \quad (\text{C.13})$$

Then the zeroth order term gives

$$H_0 u_{n\mathbf{k}}^{(0)} = \left[ \frac{\mathbf{p}^2}{2m} + \frac{\hbar}{m} \mathbf{k}_0 \cdot \mathbf{p} + \frac{\hbar^2 \mathbf{k}_0^2}{2m} + U(\mathbf{r}) \right] u_{n\mathbf{k}}^{(0)} = E_{n\mathbf{k}}^{(0)} u_{n\mathbf{k}}^{(0)}. \quad (\text{C.14})$$

The equation of first order term is

$$H_0 u_{n\mathbf{k}}^{(1)} + H'_1 u_{n\mathbf{k}}^{(0)} = E_{n\mathbf{k}}^{(0)} u_{n\mathbf{k}}^{(1)} + E_{n\mathbf{k}}^{(1)} u_{n\mathbf{k}}^{(0)}. \quad (\text{C.15})$$

While we set

$$u_{n\mathbf{k}}^{(1)} = \sum_{n'} C_{nn'} u_{n'\mathbf{k}}^{(0)} \quad (\text{C.16})$$

and define  $H'_{n'n} = \langle u_{n'\mathbf{k}}^{(0)} | H'_1 | u_{n\mathbf{k}}^{(0)} \rangle$ , we obtain

$$\begin{aligned} C_{nn'} &= \frac{H'_{n'n}}{E_{n\mathbf{k}}^{(0)} - E_{n'\mathbf{k}}^{(0)}} \\ u_{n\mathbf{k}}^{(1)} &= \sum_{n' \neq n} \frac{H'_{n'n}}{E_{n\mathbf{k}}^{(0)} - E_{n'\mathbf{k}}^{(0)}} u_{n'\mathbf{k}}^{(0)}. \end{aligned} \quad (\text{C.17})$$

Also from Eq. (15) we obtain the first order correction to the energy

$$\begin{aligned} E_{n\mathbf{k}}^{(1)} &= \langle n\mathbf{k}_0 | H'_1 | n\mathbf{k}_0 \rangle = \langle n\mathbf{k}_0 | \frac{\hbar^2}{m} \mathbf{q} \cdot \left( \frac{\mathbf{p}}{\hbar} + \mathbf{k}_0 \right) | n\mathbf{k}_0 \rangle \\ &= \frac{\partial E_{n\mathbf{k}}}{\partial \mathbf{k}} \Big|_{\mathbf{k}_0} \cdot \mathbf{q}. \end{aligned} \quad (\text{C.18})$$

While  $\psi_{n\mathbf{k}_0}(\mathbf{r}) = e^{i\mathbf{k}_0 \cdot \mathbf{r}} u_{n\mathbf{k}_0}(\mathbf{r})$ , Eq. (8) give us the *group velocity* of the Bloch electron at  $\mathbf{k}_0$ , which in the form of the first derivative of the band structure is

$$\frac{\partial E_{n\mathbf{k}}}{\partial \mathbf{k}} \Big|_{\mathbf{k}_0} = \frac{\hbar^2}{m} \langle \psi_{n\mathbf{k}_0} | \frac{1}{i} | \nabla \psi_{n\mathbf{k}_0} \rangle. \quad (\text{C.19})$$

Calculations of the second order correction to energy starts by setting

$$u_{n\mathbf{k}}^{(2)} = \sum_{n'} d_{nn'} u_{n'\mathbf{k}}^{(0)}, \quad (\text{C.20})$$

and from

$$H_0 u_{n\mathbf{k}}^{(2)} + H_1' u_{n\mathbf{k}}^{(1)} + H_2' u_{n\mathbf{k}}^{(0)} = E_{n\mathbf{k}}^{(0)} u_{n\mathbf{k}}^{(2)} + E_{n\mathbf{k}}^{(1)} u_{n\mathbf{k}}^{(1)} + E_{n\mathbf{k}}^{(2)} u_{n\mathbf{k}}^{(0)}, \quad (\text{C.21})$$

we obtain

$$\begin{aligned} E_{n\mathbf{k}}^{(2)} &= \frac{\hbar^2 \mathbf{q}^2}{2m} + \langle u_{n\mathbf{k}}^{(0)} | H_1' | u_{n\mathbf{k}}^{(1)} \rangle \\ &= \frac{\hbar^2 \mathbf{q}^2}{2m} + \sum_{n' \neq n} \frac{|\langle n\mathbf{k}_0 | H_1' | n'\mathbf{k}_0 \rangle|^2}{E_{n\mathbf{k}_0} - E_{n'\mathbf{k}_0}}. \end{aligned} \quad (\text{C.22})$$

Compared with Eq. (11) we then define the *effective mass*  $m^*$  at  $\mathbf{k}_0$  as

$$\left(\frac{1}{m^*}\right)_{\mu\nu} = \left[\frac{1}{\hbar^2} \frac{\partial^2 E_{n\mathbf{k}}}{\partial \mathbf{k}_\mu \partial \mathbf{k}_\nu}\right]_{\mathbf{k}_0} \quad (\text{C.23})$$

$$= \frac{1}{m} \delta_{\mu\nu} + \frac{2}{m} \sum_{n' \neq n} \frac{|\langle n\mathbf{k}_0 | p_\mu | n'\mathbf{k}_0 \rangle| |\langle n'\mathbf{k}_0 | p_\nu | n\mathbf{k}_0 \rangle|}{E_{n\mathbf{k}_0} - E_{n'\mathbf{k}_0}} \quad (\text{C.24})$$



# Bibliography

- [1] Ashcroft and Mermin, *Solid state physics*, Cole 1976.
- [2] Min-Fu Li, *Modern semiconductor quantum physics*, World Scientific 1994.





## Appendix D

# The Collective Excitation in The Mean Field Approximation

In the field operator formulation, the Hamiltonian of the trapped boson gas at extremely low temperature can be formulated through the binary contact interaction :

$$\begin{aligned}
 H &= \int d\mathbf{r} \Psi^\dagger(\mathbf{r}) \left[ \frac{-\hbar^2 \nabla^2}{2m} + V_{trap}(\mathbf{r}) \right] \Psi(\mathbf{r}) \\
 &+ \int d\mathbf{r} \int d\mathbf{r}' \Psi^\dagger(\mathbf{r}) \Psi^\dagger(\mathbf{r}') \delta(\mathbf{r} - \mathbf{r}') \Psi(\mathbf{r}') \Psi(\mathbf{r}). \quad (D.1)
 \end{aligned}$$

The interaction among cold atoms can be represented by the  $s$ -wave scattering length of the binary collisions. Under the mean field approach  $\Psi(\mathbf{r}) = \Phi(\mathbf{r}) + \tilde{\psi}(\mathbf{r})$ , where  $\Phi(\mathbf{r}) = \langle \Psi(\mathbf{r}) \rangle$  is the order parameter of the condensate [2]. Then the equation of motion for the condensate in the Hartree-Fock-Bogoliubov-Popov approximation is given by

$$i\hbar \frac{\partial \Phi}{\partial t} = \left[ \frac{-\hbar^2 \nabla^2}{2m} + V_{trap} - \mu \right] \Phi + g[|\Phi|^2 + 2\langle \tilde{\psi}^\dagger \tilde{\psi} \rangle] \Phi + g\langle \tilde{\psi} \tilde{\psi} \rangle \Phi^*. \quad (D.2)$$

Here  $g = \frac{4\pi\hbar^2 a}{m}$  and  $a$  is the  $s$ -wave scattering length. We will use the notations:  $n_c \equiv |\Phi|^2$ ,  $\tilde{n} \equiv \langle \tilde{\psi}^\dagger \tilde{\psi} \rangle$  and  $\tilde{m} \equiv \langle \tilde{\psi} \tilde{\psi} \rangle$ .  $n_c$  denotes the density of condensate, and  $\tilde{n}$  is the density of the non-condensate atoms. So, the equation of the excitation part is given by

$$i\hbar \frac{\partial \tilde{\psi}}{\partial t} = \left[ \frac{-\hbar^2 \nabla^2}{2m} + V_{trap} - \mu \right] \tilde{\psi} + g[2n\tilde{\psi} + m\tilde{\psi}^\dagger], \quad (D.3)$$

where  $n = n_c + \tilde{n}$  and  $m = \Phi^2 + \tilde{m}$ .

In the low temperature, the effect of simultaneously annihilation of two particles is negligible. To solve Eq. D.3 we first make the Bogoliubov transformation for the non-condensate wave function  $\tilde{\psi}$

$$\tilde{\psi}(\mathbf{r}, t) = \Sigma_i [u_i(\mathbf{r})\hat{\alpha}_i - v_i^*(\mathbf{r})\hat{\alpha}_i^\dagger] e^{-iE_i t}, \quad (\text{D.4})$$

and we then obtain

$$\begin{aligned} E_i u_i(\mathbf{r}) &= L u_i(\mathbf{r}) - g\Phi^2(\mathbf{r})v_i(\mathbf{r}) \\ -E_i v_i(\mathbf{r}) &= L v_i(\mathbf{r}) - g\Phi^{*2}(\mathbf{r})u_i(\mathbf{r}), \end{aligned} \quad (\text{D.5})$$

where  $L = \frac{-\hbar^2 \nabla^2}{2m} + V_{trap} - \mu + 2gn(\mathbf{r}) = \hat{h}_0(\mathbf{r}) + gn_c(\mathbf{r})$ . Since  $\tilde{\psi}(\mathbf{r})$  and  $\tilde{\psi}^\dagger(\mathbf{r})$  are boson operators, so the quasi-particle and quasi-hole amplitude  $u_i(\mathbf{r})$  and  $v_i(\mathbf{r})$  satisfy the normalization condition  $\int d\mathbf{r} [u_i(\mathbf{r})u_j^*(\mathbf{r}) - v_i(\mathbf{r})v_j^*(\mathbf{r})] = \delta_{ij}$ .

Instead of solving Eq. D.5 directly, we define  $\phi_i^\pm(\mathbf{r}) = u_i(\mathbf{r}) \pm v_i(\mathbf{r})$ . After some algebraic manipulations, we obtain

$$\begin{aligned} \hat{h}_0^2(\mathbf{r})\phi_i^+(\mathbf{r}) + 2gn_c(\mathbf{r})\hat{h}_0\phi_i^+(\mathbf{r}) &= E_i^2\phi_i^+(\mathbf{r}) \\ \hat{h}_0^2(\mathbf{r})\phi_i^-(\mathbf{r}) + 2\hat{h}_0gn_c(\mathbf{r})\phi_i^-(\mathbf{r}) &= E_i^2\phi_i^-(\mathbf{r}). \end{aligned} \quad (\text{D.6})$$

Expand  $\phi_i^+(\mathbf{r})$  in terms of the eigenstates of  $\hat{h}_0(\mathbf{r})$ , we get

$$\Sigma_\alpha [\epsilon_\alpha \delta_{\alpha\beta} \epsilon_\beta C_\alpha^i + 2g(\int d\mathbf{r} \phi_\beta^*(\mathbf{r})n_c(\mathbf{r})\phi_\alpha(\mathbf{r}))\epsilon_\alpha C_\alpha^i] = E_i^2 C_\beta^i, \quad (\text{D.7})$$

where  $\phi_i^+ = \Sigma_\alpha C_\alpha^i \phi_\alpha(\mathbf{r})$ , and  $\phi_\alpha(\mathbf{r})$  satisfies  $\hat{h}_0(\mathbf{r})\phi_\alpha(\mathbf{r}) = \epsilon_\alpha \phi_\alpha(\mathbf{r})$ . From the relation  $\hat{h}_0\phi_i^+ = E_i\phi_i^+$ , and the normalization condition of  $u_i(\mathbf{r})$  and  $v_i(\mathbf{r})$ , the  $C_\alpha^i$  satisfies

$$\Sigma_\alpha \epsilon_\alpha C_\alpha^{*i} C_\alpha^j = E_j \delta_{ij}. \quad (\text{D.8})$$

Finally we arrive at

$$\begin{pmatrix} u_i(\mathbf{r}) \\ v_i(\mathbf{r}) \end{pmatrix} = \frac{1}{2} \Sigma_\alpha (1 \pm \frac{\epsilon_\alpha}{E_i}) C_\alpha^i \phi_\alpha(\mathbf{r}). \quad (\text{D.9})$$

With the Bose distribution function  $\langle \hat{\alpha}_i^\dagger \hat{\alpha}_i \rangle_{BE} = (e^{E_i/k_B T} - 1)^{-1} \equiv N_0(E_i)$ , the non-condensate density can thus be represented as  $\tilde{n}(\mathbf{r}) = \Sigma_i [|u_i(\mathbf{r})|^2 + |v_i(\mathbf{r})|^2] N_0(E_i) + |v_i(\mathbf{r})|^2$ .

The condensate here is trapped in an axial symmetric double-well constructed by adding a laser generated Gaussian barrier to MOT. The GPE for the condensate part is given by

$$\begin{aligned} [\frac{-\hbar^2 \nabla^2}{2m} + \frac{1}{2}m\omega(x^2 + y^2) + \frac{1}{2}m\omega_z z^2 + U_g e^{-\frac{x^2}{2\sigma^2}} \\ + g(n_c(\mathbf{r}) + 2\tilde{n}(\mathbf{r}))] \Phi(\mathbf{r}) = \mu \Phi(\mathbf{r}). \end{aligned} \quad (\text{D.10})$$

To solve Eq. D.10 we make expansion in terms of the spherical harmonics

$$\Phi(\mathbf{r}) = \sum_l \frac{\Phi_l(r)}{r} Y_{l,m_e}(\Omega), \quad (\text{D.11})$$



We see that due to the nonspherical potential, the orbital angular momentum itself is not a good quantum number for the system, but the magnetic quantum number  $m_e$ , and parity  $P = (-1)^{(l+m_e)}$  are good quantum numbers. For the ground state condensate  $m_e = 0$ . In diagonalization of Eq. D.10, we multiply it by  $Y_{l',m'_e}^*(\Omega)$  and integrate over  $\Omega$ . The Laplacian and Gaussian barrier potential terms can be expressed as

$$\begin{aligned} E_K &= \sum_l F(r, r') \delta_{l,l'} \delta_{m_e, m'_e} \\ E_G &= \sum_l F(r, r') \delta(r - r') \delta_{l,l'} \delta_{m_e, m'_e}. \end{aligned}$$

On the other hand, the harmonic potential and nonlinear term are in the form of

$$\begin{aligned} E_{OSC} &= \sum_l F(r, r') \delta(r - r') C_{l, m_e} G_1(L, M) \\ E_{NON} &= \sum_l F(r, r') \delta(r - r') C_{l, m_e} G_2(L, M), \end{aligned} \quad (\text{D.12})$$

where  $F(r, r') \equiv \langle \Phi_{l'}(r) | \hat{O}(r, r') | \Phi_l(r) \rangle$ ,  $G_1(L, M) = W_{3j}(l, 2, l'; 0, 0, 0) W_{3j}(l, 2, l'; m_e, 0, m'_e)$  and  $G_2(L, M) = W_{3j}(l, 2n, l'; 0, 0, 0) W_{3j}(l, 2n, l'; m_e, 0, m'_e)$ ,  $W_{3j}$  denotes the Wigner-3j symbol [3]. The condensate profile is obtained by solving Eqs. D.9, D.10 self-consistently with the zero non-condensate density at the beginning.

Fig. 2 depicts the excitation energy spectra of the three lowest modes at  $T = 0$  K. The barrier height varies from  $U_g = 0$  to  $U_g = 10$  at a step of  $2(\hbar\omega)$ . This corresponds to a change from no barrier of single condensate to the almost completely separated condensates. For the three modes D(0,even), D(1,even) and D(2,even) of  $U_g = 0$  case, we reproduce the results of Ref. [1]; while we presented here the excitation energy spectra for the corresponding modes when the potential emerges from a single well into the double-well.

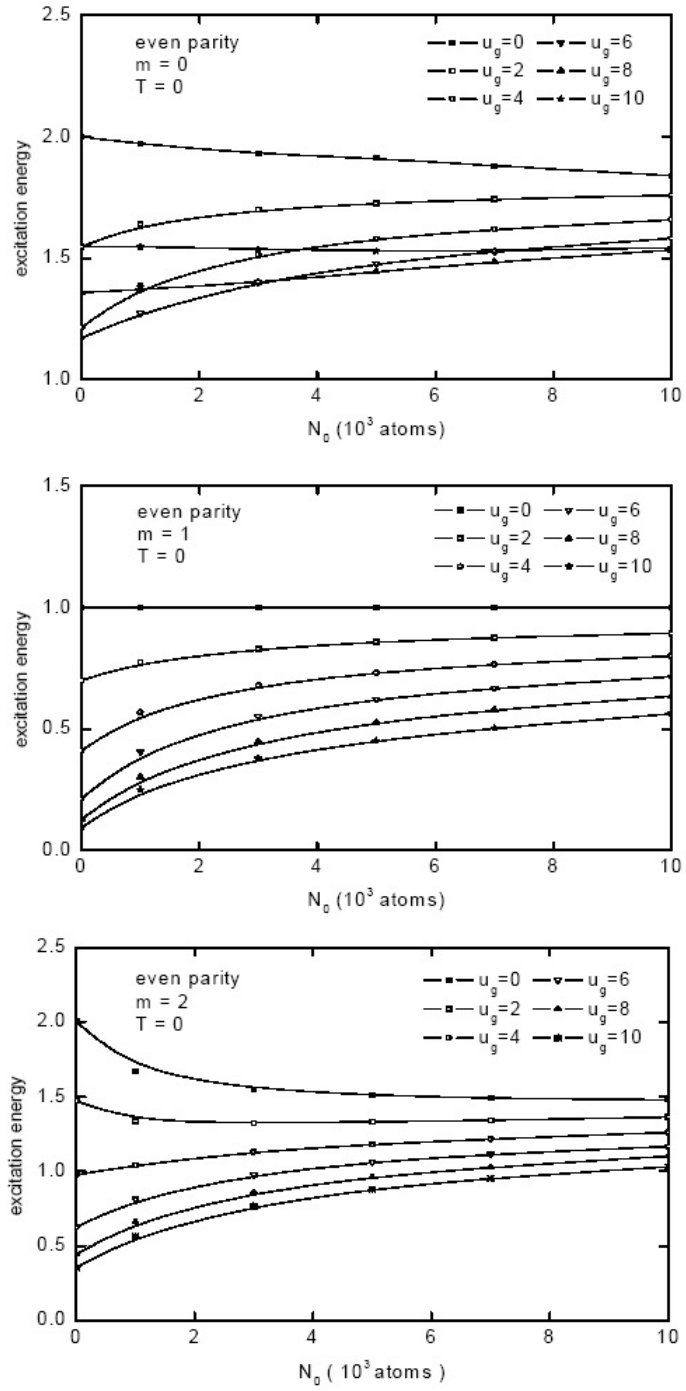


Figure D.1: Excitation energy spectra of the three lowest collective excitation modes  $D(0,\text{even})$ ,  $D(1,\text{even})$  and  $D(2,\text{even})$  respectively.

# Bibliography

- [1] M. Edwards, P. A. Ruprecht *et. al.*, Phys. Rev. Lett. **77**, 1671 (1996).
- [2] L. Pitaevskii and S. Stringari, *Bose-Einstein Condensation*, Clarendon, Oxford, 2003.
- [3] A. R. Edmonds, *Angular Momentum in Quantum Mechanics*, Princeton Univ. Press, Princeton, 1985.

